Leaving and returning home

visually-guided homing in *Bombus terrestris*

Doctoral Dissertation

by

Charlotte Doussot

Fakultät für Biologie

Universität Bielefeld

Leaving and returning home: visually-guided homing in *Bombus terrestris*.

Dissertation
zur Erlangung des akademischen Grades Doktor der Naturwissenschaften
-Dr.rer.nat-
der Fakultät für Biologie der Universität Bielefeld

vorgelegt von
Charlotte Doussot
Bielefeld, Mai 2020

betreut von
Erstbetreuer: Prof. Dr. Martin Egelhaaf
Zweitbetreuer: Dr. Olivier Bertrand

Erklärung

Ich versichere, dass ich diese Arbeit selbstständig und ohne unzulässige Hilfe verfasst habe, keine anderen als die angegebenen Quellen und Hilfsmittel benutzt und Zitate kenntlich gemacht habe.

Charlotte Doussot
Bielefeld, Mai 2020

Contents

List of Figures

List of Tables

Acknowledgements

Many people made this work and time possible but also enjoyable. At first, I would like to thanks my first supervisor Martin Egelhaaf. He trusted me to be able to conduct this project. Thanks to him, I had the opportunity to move to Germany, discover and learn the world of research. Then, I would like to thanks, Roland Kern. He helped me for the setting-up of my first project here. I would also like to thank Jens Lindemann, which has always been present for technical support, and this often when I killed several pieces of equipment. But this work would have lacked some of the complicated wanderings in calculus if I would not have had the help of Olivier Bertrand, who recently has been officially named as my second supervisor. Olivier introduced me to my new favourite non-speaking language: Python, and was always present for scientific and non-scientific discussions. Tim Siesenop's help was also tremendous. Tim helped me in most of my projects to collect some data and replaced me when I could not do experiments. And I will keep a special memory of the long conversations we often had in the corner lab. I also would like to thank Sridhar Ravi and Thierry Hoinville. They contributed in scientific discussions around some of my projects. I would like now to thank whoever made it possible for me, to have the chance to work with several outstanding students, Ronja Bigge, Magdalena Rados, Sophie Lehfeldt, Matle Leon, all did an excellent job for their different projects or as Hiwis. I am convinced that they are and will continue to be great scientists. Finally, I would also like to thanks the complete staff of the Neurobiology department for their help, making this project possible.

But because a PhD is not all about work, at least the 2% left outside of work was maybe the most life-defining experience for me. While being left alone in a country which I did not manage to learn the language, many people showed extreme kindness and tolerance and allowed me to connect to them. However, most of them are actually my dear colleagues, but for sure friends, which are: Frauke Lauterbach who has been a friend that I could trust and rely on in many moments of my time here in Bielefeld, José Monteagudo with whom I luckily shared the same office, making him one of the persons who spends the most time in my company during this period. But coffee breaks will not have been the same without Martin Müller, Jinglin Li, and the already cited Olivier and Tim. With all of them, I spent wonderful times playing board games, sharing movie nights in the lab. Recently the lab has seen several new students who also joined us in our game-nights, Silvia Rönnau and Andrea Gonsek. I wish them all the best for the following of their studies and career in biology and thank them for having brought their positive attitude in the lab.

But aside from the lab environment, another social bubble made this time in Bielefeld a fantastic experience. And for this, I have to thank two persons again José and Olivier, who introduced me to the Forró dance class. I met there many amazing people that I cannot all list here, with whom I shared a lot of enjoyable moments, at parties or on the Siegfriedplatz, among them, there are Elena, Julia, Ivan... Ivan has always been there as a friend and is an inimitable pizza chef. I wish him all the luck as a freshly starting PhD student in sociology.

At last but definitely, the most important I want to thank Rebecca for her constant support in the tough moments of finishing this thesis, her support never failed. I also thank her for being my forever favourite dance partner.

Finally, all of this will not have been possible without my parents Thérèse and Alain Doussot, who supported me through my all-school education and pushed me until here. They helped me to move here and even brought a sofa on the car roof from Normandy to Bielefeld. They always showed psychological and financial help, sacrificing part of their life to allow their daughters to succeed. Which brings me to thanks my two sisters Aurélie and Elodie, both were, are and will stay constant supporters. Both are incredibly talented and bright engineers which I admire. Elodie is now a mother, and consequently, I am the happy aunt of Hortense, which is for now, in total objectivity of course (until the next one at least), the cutest baby on Earth. I would also like to have a thought for my guitar teacher, Guy Chevallier, who passed away recently, I discovered the guitar thanks to him more than 20 years ago. I definitely keep music and guitar as part of my life, as both make some hard days of work lighter.

So thanks to all of you, but now, if you're reading this, it means you have to stop procrastinating and should start to read the real thing.

Abstract

Returning to a previously visited place is a task of real importance, which is called "homing". For insects like bumblebees, flying daily between their nest and flower-covered meadows, this task becomes a real feat given the tiny size of their brains and the generally discreet entrance to their nest. In the case of *Bombus terrestris*, the nest entrance is often just a small hole in the ground that is difficult to see. The mechanisms explaining how bumblebees find the entrance to their nest are still scientifically debated. In my thesis, I investigate some hypotheses on these mechanisms and their plausibility. In particular, I focus on visual-guidance strategies that bumblebees might use to return to their nest.

In the first part of the thesis, I asked the question: Which visual information about the nest surroundings do bumblebees remember to allow them to return home again? To answer this question, I compared the behaviour of bumblebees in a specific cue-conflict setting with the behaviour of well-established models of visually guided homing, and one model of my design. The different models differ in the number, and nature of the panoramic images acquired and memorised upon departure from the nest. They also differ in how, during return, the current view is compared with unique or multiple memorised views. In my experimental setting, the bumblebees were trained to return to their nest with two sets of visual landmarks indicating their inconspicuous nest-hole. Then, I recorded their return journey after these cues were brought into conflict to different degrees and displaced in the environment from the original learning condition. Consequently, the bumblebees had to manage to return despite the conflicting indications provided by the two sets of visual cues. In result, bumblebees did not search at a compromise location but searched at the different places indicated by each set of visual cues. When comparing this behaviour with the prediction made by the different models, I found that some of the models performed only poorly, especially those where only one panoramic view at the nest location is taken into account. Models based on several panoramic views in the vicinity of the nest entrance predicted the location where bumblebees searched for their nest much better. A lower number of such views seems to be required if the views also contain distance information in addition to contrast information.

In the next part of my thesis, I dealt with the question of how bumblebees cope with a visual ambiguity about their nest-location during return by taking 3D development of the flight trajectories into account. The search behaviour of insects has rarely been investigated under visual conflict situation; therefore, I provide a detailed analysis of the bumblebees search behaviour when the conflicting cues indicate two possible home-locations. During some of the test situations, bumblebees switched from one location to the other. Eventually, after some time, they found their nest-entrance, which at this point is not indicated by any visual cue. Based on different quantitative analyses, I found that the switching behaviour is prevalent during situations with a small conflict between the cues. In contrast, during conditions of large conflict, just one location will be preferably visited. To further charac-

terise search behaviour, I performed a clustering analysis, including variables of the flight trajectories not considered so far: time and altitude. Some groups of return flights emerging from this analysis show a switch in search behaviour between the conflicting cues as well as frequent changes in height, with both features decreasing overtime during the flights. I hypothesised that changes in altitude might be critical to follow the homing direction indicated by a vision-based homing strategy enabling a switch from one cue-based search location to the other.

As suggested by the first part of the thesis, depth-information might be critical for later return. Therefore, I asked in the third part of the thesis: What is the reference frame of a relative distance map acquired and memorised during the departure flight from the nest? By recording the first exit flights of bumblebees from their nest-hole, i.e. when bees gather and learn information on their surroundings, and by characterising their head movements, I was able to show that bumblebees, like other flying insects, limit rotations to brief periods. However, I observed residual remaining head rotations during the intervals of relative head stabilisation. Depending on the exact characteristics of these residual rotations, the relative distance-map which could be derived from the apparent motion of the surroundings during the periods of relative head stabilisation might be either centred at (1) the bee, (2) the nest-location or (3) any other location in space. I found that the residual head rotations as occurring during the first departure flights from the nest-hole do not allow building a nest-centred map of the environment. Moreover, I could not provide sufficient evidence in favour of a bee-centred spatial representation of the environment. Finally, I discussed the implications of the reference frame in the context of the different model tested in the first part of the thesis.

As an overall conclusion of this work, the acquisition of distance information about the nest surroundings and the active behaviour of bumblebees while learning and returning-home is suggested to be decisive to ensure their arrival. The use of distance information and the behaviours described in the second part of the thesis might also be used by other insects that need to return to an inconspicuous location, such as ants or wasps, and may have the potential to inspire the development of navigation models that can be used by artificial autonomous agents, whether flying or not.

Zusammenfassung

Die Rückkehr an einen zuvor besuchten Ort ist für viele Tiere eine wirklich wichtige Aufgabe, die als "Homing" bezeichnet wird. Für Insekten wie Hummeln, die täglich zwischen ihrem Nest und blumenbedeckten Wiesen hin- und herfliegen, wird diese Aufgabe angesichts der winzigen Größe ihres Gehirns und des im Allgemeinen kaum erkennbaren Eingangs zu ihrem Nest zu einer besonderen Herausforderung. Im Fall von *Bombus terrestris* ist der Nesteingang oft nur ein kleines kaum sichtbares Loch im Boden. Die Mechanismen, die erklären, wie Hummeln den Eingang zu ihrem Nest finden, sind wissenschaftlich immer noch umstritten. In meiner Dissertation untersuche ich einige Hypothesen zu diesen Mechanismen und deren Plausibilität. Insbesondere konzentriere ich mich auf visuelle Suchstrategien, die Hummeln zum Finden ihres Nests verwenden könnten.

Im ersten Teil der Arbeit stellte ich die Frage: An welche visuelle Information über die Nestumgebung erinnern sich die Hummeln, um wieder nach Hause zurückfinden zu können? Um diese Frage zu beantworten, verglich ich das Verhalten von Hummeln in einer spezifischen „Cue-Conflict“ Situation mit dem Verhalten von gut etablierten Modellen für visuelles Heimfinden sowie mit einem von mir entwickelten Modell. Die verschiedenen Modelle unterscheiden sich einerseits in der Anzahl und Art der Panoramabilder, die beim Verlassen des Nestes gespeichert werden, und adererseits, wie bei der Rückkehr die aktuelle Ansicht der Umwelt mit den gespeicherten Ansichten verglichen wird. In meiner Versuchsanordnung wurden die Hummeln darauf trainiert, zu ihrem Nest zurückzukehren, wobei zwei Konstellationen von visuellen Merkmalen auf ihr Nestloch hinweisen. Dann registrierte ich die Rückflüge, nachdem die beiden Merkmalskonstellationen gegenüber dem ursprünglichen Lernzustand in unterschiedlichem Maße gegeneinander verschoben und so in Konflikt zueinander gebracht worden waren. Die Hummeln mussten folglich trotz der jetzt widersprüchlichen Information die Rückkehr schaffen. Im Ergebnis suchten die Hummeln nicht an einem Kompromissort, sondern an den verschiedenen Orten, die durch die beiden visuellen Merkmalskonstellationen jeweils angezeigt wurden. Beim Vergleich dieses Verhaltens mit den Vorhersagen der verschiedenen Modelle stellte ich fest, dass einige der Modelle nur schlechte Vorhersagen lieferten, insbesondere diejenigen, bei denen nur eine Panoramasicht am Neststandort berücksichtigt wurde. Modelle, die auf mehreren Panoramaansichten in der Nähe des Nesteingangs basieren, sagten den Ort, an dem die Hummeln ihr Nest suchten, viel besser voraus. Eine geringere Anzahl solcher Ansichten scheint erforderlich zu sein, wenn diese neben Kontrastinformation auch Entfernungsinformation enthalten.

Im nächsten Teil meiner Dissertation befasste ich mich mit der Frage, wie Hummeln mit visuellen Mehrdeutigkeiten über ihren Neststandort bei der Rückkehr umgehen, indem ich die 3D-Entwicklung der Flugbahnen berücksichtigte. Das Suchverhalten von Insekten wurde bisher nur selten in visuellen Konfliktsituationen untersucht. Deshalb führte ich eine detaillierte Analyse des Suchverhaltens von Hummeln durch unter Bedingungen von widersprüchlicher Information über den Neststandort. In einigen Testsituationen wechselten die

Hummeln von einem möglichen Nestort zum anderen. Schließlich fanden sie ihren wirklichen Nesteingang, der unter diesen Bedingungen nicht unmittelbar durch visuelle Merkmale angezeigt wurde. Auf der Grundlage verschiedener quantitativer Analysen fand ich heraus, dass das Wechselverhalten zwischen den beiden möglichen Neststandorten besonders häufig in Situationen mit einem kleinen Konflikt zwischen den visuellen Merkmalkonstellationen vorkommt. Im Gegensatz dazu wird unter Bedingungen eines großen Konflikts vorzugsweise nur einer der Orte aufgesucht. Um das Suchverhalten weiter zu charakterisieren, führte ich eine Clustering-Analyse durch, die bisher nicht berücksichtigte Flugbahnvariablen miteinbezog, nämlich die Zeit und die Flughöhe. Einige Gruppen von Rückflügen, die sich aus dieser Analyse ergaben, zeigen einen Wechsel im Suchverhalten zwischen den widersprüchlichen Merkmalskonstellationen sowie häufige Höhenänderungen an, wobei sich die Häufigkeit der Wechsel während der Flüge verringerten. Ich stellte die Hypothese auf, dass Höhenänderungen entscheidend sein könnten, um das Ziel zu finden, insbesondere wenn dieses nur durch einen Wechsel zwischen den Suchorten, die durch die unterschiedlichen Merkmalkonstellationen angezeigt werden, gefunden werden kann.

Wie im ersten Teil der Dissertation vorgeschlagen, könnte Tiefeninformation für die spätere Rückkehr der Hummeln zum Nest entscheidend sein. Deshalb habe ich im dritten Teil der Arbeit gefragt: Was ist der Bezugsrahmen einer relativen Entfernungskarte, die während des Abfluges vom Nest erworben und gespeichert wird? Durch Aufzeichnung der Kopfbewegungen der Hummeln während ihrer ersten Ausflüge aus dem Nestloch, d.h. wenn sie Information über ihre Umgebung sammeln und lernen, konnte ich zeigen, dass sie, wie andere Insekten auch, Kopfrotationen auf kurze Zeiträume beschränken. Allerdings beobachtete ich verbleibende Restkopfrotationen während der Intervalle der relativen Kopfstabilisierung. Abhängig von den genauen Charakteristika dieser Restrotationen kann die relative Entfernungskarte, die aus der scheinbaren retinalen Bewegung der Umgebung während der Perioden der relativen Kopfstabilisierung gewonnen werden könnte, entweder (1) auf die Hummel, (2) auf den Neststandort oder (3) auf irgendeinen anderen Ort im Raum zentriert sein. Ich fand heraus, dass die Restrotationen des Kopfes während der ersten Abflüge aus dem Nestloch es nicht erlauben, eine nestzentrierte Karte der Umgebung zu erstellen. Außerdem konnte ich keine ausreichenden Belege für eine bienenzentrierte räumliche Repräesentation der Umwelt gewinnen. Ich diskutiere die Auswirkungen des visuellen Bezugsrahmens im Zusammenhang mit den verschiedenen im ersten Teil der Arbeit getesteten Modellen.

Als allgemeine Schlussfolgerung dieser Arbeit wird vorgeschlagen, dass die Erfassung von Entfernungsinformation über die Nestumgebung und das aktive Verhalten der Hummeln während des Lernens beim Verlassen des Nests für die spätere Rückkehr zum Nest entscheidend sind. Die Verwendung von Distanzinformationen und die im zweiten Teil der Arbeit beschriebenen Verhaltensweisen könnten auch von anderen Insekten, die an einen unauffälligen Ort zurückkehren müssen, wie z.B. Ameisen oder Wespen, genutzt werden und könnten das Potenzial haben, die Entwicklung von Navigationsmodellen zu inspirieren, die von künstlichen autonomen Agenten, ob fliegend oder nicht, verwendet werden können.

Résumé

Retourner dans un lieu précédemment visité est une tâche d'une réelle importance, que l'on appelle le "homing". Pour des insectes comme les bourdons, qui volent quotidiennement entre leur nid et les prairies couvertes de fleurs, cette tâche devient un véritable exploit étant donné la taille minuscule de leur cerveau et l'entrée généralement discrète de leur nid. Dans le cas de *Bombus terrestris*, l'entrée du nid n'est souvent qu'un petit trou dans le sol difficile à voir. Les mécanismes expliquant comment les bourdons trouvent l'entrée de leur nid sont encore scientifiquement débattus. Dans ma thèse, j'étudie certaines hypothèses sur ces mécanismes et leur plausibilité. En particulier, je me concentre sur les stratégies de guidage visuel que les bourdons pourraient utiliser pour retourner à leur nid.

Dans la première partie de ma thèse, j'ai posé la question : Quelles informations visuelles sur l'environnement du nid les bourdons se souviennent-ils pour leur permettre de retourner chez-eux ? Pour répondre à cette question, j'ai comparé le comportement des bourdons dans un environnement spécifique, celui-ci incluant un conflit visuel, avec le comportement de modèles bien établis reproduisant un retour à la maison guidé visuellement, ainsi qu'un modèle de ma conception. Les différents modèles diffèrent par le nombre, et la nature des images panoramiques acquises et mémorisées au départ du nid. Ils diffèrent également dans la façon dont, au retour, la vue actuelle est comparée aux vues uniques ou multiples mémorisées. Lors de l'expérience, les bourdons ont été entraînés à retourner à leur nid avec deux groupes de points de repères indiquant l'entrée discrète du nid. Ensuite, j'ai enregistré leur vol de retour après que ces repères furent mis en conflit à différents degrés, et déplacés dans l'environnement par rapport à la condition d'apprentissage initiale. Par conséquent, les bourdons ont dû réussir à retourner à leur nid malgré les indications contradictoires fournies par les deux repères visuels. Les résultats montrent que les bourdons n'ont pas fait un compromis entre les deux repéres visuels, mais ont cherché aux deux endroits indiqués par ceux-ci. En comparant ce comportement avec les prédictions faites par les différents modèles, j'ai constaté que certains modèles n'étaient que peu performants, en particulier, ceux qui ne prennent en compte qu'une seule vue panoramique à l'emplacement du nid. Les modèles basés sur plusieurs vues panoramiques à proximité de l'entrée du nid, ont prédit beaucoup mieux l'endroit où les bourdons cherchaient leur nid. Un nombre plus faible de ces vues semble être nécessaire quand celles-ci contiennent également des informations de distance en plus des informations de contraste.

Dans la partie suivante de ma thèse, j'ai traité la question de savoir comment les bourdons font face à une ambiguïté visuelle sur la localisation de leur nid, notamment en prenant en compte le développement en 3D des trajectoires de vol de retour. La façon dont les insectes recherchent a rarement été étudiée en situation de conflit visuel ; c'est pourquoi je fournis une analyse détaillée du comportement de recherche des bourdons lorsque des indices contradictoires indiquent le nid à deux locations possibles. Dans certaines situations, les bourdons sont passés d'un endroit à l'autre. Au bout d'un certain temps, ils ont fini par

trouver leur nid, qui, à ce stade, n'est indiqué par aucun indice visuel. Sur la base de différentes analyses quantitatives, j'ai constaté que les bourdons permuttent plus souvent entre les deux locations quand ceux-ci sont testés dans des situations de léger conflit visuel. En revanche, dans des conditions où le conflit est important, un seul endroit est en préférence visité. Pour caractériser davantage le comportement de recherche, j'ai effectué une analyse de "clustering", incluant des variables décrivant les trajectoires de vol qui n' étaient pas considérées jusqu'à présent : le temps et l'altitude. Parmi les groupes formés à partir des vols de retour, certains montrent systématiquement cette permutation entre les deux indices ainsi que des changements fréquents d'altitude. Ces deux caractéristiques diminuant au fil du vol. J'ai émis l'hypothèse que les changements d'altitude pourraient être essentiels pour suivre la direction indiquée par une stratégie de homing basée sur la vision, permettant ainsi au bourdon de passer d'un endroit de recherche indiqué par un groupe de repères à l'endroit indiqué par l'autre groupe de repère.

Comme le suggère la première partie de la thèse, les informations de distance pourraient être essentielles pour un retour ultérieur. C'est pourquoi j'ai posé la question dans la troisième partie de la thèse : A quelle référence les distances acquises et mémorisées lors du premier vol au départ du nid sont-elles attachées ? En enregistrant les premiers vols de sortie des bourdons, c'est-à-dire lorsqu'ils recueillent et apprennent des informations sur leur environnement, et en caractérisant leurs mouvements de tête, j'ai pu montrer que les bourdons, comme d'autres insectes volants, limitent les rotations à de brèves périodes. Cependant, j'ai observé que leurs têtes accomplissent des rotations résiduelles pendant les intervalles de stabilisation relative. En fonction des caractéristiques exactes de ces rotations résiduelles, une représentation des distances relatives, celle-ci dérivée à partir du mouvement apparent de l'environnement sur la rétine, pourrait être centrée soit sur (1) le bourdon, (2) ou l'emplacement du nid ou (3) tout autre emplacement dans l'espace. J'ai constaté que les rotations résiduelles de la tête, telles qu'elles se produisent lors des premiers vols au départ du nid, ne permettent pas de construire une carte de l'environnement centrée sur le nid. De plus, je n'ai pas pu fournir de preuves suffisantes en faveur d'une représentation spatiale de l'environnement centrée sur l'insecte. Enfin, j'ai discuté des implications du cadre de référence de cette représentation dans le contexte des différents modèles testés dans la première partie de la thèse.

En conclusion générale de ce travail, il est suggéré que l'acquisition d'informations de distance sur l'environnement du nid, et le comportement des bourdons pendant l'apprentissage et le retour au nid sont décisifs pour assurer leur arrivée. L'utilisation des informations de distance et les comportements décrits dans la deuxième partie de la thèse pourraient également être utilisés par d'autres insectes qui ont besoin de retourner à un endroit peu visible, comme les fourmis ou les guêpes, et pourraient inspirer le développement de modèles de navigation pouvant être utilisés par des agents artificiels autonomes, qu'ils volent ou non.

1 General Introduction

1.1 The concept of navigation

When asked how an animal survives in the wild, most people will answer that it must be able to feed, hide, protect itself and adapt to its environment. Interestingly, navigation and orientation, while essential to most animals, are usually not considered as an answer to this question. Orientation and navigation are universal abilities that most species actively use to accomplish diverse tasks. Hence, the mechanisms underlying navigation are likely to be strongly shaped by natural selection. Therefore, one would expect animals to have evolved to become exquisite navigators.

However, when we look at ourselves, we seem to contradict this general statement. Indeed, in today's western world, most of us rely on GPS devices to find our way around a city or follow human-made signalization. And when asked to retrieve our car in a parking lot, or a fruitful clam-digging spot on the seaside from last year, despite having already visited these locations, we often find this exercise difficult. The history of man-made navigation tools is long and proves the efforts made to make navigation easier and thus to enable prowess: from the Vikings' sun stone in the 900s, when they sailed from Norway to Greenland and North America [111], to the satellite GPS, now integrated in all smartphones. While humans have developed a "big brain" over the course of evolution, which

allowed them to create such tools, it is likely that many of them will unfortunately be lost once they are deprived of these tools. However, this is not the case for all of us; many learn from an early age to use cues in their environment to navigate. For example, the night sky is used by fishermen, who follow the movement of the stars to estimate the distance travelled, or hunters who learn to use simple visual cues [85]. To facilitate navigation, humans shape their world by the use of signs or man-made constructions like roads or signalization, leaving only a minority of us able to rely on natural cues. Therefore, an individual's life-style can have a significant impact on its navigational abilities, whereas for other animals, these qualities are mostly innate, and primarily rely on the use of their direct natural environment. In this regard, animals are arguably better models to study innate navigation abilities, since these are not biased by the experience of using sophisticated tools.

Animals have always fascinated us with their navigational exploits. In fact, we can all remember the many stories of lost pets, which have been reunited with their owners after a journey of sometimes several kilometres and many over examples can come to mind to illustrate animal navigation.

But first, it is necessary to define what is really meant by the term "navigation". First of all, innate directed movements that can be triggered as an immediate response to a stimulus (Kinesis), or that are directed towards or in reference to a stimulus (Taxis), are not considered as processes of navigation [108, 131]. This leaves us with a more complex form of spatially directed movements that include spatial orientation and navigation. **Spatial orientation** can be defined as a movement with reference to an object or pattern in the environment, which acts as a **compass** and provides the animal with a direction to follow [145, 108]. In nature, there is a plethora of compasses that might be used, such as the sun, the earth's magnetic field or even a conspicuous hill or tree in some distance to the

animal. To illustrate a phenomenon of spatial orientation, we can think of nocturnal dung beetles that use the arrangement of stars provided by a clear night sky to push their dung ball in a straight line away from the dung pile, which is used as a food source or breeding chamber for its larvae, [51]; thus, ensuring an optimized course to avoid the nicely shaped ball being stolen by another beetle.

Navigation can be seen as a sub-type of spatial orientation and is often considered as a movement towards a goal based on its direction, but also based on its distance from the animal or from a known location. The notion of distance makes navigation more elaborate than a simple orientation mechanism [131]. Indeed, getting an idea of the distance to a goal is a rather complex process, especially since, unlike us, animals cannot look at their phone or a map.

Despite being sophisticated abilities, orientation and navigation are accomplished on a daily basis by most animals when they return home, e.g. to a food source or to a breeding site. These daily routines, requiring the animal to move from one familiar place to another, is a phenomenon called "**homing**", and it is the focus of this chapter and an overarching issue of this thesis.

1.2 Terminology of Homing behaviours

Intuitively, a behaviour can be considered as homing when an animal returns to where it lives. However, the behaviours adopted when returning

home are also found when returning to other behaviourally relevant places, such as a familiar food source or a mating site. Therefore, in the following, homing will include all locomotion from any location B back to a goal location A.

Navigation from a point B to a point A can be classified under the generic term "homing", although, it cannot be conceived as a single type of behaviour. Indeed, the complete return-trip to point A, can be divided in different sections or phases, where different mechanisms and strategies might be in used by the animal. Therefore, the study of homing requires careful definition of the behaviours or navigation strategies used. Research on animal navigation led to the proposal of several classification schemes to define the different homing phenomena: for example, the early classification proposed by Papi 1992 [131], the one suggested by roboticists, which ranks the different processes according to their complexity [70, 172], and more recently, the classification proposed by Mandal 2018 [108], mostly based on the work of Papi 1992, with the addition of concepts developed after Papi's work was proposed. In the following, a taxonomy of homing behaviours based on the above-mentioned classifications will be summarised. This is intended to facilitate the understanding of the phenomenon of homing within the framework of this thesis, but also to broaden the scope of this work.

In the classification used here, the homing behaviours will be separated into two categories. The first category comprises the behaviour adopted when the goal or the close environment of the goal can be perceived by the animal directly from its current position. This behaviour is termed **local homing** behaviour. The second category comprises all the other behaviours used when the immediate goal's environment cannot be perceived from the animal's current position. This category of behaviours is called **far-range homing** (Fig 1.1). Within each category,

the strategies underlying the respective behaviours will be described on a scale of complexity from the perspective of the animal. Interestingly, most of these strategies play a role in both local and far-range homing.

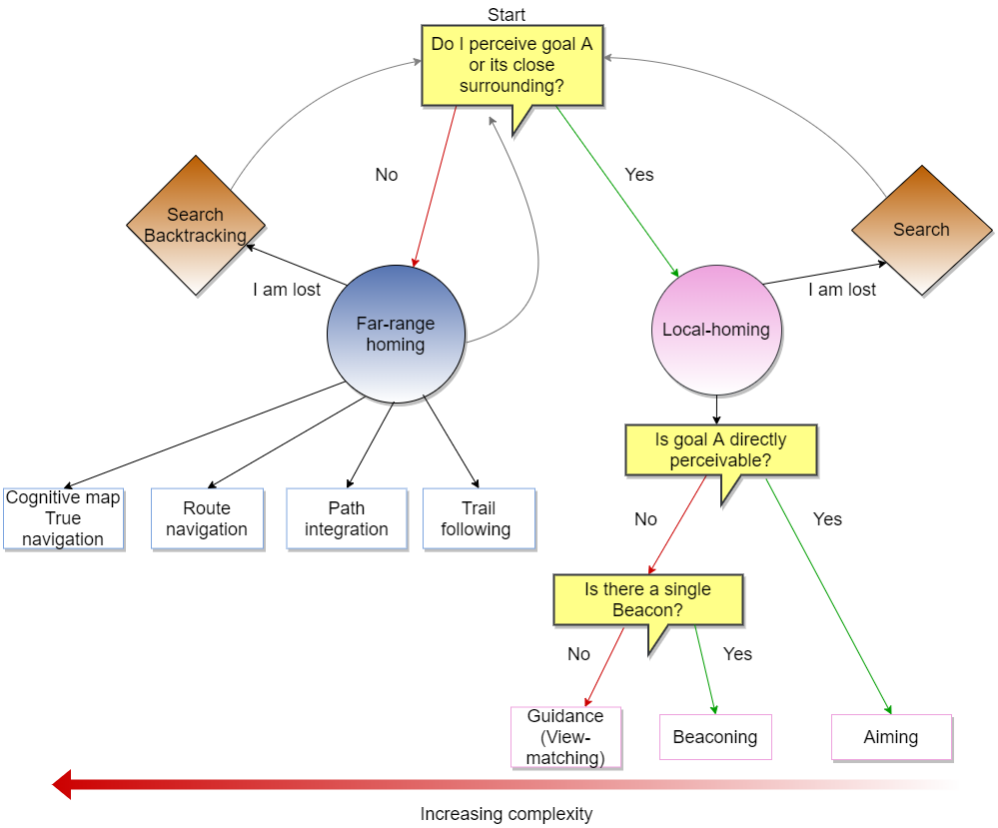

Figure 1.1: Classification of homing strategies. The flow-chart starts with the question in the upper box, and divide the strategies between local homing (pink box) and far-range homing (blue box). Answers to the questions (yellow boxes) are yes (green arrow) or no (red arrow). The grey arrows show a possible return to the first question following the accomplishment of a strategy.

1.2.1 local homing

local homing strategies involve processes such as aiming, beaconing and piloting (Fig 1.1) [70]. **Aiming** is done when the goal is explicitly perceived by the animal, in which case the animal simply has to head towards it (Fig 1.2). **Beaconing** indicates navigation relative to a perceptible object, a 'landmark', in the vicinity of the yet invisible goal (Fig 1.2). The third type, piloting or guidance, is more complex because it requires to estimate the location of the goal, which is not perceptible, based on the spatial arrangement of several external cues placed around it. **Guidance** relies on finding the solution to the problem of triangulation between different objects, which can be solved in many ways depending on the abilities of the animal studied (Fig 1.2). For example, insects which succeed in solving the task of guidance are thought to bring in line the memorised bearing of the objects from the perspective of the goal location, with their actual view of these objects [26]. As another example, a mouse trained to swim towards a submerged invisible platform in the presence of distal room-cues, i.e. in the classical Morris water maze setting, will direct its search for the platform according to the location of these **allothetic** cues, once they are moved. Hence, these cues are used by the animal as external references to retrieve the platform [120]. Finally, if the goal is not found, the animal will enter into a search behaviour (explained later).

1.2.2 Far-range homing

The second category of homing strategies, far-range homing, includes behaviours that are used when the goal and its immediate surroundings are not perceptible from the animal's current location. Several behaviours can be adopted to find a distant goal, such as trail-following,

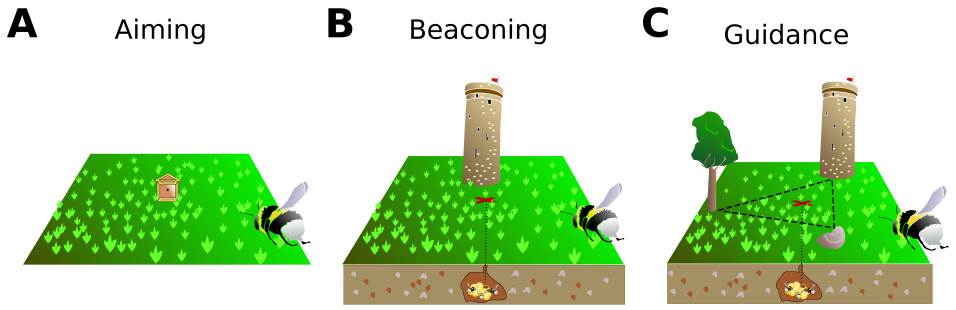

Figure 1.2: Illustration of three visual local homing strategies. Homing-trip of a bumblebee when it returns to its nest that is either in a visible box above ground (A) or below ground (B, C) with a barely visible nest entrance. (A) **Aiming**: Since the hive-box can be seen by the bumblebee, it can return by aiming at the box. (B) **Beaconing**: A castle is located behind the location of the inconspicuous nest-entrance, represented here by a red cross. If the bumblebee remembers that the castle indicates the location of the nest entrance, it can direct its flight towards the castle to return home. (C) **Guidance**: The imperceivable nest-hole is surrounded by three visible terrestrial landmarks. By geometrically solving the arrangement between the castle, rock and tree as in its memory, it is possible for the bumblebee to pinpoint the location of the nest-entrance.

back-tracking, path-integration, route-based navigation or true navigation (Fig 1.1). During **trail-following**, the animal uses a cue, such as an odour, forming a trail that was left behind by a fellow animal or by itself on a previous journey. An example are Chitons leaving mucus behind them during their movement in the substratum [30]. Differently, some animals may use pre-existing tracks to direct their homing, such as pigeons and honeybees that can use man-made roads to navigate their way [105, 44]. Additionally, another simple strategy is to go backwards, i.e. back-tracking. **Back-tracking** can be used to find the location of the goal in consequence to an unfortunate displacement. For example, ants displaced by researchers as they approached their nest walk into the opposite direction of the displacement; thus, back towards their nest [198].

A highly important strategy is **path-integration** (PI), also known as dead-reckoning as Darwin called it in nautical terminology [52] (Fig 1.3). Path-integration is arguably one of the most fascinating abilities of animals. By using an external (allothetic) compass, for example the sun or the pattern of polarized light in the sky indicating to the animal its orientation in its environment, and the integration of its own travelling distance, for example by counting the number of steps (an **idiothetic cue**, i.e. the reference is the individual), the animal can determine its current position relative to the origin of its journey i.e. the goal location (Fig 1.3). Therefore, by continually integrating its often tortuous journey towards the current position, the animal can return to the place of departure in a straight path. PI gives the animal access to a so-called homing-vector that indicates the direction and distance of the "home" at each new step, until this one is eventually nullified when the animal reaches its goal or surrounding (i.e. a zero-vector). Consequently, PI is also called **vector-navigation**. This behaviour has been studied in quite some detail in desert ants [123], crickets [10], but also less intensively in mammals [64].

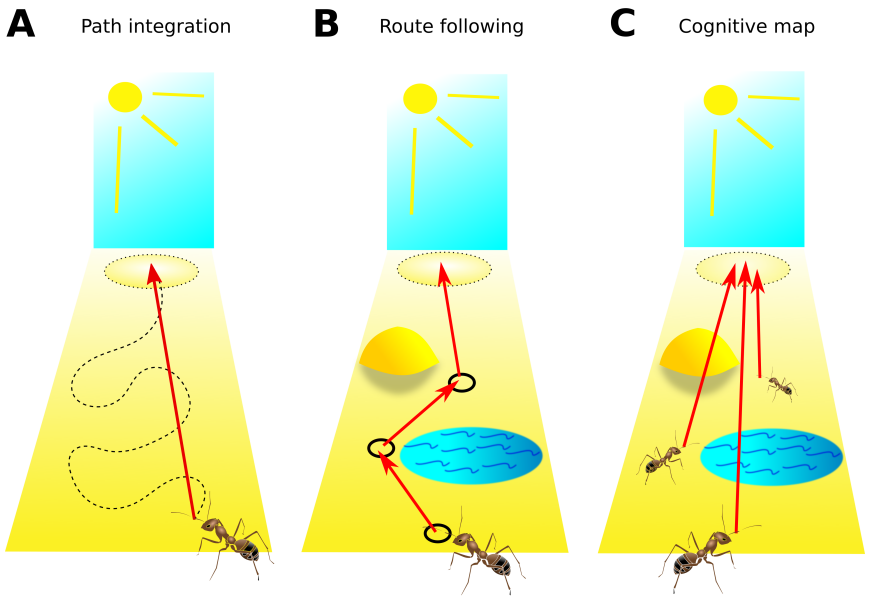

Figure 1.3: Illustration of three far-range homing strategies. The nest location is not yet visible neither its surrounding, the later represented by a dotted circle, indeed the ant is too far away from this one. A: **Path-integration**, after completing its outward journey (dotted black line), during which it integrated its steps number and its orientation relative to the sun compass, the ant can access the home vector pointing directly to the starting location (red arrow) .i.e. the nest. B: **Route-following**: a vector, called local-vector, is associated to each node of the habitual ant's route, define in this example by the different visual landmarks and align in the world coordinate system with a compass e.g. the sun. The ant at each node will follow the indication given by the corresponding red arrow to return to its nest or its surrounding. C: **Cognitive map**: the ant knows the relation between the different elements of its familiar environment, therefore, wherever in this environment it can directly return to its nest or surrounding.

A more complex far-range homing strategy is **route-based navigation**. A route is composed of several segments. A segment starts and ends

at a node. A node is the starting- or end point of a road or an intersection. In between nodes, the animal moves along a specific direction (Fig 1.3). In other words, a distinct behaviour can be assigned to each segment that is initiated by its start node and terminated at its end node. This process is also called **recognition-triggered response**. In this way, each node is associated with a direction in which to move next. In other words, a local vector is associated with each route segment. Evidence for this type of behaviour has been provided many times for ants navigating in a cluttered environment using vision to define the different nodes [110, 41]. However, this navigation strategy does not allow new roads to be established and does not cope with obstacles on the track blocking the animal's direct locomotion to the next node. Thus, this behaviour is not likely to be used independently of other navigational strategies.

Navigating by means of a **cognitive map**, is a process that is most complex from a computational perspective. A cognitive map is often referred to as the representation of the allothetic cues' locations in the environment as well as the location of the goal, including the true linear and angular distances between the cues. In this way, the animal can take a new shortcut and "plan" its journey home when it is displaced in its familiar environment (even beyond a habitual route) (Fig 1.3). The existence of a cognitive map has been widely accepted for mammalian navigation, notably through the discovery of specialized cells located in the hippocampus such as grid cells, boundary cells, and head direction cells that allow the animal to map its environment [121, 54]. Nevertheless, the existence of cognitive maps in other species, such as bees, is still very controversial [113, 29], as observations of complex homing behaviour in bees has been suggested to be explainable by the combination of several simple strategies rather than by the use of a cognitive map [195].

Whereas homing based on a cognitive map only works in familiar en-

vironments, **true navigation** is probably the most complex mechanism: it is assumed to work even if the animal has been displaced to a location where it has never been before and is still able to return to its goal. This remarkable behaviour has been reported for several mammals such as bats [173], but also in birds (pigeons [62]), and for invertebrates such as lobsters [16]. These exceptional capacities are assumed to be related to the use of terrestrial magnetic fields.

If a navigation strategy does not lead the animal exactly to its goal for whatever reason, or if the animal is displaced to an unknown location, **search behaviour** is initiated (Fig 1.1). This search may be "systematic" and focused on the assumed goal location, or "optimal", better known as "**Levy-walk**". **Systematic searching** has been well described for ants [116] and desert isopods [79]: by searching for its nest, the animal walks in a spiral around the presumed nest position as it is indicated by its PI. On the other hand, a Levy-walk search is crudely characterised by the animal covering a small area by walking in sequence of small segments of variable length (straight path) each in a different direction, then interrupted by a longer path towards a new location [84]. This kind of search behaviour can be observed in animals looking for an invisible goal when they do not have *a priori* knowledge about where it may be located. Adopting this strategy, the probability to revisit twice the same location is low. Examples of Levy-walk searching patterns have been reported for marine predators looking for prey [154]. In the context of homing, it has been reported that Levy-walk search is carried out by honeybees searching for their hive after being captured and released at a distance from it, i.e. in a situation where the animal did not have *a priori* knowledge about the hive's location [140].

The above examples provided some evidence that at least some insects species are extremely skilled navigators and appear to perform a

variety of navigational strategies. Accordingly, insects often triggered a lot of attention in navigation research. Therefore, the following paragraphs will summarize why insects are so fascinating in the context of navigation.

1.3 Insects as model species to study homing

1.3.1 Introduction to the study of insects homing

Insects belong to the phylum of arthropods, which makes up the vast majority of the animal biomass, and the insect class is extremely diverse with about 1 million species described [5, 28]. Consequently, insects have always fascinated and their study, "entomology", goes back as far as 2000 years [151]. However, the study of insect homing started, as far as we can tell, only around 150 years ago with Jean Henri Fabre who, after releasing megachilid bees and sphecid wasps up to 4 km from their home, found them the same day back at their nest. Since then, the interest in understanding the insects' navigational abilities has never ceased [131]. The growing interest in building efficient autonomous technical navigation systems, such as drones, as well as the desire to understand insect species essential to our ecosystems but being threatened by the excesses of globalization, have pushed in recent years the study of insect navigation and guidance capabilities much further.

Insects are skilled navigators, especially when considering their size,

the distance they travel and their tiny brains. One of the most spectacular examples is the monarch butterfly *Danaus plexippus*, migrating in autumn from the Eastern USA to some mountain overwintering sites in Central-Mexico [20]. During this journey, the monarch butterfly can travel 130 km per day. However, this fascinating behaviour cannot be considered as homing behaviour, as the monarch butterfly does not survive more than one year and is therefore unlikely to return to the United States, as the migration cycle takes place over two generations [19].

However, a specific group of insects is the perfect example for the study of homing abilities: the central-place-foragers, as it will be explained in the next paragraph.

1.3.2 Central-place foragers

Unlike other insects, eusocial hymenoptera, including wasps, ants and bees, are known as central-place-foragers [129]. The term **central-place forager** refers to the fact that some individuals in the colony called foragers, travel every day back and forth between the colony and feeding places to bring back food for the larvae and colony. In the case of large bee hives, foragers may explore an area of up to 100 square kilometres. Although bees have excellent navigational skills, ants are nevertheless more widely studied and most models of homing behaviour have been developed based on behavioural observation of ants. This is because of their limitation to travel on foot so, close to the ground. Therefore, it is more convenient to monitor their foraging tracks than the more extensive routes characteristic of flying hymenopterans. Ant species navigate in a wide variety of habitats and exhibit a large assortment of behaviours depending on the species studied. And all the navigational strategies they use are included in their navigational-toolkit.

1.3.3 The navigational toolkit of ants

The ant **navigational-toolkit** is the best example to illustrate the complexity of the different homing phenomena mentioned above. The notion of the ant navigational-toolkit was introduced by Rüdiger Wehner for desert-ants [188]. The toolkit provides the ant with several navigation strategies. For example, there are ants, such as the Malaysian Leptogeny, that use pheromones to guide their fellow ants to a recently killed prey in order to transport it to the nest [112, 23]. Other ants also use pheromone trails, but this time without recruiting the whole group along the trail, as in the case of wood ants, leaf-cutting ants and harvesting ants. But when walking along a pheromone-trail, there may be an ambiguity about the direction in which to move because it does not provide information on orientation. Therefore, like for other ants species which do not use a pheromone-trail, those ants will resolve this orientation ambiguity by using other prominent strategies built into their navigational-toolkit: notably their PI, the guidance by visual cues when available, and search behaviour [131]. In addition to these probably most relevant behaviours, there are others such as back-tracking [198], beaconing based on olfactory cues [160]. Ants living in cluttered environment use a succession of terrestrial visual cues, each associated with a direction, to allow them to follow a route. However, despite much research it is not yet clear how this strategies work together in order to guide the animal home.

A possible answer to this question is given through modelling analysis, which could reproduce many experimental results on hymenopterans by combining the diverse home-directions provided by the different strategies. This combination is based on the "**certainty**" of each strategy, i.e. the expression of the animal's judgment on the reliability of this strategy [80, 184, 48, 166]. This decentralized architecture of the navigational toolkit of ants, where each strategy is used separately or in

parallel, contrasts with the idea of a centralized structure, which underlies the cognitive map concept [113]. Furthermore, a decentralized architecture is considered to be closer to the computational capabilities of the insect brain, as suggested by a recent modelling study following a model constrained by the insect brain structures [166]. Therefore, the use of a cognitive map by insects is unlikely, because there is no experimental evidence that could not be replicated with a decentralized approach. In conclusion, it seems that the direction followed by a homing animal is based on what has been called the "certainty" of these guidance strategies.

Yet, the certainty accorded to these strategies is not immutable and this one might change depending on the accomplished task. For example, which strategies are considered more reliable by the animal during local homing? To discuss this question, the example of another insect will be used, *Bombus terrestris*, which is less studied than ants, but which has several advantages for the study of local homing ,as explained in the following. Besides, it has been the experimental animal used in this thesis.

1.4 *Bombus terrestris*

1.4.1 Biology of *Bombus terrestris*

Bumblebees are **eusocial hymenopterans**, which means that they follow the three rules of **eusociality**: (1) individuals take care of the food of the whole colony, (2) there is a division of labour and reproduction

(not all individuals can reproduce), and (3) there is an overlap between generations [189]. *Bombus terrestris* often build their nests in old burrows of rodents, i.e. underground. In this location, conditions are optimal for the maintenance of the entire colony and the larvae. A colony of *Bombus terrestris* can reach up to approximately 400 individuals. Inside the hive, a queen and her daughters can be found, the latter being genetically closer to each other (average of 75% shared genes) than to a possible offspring (only 50% relatedness), if assuming the queen mated only once. The important similarity between sisters is due to their father being an haploid individual emerging from an unfertilized egg, thus sharing 100% of his genetic material with his own children, and to the genetic material inherited from their diploid mother (50% relatedness between mother and daughter). This relatedness may support cooperation between the sisters. The work within the nest is divided between the females, because males emerging from unfertilized eggs are likely to leave the nest after a few days [72] and only aspire to feed and mate with young queens. Unlike honeybees, the division of labour in a bumblebee nest is more flexible, as a bumblebee can switch from one role to another on a daily basis depending on the current needs of the colony: guarding the entrance, taking care of the brood or foraging. Foragers are not so numerous, rarely more than ten per hive, often with a great variability in performance from 3 to 15 flights per day [65, 192]. During their foraging flights they can cover several hundred meters [130]. Thus, the foragers are very efficient relying on their navigational skills. Therefore, they are a good model for the study of local homing. Moreover, *Bombus* is resistant to many diseases and weather conditions, and appears to behave in indoor experimental settings in a very similar way as under outdoor conditions [15, 57]. For these reasons, bumblebees have been extensively studied in a multitude of experimental settings for their navigational capabilities. Examples are analyses of their learning flights close to the nest-hole [107, 142, 134], the performance when crossing holes in obstacles on their way back to the

hive [139], route following based on colour cues [8] crossing an environment of densely cluttered objects [71], navigating in turbulence [47], and following an outdoor foraging routine [192, 104, 130]...

1.4.2 The navigational toolkit of *Bombus terrestris* for homing:

To accomplish these behaviours, bumblebees, like ants, can rely on a plethora of senses and navigational strategies. To navigate their environment, bumblebees may rely on their PI (see below), or on allothetic cues such as terrestrial visual cues for guidance [107, 142] or on following habitual foraging-routes [104], but also olfactory cues of flowers [96] or a scent-trail left by a conspecific while walking [34]. Moreover, bumblebees have been concluded to even use electrical cues for recognising a particular food source [88].

The choice of a particular strategy or tool may differ between returning to a food source or home. It may as well differs if considering local or far-range homing. The following only focus on the final phase of return flights of bumblebees, i.e. when arriving in the surroundings of the nest-entrance (i.e local homing). Therefore, in this context, some strategies of this toolkit may be unlikely to be used, such as guidance by electrical or odour cues, since these are mainly associated with flowers. Although olfactory cues originating from the hive may be perceived in the close proximity of the nest entrance, no study shows a clear use of these yet. Above, it has been mentioned that strategies classified as far-range homing could also be used during local homing. This could be the case here for PI and route-following, which might be used in addition to a strategy of visual guidance when the bee is in the nest-entrance surroundings. However, the different homing strategies might be judged as more or less

reliable by *Bombus terrestris* during local homing. Hereafter, the use of PI is described in the broader context of flying hymenopterans, providing an introduction to several relevant concepts important to keep in mind for the understanding of this thesis.

1.4.3 Path-integration of flying hymenopterans

To discuss the reliability of the PI it is worth explaining how it works in the case of bumblebees or other flying hymenopterans. As do walking insects, bumblebees use the whole range of existing compass cues provided by the environment, like the sun and the polarized light [39]. However, it is obvious that flying animals cannot rely on counting the number of steps performed as an odometer (i.e. an idiothetic cue) like walking ants do. Instead, flying hymenopterans are likely to estimate the distance travelled through vision. When flying a straight course, they can estimate how far they have been travelling from the integration of the displacement of the visual environment on their eyes, in other words from the **optical-flow** (OF) [39, 50, 159]. When flying on a straight course, the geometrical optic-flow, as define by Koenderink [92], is dependent on the distance to object, the altitude of the flight and the landscape topography, as well as on locomotion velocity. Therefore, during return, a change in altitude, topography or flight-velocity different from the outbound journey, may induce an ambiguity about the integrated distance based on the OF, which could lead the insect to either over- or underestimate the distance to the goal [159, 63, 135].

A representation of the OF is supposed to be estimated by motion detection mechanisms in the brain by **motion-sensitive neurons** located in the optic-lobe. These neurons were shown to respond to the three dimensional structure of the environment during translatory movements

[114, 12, 91, 78, 174]. However, these neurons cannot respond in a texture- or contrast-free environment. Experiments on honeybees showed that, indeed, the integration of distance during PI is affected by the texture and 3D layout of the environment. For example, the honeybee's odometer runs at a slower pace when flight is performed over water with its relatively featureless surface [167]. However, this kind of dependence on contrast and texture has not been observed in other behavioural contexts [153]. Since in most natural situations outbound and return flights of bumblebees are likely to take place under similar environmental conditions and potentially at a similar flight height, the ambiguities in OF estimation introduced by the geometry and the motion-detection mechanism might not be critical. However, given all these ambiguities, the information provided by the odometer might be slightly imprecise when the bee is in the close surrounding of the nest trying to pinpoint its entrance [159].

However, PI even when based on a more precise odometer, such as step counting, is sensitive to incremental noise the more tortuous the outward path is [32]. Moreover, the longer the journey is, the more positional uncertainty accumulates when estimating the goal location [196]. Therefore, bumblebees and other flying hymenopterans will rely to a large extent on terrestrial visual cues to reach their nest [169].

1.4.4 The start of the journey: the learning flight

The nest of *Bombus terrestris* can be detected from outside only by a small hole in the ground, making it almost unnoticeable to a naïve observer. However, bumblebees succeed to return to their nest by using its visual surroundings. How does this tiny animal manage such a demanding task? The return trip is not the starting point of local homing. Indeed, the key to a successful return starts earlier, i.e. when the animals are thought

to memorize the visual environment of the nest-hole during their first outbound trips. Upon departure, they perform complex flight manoeuvres viewing for most of the time at their nest entrance, circling around it [134, 107, 46]. During this flight phase the bumblebee's frontal visual field is oriented mostly to the nest-hole [134, 107]. On the next departures for foraging trips from the nest-hole, this kind of flight manoeuvres become shorter and shorter and eventually disappear, unless a visual alteration was given to the nest's visual surroundings, which then triggers a new series of such flight manoeuvres [98, 106]. These choreographies differ in detail between species, but follow the general concept called "**turn-back and look behaviour**" [98, 201, 170, 99, 46]. This behaviour is commonly named **learning flights** or walks, for flying and walking hymenopterans, respectively [67, 185].

Recordings of learning flights exist for several hymenopteran species, such as wasps, honeybees and bumblebees [201, 202, 134, 6]. In ants, it has been possible to characterise learning walks in some detail [68], revealing, for example, that ants perform specific walking "pirouettes" mostly directed to their nest entrance. In the case of bumblebees, this kind of recordings often lack sufficient precision to allow determining exactly where the animal has been looking at during the learning, which might be a critical piece of information to unravel what has been learned in the visual surrounding. The importance of tracking the gaze direction during a phase of learning can be reflected in a more intuitive example, following the illustration depicted in (Fig 1.2C). If we imagine a biologist who wants to return to the bumblebees' nest-location to position a recording camera, we could notice that her eyes will look around the location, and eventually she will direct her gaze longer on remarkable visual landmarks, such as the tree. In this example, the gaze direction seems to provide evidence about what features in the environment the biologist might use for later return. But in insects, the direction of gaze is difficult to determine because of

their small size and rapid movements hampering video tracking at high spatial and temporal resolution. Since - in contrast to humans - the eyes of insects are unable to move much within the head capsule, eye movements can immediately be derived from the recordings of head movements, which is, however, a complicated issue if to be done in 3D. Studies on head movements during learning flights have already been carried out in wasps [165], and – in this thesis - on bumblebees (see Chapter 3). These studies may provide hints about what is learned about the visual environment during learning flights and potentially answers to the question: is this learning taking place continuously during the entire learning flight, or only at specific moments along the flight trajectory when, for example, the insect views the nest-hole in a given retinal area [165].

1.5 Finding the nest-entrance

1.5.1 Classification of visually-based local homing strategies

Based on existing estimates of insect orientation relative to the nest-hole during learning flights and by observing their return behaviour, a variety of hypotheses have been developed on what insects learn about the nest's visual surroundings and how this information might be used to find their way back-home after a foraging trip. These hypotheses have been proposed both by biologists and bio-inspired roboticists, the later aiming

at parsimonious technologies and referring to agents rather than insects. These vision-based homing strategies can be roughly divided into two different categories: **holistic** homing strategies and **non-holistic** homing strategies. In the context of this thesis a holistic homing strategy means that a representation of the whole visual environment is memorized and used, whereas in a non-holistic strategy objects ('landmarks') are segmented from the rest of the environment and represented as individual entities Fig 1.4. I will firstly explain with an example how non-holistic strategies work. If using a non-holistic strategy to return to its nest, the bumblebee in the environmental setting shown in (Fig 1.2) needs to have memorized explicitly upon departure the tree, the castle and the rock as well as their relationship. During return, depending on the type of non-holistic strategy, the bee could (1) match its current view of the landmarks with their respective representation in its memory, a process called **correspondence-method** or could (2) derive a direction in the world coordinate system of the selected landmarks without the need to establish pairs between their current representation and their location in the memory [118]. Conversely, when using a holistic strategy there is no need to select the landmarks. In our example Fig 1.2, the bumblebee could remember one or several complete views of its nest surroundings, where not only the object labelled as landmark in the earlier non-holistic strategy (tree, castle...) would be represented.

In what follows, we will provide a non-exhaustive list of these strategies inspired by the classification of Möller and Vardy 2006 [118]. However, the definition of holistic and non-holistic strategies followed in this work, differs from theirs. Finally, note that like the classification of general homing behaviours described above, some visual local homing strategies may be more ambiguous than others so can be attributed to both categories of homing strategies, holistic and non-holistic.

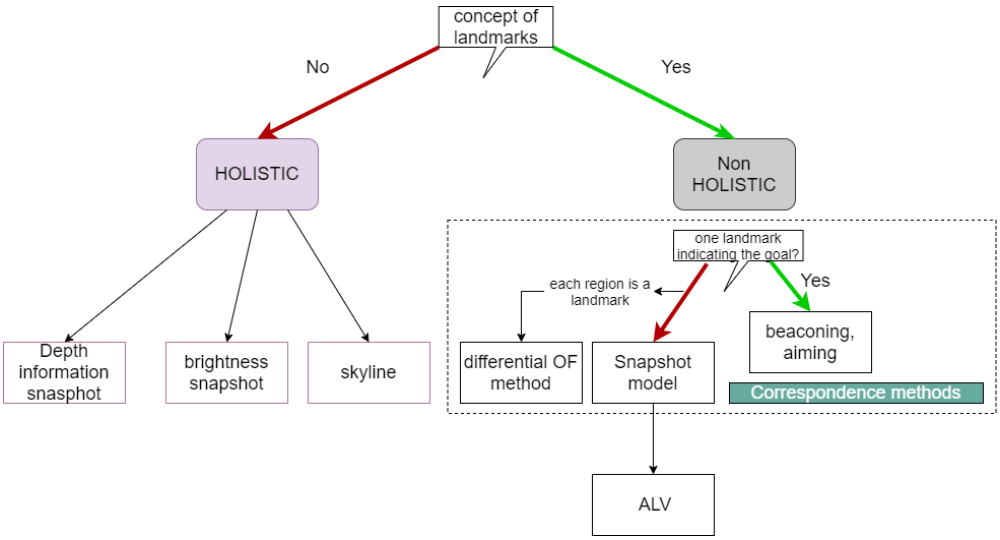

Figure 1.4: Classification of vision-based local homing strategies. Sorting of different visually-based homing strategies between holistic (purple) and non-holistic (grey). Among the non-holistic strategies those relying a correspondence methods are represented by a dotted rectangle. Answers to the different question are yes (green arrows) and no (red arrows).

1.5.2 Non-holistic strategies

When trained in classical learning paradigms not related to navigation, bumblebees are able to learn many properties of visual objects such as their shape and colour [156, 190, 103], indicating that bumblebees during local navigation might learn landmarks in the vicinity of their nest also based on such visual features in order to use this information on their return trip. There are different strategies how these visual cues can guide the return trip. For example, if a single highly visible beacon is placed next to the nest-hole, bumblebees are attracted by it and can easily return home (beaconing and aiming) [169, 157]. This strategy is simple and would make it possible to return home in many situations if such a beacon were present. However, nature in most cases does not provide bumble-

bees with a single distinct landmark placed directly at the entrance to the nest. Indeed, several landmarks are often placed around the nest, forcing bumblebees to use a guidance strategy to the nest-hole based on the location of these landmarks. Therefore, the animal must remember each of them. However, bumblebees and most insects have a large field of view that provides them with an almost complete **panoramic-view**, so this panorama could be used to memorise in parallel all the landmarks near the nest entrance [131, 27].

A bumblebee leaving its nest could, during its learning flight, remember one or more panoramic views, also called snapshots, including landmarks around the nest entrance. Later, on its return, the bumblebee could try to match its current view of the landmarks with the stored image. Experiments with honeybees trained to return to a food source indicated by one landmark, revealed that they direct their search closer or further away from the landmark if it is smaller or larger than the original during the learning situation. This finding suggests that bees have not learnt the distance between the landmark and the food source but rather how large the landmark appears when viewed from the food source [26]. In another experiment bees were trained with three landmarks next to the food source. In a test situation with the three landmark placed in a new constellation, in such way that the search could be done where either (1) the angle between landmarks fit the original constellation or where (2) the distance to the landmarks is the same as in the learning situation, during test honeybees searched for the feeder at the location where the angle between landmarks was the same as during learning (1). This observation illustrates the idea of **template-matching** and indicates that insects confounded distance and size, and that their memory appears to be based on a two-dimensional rather than a three-dimensional representation of the environment [27]. Similar findings were obtained for ants [186]. This behavioural performance can be accounted for by the

snapshot-model described by Cartwright and Collett 1983 [27], Fig 1.4, where the insect attempts to make correspond the retinal appearance of stored landmarks to the current view of the landmark array. This model, however, requires the animal to distinguish the landmarks from the rest of its environment. Although this has not been a problem in the experimental situation of Cartwright and Collett (1983) where the objects were black cylinders and the background homogeneously white, problems may arise in more complex natural environments.

Based on this classical snapshot-model, roboticists designed an algorithm to extract the landmarks from the retinal images using a thresholding procedure applied to the visual input. As a consequence of this procedure, the memory is reduced to a black and white representation of the environment where only the most visible landmarks can be distinguished (the Average Landmark Vector model [95]). This algorithm differs from the snapshot model, because it is not necessary for the agent to match the landmarks. Indeed, a single direction is directly computed from the set of landmarks. This model is therefore not based on a correspondence method, but rather needs a compass to align the directions to the landmarks in the world coordinate system. There are several other models proposed by roboticists that rely on certain parameters of landmarks, such as their contours [117], colours [73], or corners [179] to explain local homing.

1.5.3 Holistic strategies

A model can be considered holistic to varying degrees. In our approach, a holistic model uses a visual feature, such as a colour value, to characterise the entire environment. But importantly, without segmentation into individual objects. Following the colour example, if only one colour

is to be used e.g blue, the visual environment would be then remembered as shades of blue, dismissing other colours and putting emphasis on blue patterns; consequently, this representation could be memorized for later return. To allow homing, it is necessary to make a global comparison between the stored holistic view and the current view. As no landmarks are used for homing, it is therefore necessary to align the views by using a compass, but details on the need for a compass are explained more thoroughly in chapter 2 of this thesis.

In an holistic strategy, the view stored in memory, can be described as a **2D panoramic snapshot** with the horizontal axis of the image being the eye azimuthal axis and the vertical axis its elevation. There is a multitude of information that can be encoded in a panoramic snapshot, for example, **brightness**. It has been demonstrated that brightness or intensity values contain effective information to potentially direct an insect to its goal, even in a natural scenario where no distinct landmarks are available [203]. While moving, the insect is directed to the location where the difference between the brightness snapshot taken at the nest site and the current view is minimized. Indeed, when this difference is calculated at several locations sampled around the nest entrance, it increases steadily as one moves further away from the nest. Therefore, ideally, the insect can simply move towards the minimum difference.

Two other kinds of visual information that may be contained in a panoramic snapshot are the skyline and the depth structure of the environment. In short, the **skyline** is the border between the landscape and the sky. A separation between the sky and the landscape is computationally simple and available directly eg. through the UV-green contrast [163]. Due to the absence of post-processing and the omnidirectionality of the skyline, this method is classified as holistic. The use of the skyline for homing is a promising approach, because it is invariant to a rotation of

the snapshot that is often imposed by movements of the animal, especially in the case of flying insects [164].

Depth-information can also be obtained from vision, more precisely, from the optical flow. In short, during translation, objects in the immediate vicinity of the observer move more rapidly over the retina than more distant ones, a phenomenon called **motion-parallax**. Accordingly, the retinal displacement of a near object will be larger than the apparent-motion of one placed further away. Motion-parallax is obvious to human observers when viewing the landscape while driving on a highway: trees along the road disappear quickly from our field of view, while a distant farm remains in view much longer. Evidence for the use of information derived from optical flow has been obtained in studies on honeybees: they can retrieve their feeder even if indicated by camouflaged landmarks alone, these being only distinguishable during translational flight manoeuvres. As a result, the insect most likely stores distance information about such camouflaged objects, since brightness or skyline cues are not available in this scenario. Therefore, flying hymenopterans may be able to store snapshots based on optic-flow-induced depth information relative to the observer [56, 57, 107, 46].

Different types of OF snapshots have been proposed by Vardy and Möller 2005 [178] to be used for a guidance strategy. Here **differential-OF** techniques are employed, which are based on the intensity information of an image and not on depth-information. Indeed, OF can also represent the pattern created by the apparent motion and velocity of brightness patterns in the image [82]. There is evidence that such an OF model can reproduce the homing behaviour of locusts in an artificial arena [109]. It is rather difficult to classify such a model as holistic or non-holistic since each region of the image is considered a landmark; so it is necessary to establish a correspondence between them ([178], Fig 1.4).

All these models are based on different techniques to provide the insect with a direction in which it should move during homing. However, in bumblebees, unlike ants that stop several times and scan their visual environment when following a route [197], there are no good behavioural data available showing how bumblebees may actively shape their behaviour and flight pattern to move into the direction given by one or more of these vision-based homing strategies.

1.6 Conclusion

Insects are remarkable navigators that use a variety of strategies and senses to move from one place to another: for example, they can follow a pheromone trail or the information provided by a compass, but they rely mainly on information about their visual environment. Insects like bumblebees have compound eyes with an almost omnidirectional field of view, which allow them to perceive nearly their entire environment but with a low resolution. Both of these characteristics make vision to be the preferred sense in many navigational tasks [115, 194], especially when returning home. Returning home is a very important task for the survival of social insects. Therefore, understanding how an insect, such as the bumblebee, learns information about the visual surroundings of its nest and how it uses this information to return home, lead to many hypotheses which must take into account the computational abilities of an insect and the feasibility of the chosen strategy in its environment. To better understand all these issues it is important to gain knowledge

on how bumblebees actively shape their behaviour in the context of the challenging task of local homing.

1.7 Thesis Outline

With all this terminology in mind, I can now introduce the framework for my thesis. This work attempts to unravel some still open problems about the visual guidance strategies used during local homing of *Bombus Terrestris*. I focus on two specific phases of homing: (1) the late phase of the return journey, when the bumblebees arrive in the vicinity of their nest, trying to locate their almost invisible nest-entrance, and (2) the very early phase of outbound flights, i.e. when they leave their nest for the first time performing a learning flight.

The first two chapters will be devoted to the return journey. In chapter 2 of this thesis, I analyse some of the different visually-based local homing strategies, these being holistic or not. I combine behavioural analysis and computational modelling. In an indoor arena, where bumblebees had to return to their nest from a feeding chamber outside the test arena after their visual environment was altered, I could identify a visual guidance strategy, which predicted the location where bumblebees searched for their nest. This strategy requires bumblebees to remember several holistic panoramic views taken around the nest location as they leave it and relying on both contrast and depth-information.

Chapter 3 is a more detailed analysis of the behaviour expressed by

bumblebees in the paradigm used in Chapter 2. I focus on characterising the search behaviour over time and altitude (i.e. changes in flight altitude) that bumblebees perform to find their nest. These two aspects are often omitted in conventional analyses. Based on this analysis, I suggest a novel hypothesis about the functional importance of change in height, especially in the context of local homing when the bumblebee needs to search for the nest-hole if the local homing mechanism fails to guide the bee toward it after the environment had changed compared to the learning situation.

In Chapter 4, I scrutinise the choreography of learning flights and the orientation of the bumblebee's head in space in a indoor scenario different from the one used in the previous chapters. By monitoring the head and, thus, the eye movements of bumblebees at an unprecedented spatial resolution I analysed how bumblebees shape the optic-flow-based depth-information through an active vision strategy. Then I discuss the potential consequences of this active-vision strategy on the subsequent return flights, particularly using the homing-strategy identified in the previous chapters as sufficient to account for my experimental results.

Finally, concluding remarks on the whole of this work will be given in the last section.

2 Comparative study of visually based homing models during visual conflict

2.1 Abstract

Returning home is a crucial task accomplished daily by many animals, including humans. Insects like bumblebees or ants are good study models to discover efficient navigation strategies used to go back home. When they arrive in their nest surroundings, most of them are known to rely on learned visual information to pinpoint their nest entrance. Therefore, in the last decades, many hypotheses have been raised to explain the challenging task of visually-guided local homing. These hypotheses are often simplified, making them plausible to be used by the small insect brain. These hypotheses have often been tested in a scenario where no ambiguity about the home entrance existed; thus, several of them were shown to replicate the homing behaviour of insects. In this study, to be able to compare the validity of these visually-based strategies systematically, we used a paradigm creating ambiguity about the home entrance with respect to the learned visual cues. Thus, we could compare the different models' behaviour with the behaviour of insects. We trained bumblebees of the species *Bombus terrestris* in a specific visual scenario, which

during tests, was altered, to set the visual cues into conflict. The homing models were expected to predict the locations where the bumblebees searched for their nest during return flights. From our results, we were able to pinpoint characteristics affecting the models' prediction: such as remembering multiple holistic views of the surroundings at different locations, the location of these views in respect to the nest entrance and local landmarks, and finally the encoding of distance information. From these characteristics, we could develop a complementary and biologically plausible hypothesis to the pre-existing ones, using views encoding distance information derived from the optical-flow.

2.2 Introduction

RETURNING HOME, often termed homing, refers to the process of navigating from a location, such as a food source, to the home surroundings. In the animal kingdom, even tiny invertebrates, like some insect species, accomplish this complex task. Insects cover vast distances to collect food, but they can return to their home surroundings by using and combining different navigational strategies. They can follow a visually familiar route [74, 193], a scent trail [49, 37], or combine directional information from a compass (e.g. polarised light [93], sun or moon position [97, 182]) with the distance travelled, i.e. the path integration [123, 184]. In ground-nesting Hymenopterans, when the insect finally arrives in the familiar surroundings of the home location, its nest entrance

remains mostly inconspicuous from the outside. To pinpoint its entrance, the insect performs a specific behaviour called “local homing”.

During local homing path integration is a possible source of information, but its indication at this point of the journey might be imprecise due to the accumulation of noise [32, 33, 196, 7, 80]. In addition, in flying insects, the imprecision of path integration might be even more considerable, due to external factors like the wind [177]. Hence, during local homing, ground-nesting hymenopterans rely mostly on sensory information such as visual, olfactory, or tactile cues [170, 142, 18, 22, 21, 152]. Vision is one of the most used modalities by a wide range of navigating insects, making this sensory modality a pre-dominant and essential tool for local homing [36, 38, 199].

Despite its importance, many questions about the visual information used during local homing remain open. Indeed, the visual cues surrounding an insect nest can be dense and inconsistent (e.g., shadows on the ground that may change over the day [201]), making the visual surroundings a complex source of information. Hence, which information the small insect brain stores and how it uses it later to return home, is a question not only biologists tried to answer, but also roboticists, aiming to build autonomous agent. Accordingly, they proposed visually based homing models allowing for low computational costs as permitted by an insect brain [203, 56, 95, 55, 125, 178]. These models can home by using different visual cues stored in their memory (e.g. a panoramic snapshot [203], bearings of visual landmarks [95]), and could replicate some successful local homing behaviours, making them plausible hypotheses to visually-guided homing.

To disentangle these visually based homing models in the context of local homing, we conducted behavioural experiments with bumblebees,

Bombus terrestris, and compared their behaviour to the performance of different models. We trained bees to find their inconspicuous nest entrance in a compass-free environment simplifying an outdoor scenario. To help their return, we provided them two constellations of visual landmarks, both indicating the nest-hole location. To assess how bumblebees used these visual cues for local homing, we recorded return flights of bumblebees from a food source to their nest-hole, after the cues were displaced. We tested for several degrees of visual conflict between the different landmark constellations and analysed where the bumblebees would search for their home. Then, we tried to account for the experimental results by simulations of visually based homing models.

By using this visual conflict paradigm, we could systematically challenge the different models by only changing the visual input but not the nature of the cues. Therefore, this simple paradigm is an excellent tool to distinguish between the explanatory power of different homing models, and eventually unravelling the mechanisms underlying visual homing.

2.3 Materials and Methods

2.3.1 Experimental design

We used three healthy hives of *Bombus terrestris* provided by Koppert B.V., The Netherlands. The bees had direct access to pollen in the hive. The hive was connected with a transparent tubing system to a large cylin-

drical flight arena (of 75 cm radius and 90 cm height) (Fig 2.1A). The bumblebees entered the arena through a 1 cm hole in its ground. The entire arena floor was covered with small wood chips to hide the nest-hole efficiently; they were frequently shuffled around to avoid bumblebees to use potential odour cues set by others. The arena was covered with two acrylic plates (not present in Fig 2.1A) to prohibit the bees from escaping the flight arena. The arena wall was divided into a bottom part of 80 cm height, which could be rotated around the vertical axis of the arena, and an upper part of 10 cm height, which was fixed (Fig 2.1A). The bumblebees could leave the arena and access a foraging chamber through a 1.5 cm diameter hole in the fixed part, where feeders presented them a sweet aqueous solution (a mixture of 30 % saccharose and honey drops).

In the flight arena, two constellations of visual cues were provided to the bumblebees. The first constellation consisted of 3 black cylinders (15cm height and 2 cm diameter each), arranged at a distance of 10 cm around the nest-hole. The second was a pattern of three red stripes on the white wall of the flight arena (80cm height and 12cm width). These background stripes were asymmetrically arranged, with two of them placed next to the nest-hole (Fig 2.1B). The bars were red for tracking purposes (bumblebees are not sensitive in this spectral range and would perceive them as dark [155]). A white mesh cloth covered the ceiling of the room to restrain access to external cues (Fig 2.1A).

A bumblebee flying from the foraging chamber back to the hive was recorded by two synchronized high-speed cameras (Falcon2 4M, Teledyne DALSA, Inc.) with a resolution of 2048*2048 pixels at 74 frames per seconds. The two cameras were viewing the set-up at different angles, giving a top view and a tilted view of the arena. Ten LEDs (OSRAM, 350 lm) mounted on a wooden ring above the cylinder illuminated the

arena, and 16 paired neon tubes (Biolux 965, Osram, Germany) arranged symmetrically in the room served as additional light sources.

We started the recordings as soon as a bumblebee entered the flight arena. Recordings lasted up to 5 minutes or until the bee found the nest entrance. From the two calibrated cameras (Matlab toolbox DLTdv 5, Hedrick's lab), we tracked the position of the bumblebees with a custom-made Python script, based on OpenCV. The videos were then manually reviewed with the software IVtrace (`https://opensource.cit-ec.de/projects/ivtools`), so the bee's position and orientation could be manually corrected in case of a tracking error.

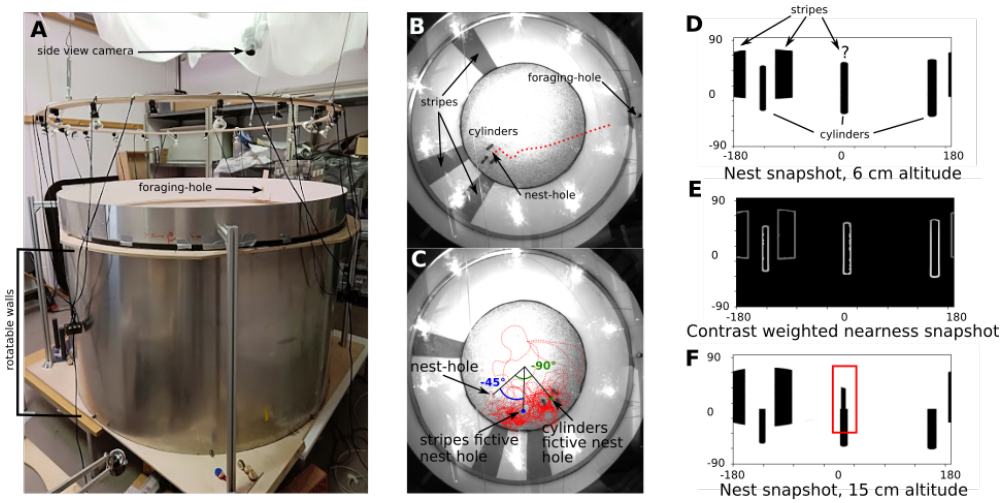

Figure 2.1: Experimental set-up: A: Photography of the experimental set-up composed of a cylindrical flight arena, a suspended ring holding part of the lighting, and a white mesh covering the camera holders (only side camera visible in picture). B: Training condition, image from the top view camera during recording, with two of the three stripes on the arena wall placed behind the nest-hole and three cylinders placed around the nest. Overlaid trajectory, red dotted line, of a return flight during the training phase. C: Picture of a test condition, cue conflict condition -45/-90; the cylinders' fictive nest, green circle, is placed at an angle of -90° from the nest-hole viewed from the centre of the arena, then the stripes' fictive nest, blue circle, at -45° from the nest-hole. The picture is overlaid by one sample trajectory corresponding to the cue conflict condition (red dotted lines). D: Nest snapshot, equirectangular projection of the simplified bee view, taken at 6 cm above the nest-hole location in the simplified rendered environment. Note that the third bar is occluded by one cylinder. E: Image of the contrast-weighted nearness nest-snapshot in the rendered environment at 6 cm altitude. F: Nest-snapshot at an altitude of 15cm. The third bar is now only partly occluded.

2.3.2 Training and test procedure

We let the bees exploring the set-up for three days in the arrangement shown in Fig 2.1B. Bees could fly only between 7 am and 7 pm; then

the lights were switched off to reproduce a naturalistic day-night-cycle. After this exploration and learning phase, relatively straight trips from the foraging chamber back to the nest entrance could usually be observed (Fig 2.4A & Fig 2.1B). To test how the bees behaved under a visually conflicting condition, we trapped at least 5 foragers while these were feeding in the foraging chamber. Then, while all other bees were constrained in the hive, the two types of visual cues in the flight arena were put into conflict by rotating the wall and displacing the cylinders constellation (Fig 2.1C). After this manipulation, we allowed a single bee to re-enter the flight arena from the foraging chamber and recorded its flight. If the bumblebee did not show any attempt to find its nest (i.e., never flew close to the ground as they usually do when searching for the nest) the video was not analysed. A searching bee had up to 5 minutes to find back to its nest. If it did not find the nest in this time interval, it was caught and placed manually back into the hive. The experiments were performed in the late morning for approximately two hours until all the trapped bees were tested. Then, the training condition was set back, so bees could fly in the non-conflict situation (Fig 2.1B) until the next day set of experiments.

Several conditions were tested, all shown in Fig 2.4. Test situations would create two fictive nests at different locations if either one or the other type of cue (stripes or cylinders) determines the location of the nest entrance. The nomenclature for the different conflict conditions is based on a pair of numbers and a third number (e.g. 90/-90, 180°). The first number indicates the angle as seen from the arena centre, between the real nest hole and the fictive nest determined by the cylinders, and the second one, the angle between the real nest-hole and the fictive nest determined by the stripes. The third number indicates the directed conflict angle between the two fictive nests. In total, 12 cue-conflict conditions were tested.

2.3.3 Behavioural analysis

During the 5 minutes test, bumblebees usually flew at low altitudes in the arena searching for their nest-hole in the ground. We first estimated at which altitude bumblebees spent most time by analyzing their distribution along the arena z-axis (i.e. the altitude axis) (Fig 2.2). We observed that bumblebees spent 75 percent of their time at flight heights below 20.63cm. Hence, an upper threshold of 20.63 cm was used to exclude behavioural sequences not related to the search for home. Besides, we used a lower limit of 3cm to exclude the walking behaviour of the bumblebees, since we focus only on flying behaviour more representative of their natural behaviour.

To investigate where the bumblebees flew searching for their nest according to the two types of cues, we estimated the probability density function of the bee's location, along the x and y-axis of the arena (with z between 3cm and 20.63 cm) by a 2D kernel density estimation (KDE, Python library Scipy.stats). The KDE bases its estimation on a smoothing parameter (estimated here thanks to the Scott's rule [127]) (see results Fig 2.4). Because some bumblebees find the nest in less than five minutes, we normalized the distribution for each flight, expressing the location distribution as a proportion of the time spent in the arena. Finally, these results were pooled across bees for each condition to ease comparison and normalized to account for different numbers of tested animals between conditions.

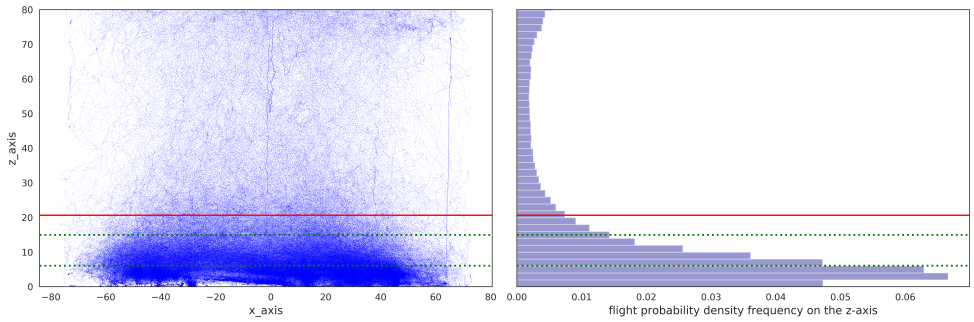

Figure 2.2: Overall spatial distribution of all flights of bumblebees in the arena under cue-conflict conditions. A: representation of all the flights obtained under cue conflict conditions (n=107 flights) along the x-axis and z-axis inside the arena. The bee's position at each point in time is represented as a blue dot. The red line represents limit where 75% of the behaviour is happening along the z-axis. The two green dotted lines are the two altitudes for which a set of images has been taken from the perspective of a bee (6cm and 15cm). While searching for the nest-hole in cue conflict situations bumblebees fly relatively close to the ground. Nevertheless, numerous data points are visible at higher altitudes; this is due to bumblebees giving-up on searching or colliding with the perspex lid at 90 cm above the ground. Vertical paths can be due to a bee falling from the entry hole or crawling up one of the bar since their texture offered some grip. B: Histogram representing the frequency distribution of flights along the z-axis. Overlaid with the same limits as in A.

2.3.4 Homing Algorithms

Simulated bees, later called agents, using a visually-guided homing mechanism need to gather information about the visual environment. Therefore, we rendered a simplistic version of the set-up in a graphic software (Blender, Version 2.79). This simplistic version takes into account only potentially relevant visual cues, i.e., the arena wall with the stripes and the cylinders. Thus, the entrance to the arena from the feeding chamber and the nest-hole were not modeled to focus the model comparisons only on the conflicting cues (Fig 2.1D). Consequently, some cue-conflict

conditions were visually identical inside the rendered arena (e.g., cylinders/stripes: 45°/-135° and 90°/-90°), reducing the set of conditions to be tested to only seven (Fig 2.6). From the rendered arena, we took a series of panoramic images oriented along the x-axis (i.e. with the azimuthal null viewing direction along the x-axis of the arena), spaced on a grid by 2 cm, making a total of 7211 views. Since bees flew for most of the time below 20.63 cm (see above), the rendering procedure was done on two grids at different altitudes: 6cm (approximating the median value), and 15 cm (the mid-altitude of the fourth quantile)(Fig 2.3B). The gathered images are equirectangular panoramic snapshots (-180 to 180° in azimuth and -90 to 90° in elevation, with a resolution of 1px per degree) supposing the eye of the agent to be spherical. Based on these sets of rendered images, five different vision-based homing algorithms were tested. Besides, an additional homing algorithm based on explicit knowledge of the cue positions was tested (Fig 2.3B, Table 4.1). All homing algorithms used the memorized representation of the training condition (Fig 2.1B&D), i.e. the situation without cue conflict.

Figure 2.3: Schematic of the different tested models. A: Average landmark vector (ALV); the stored vector in the memory is the ALV at the nest-hole location (red arrow). The $\vec{ALV}nest$ is the average of each landmark vector ($\vec{LV}$) at this location (grey arrows).The ALV at the current location is calculated in the same manner (blue arrow), and the $\vec{ALV}nest$ is subtracted to this one. The result is the home vector $\vec{HV}$ represented with a green arrow. B: the gradient -descent model based on the image rotational difference function (rotIDF); the minimum rotIDF is calculated at each grid position, the potential obtain is plotted on a downsampled grid and a colormap (from black minimum to white maximum). The agent descent the potential; thus, move in the direction of the darkest neighbouring point of the grid. The current-view is overlaid with the rotIDF (blue line). The nest snapshot stored in memory shows a 0 minimum in its rotIDF at the middle of the image i.e. 0° orientation. Important: the value of the rotIDF's minimum at the current location, is the only information used to create the potential. To note, the minimum rotIDF value on the represented potential is not null at the nest due to the downsampling of the grid for illustration purposes hence, not falling below the exact nest location, where this one is indeed null. C: The multi-snapshot model. 4 views, constituting a set of view, are taken outside of the cylinder constellation on a 15 cm radius circle. Each view is overlaid by its rotIDF function with the current-view. Each view refers to a heading direction of the same colour (red, blue, yellow and grey). The green arrow represents the weighted circular average of all headings, it is the $\vec{HV}$. D: The multi-snapshot model based on contrast-weighted-nearness (CwN) views. 4 CwN-snapshots at 15 cm from the nest are taken. Each view is overlaid its similarity function with the current view, leading to different heading directions (coloured arrows). The weighted circular mean of those different headings is the green arrow indicating the $\vec{HV}$ direction.

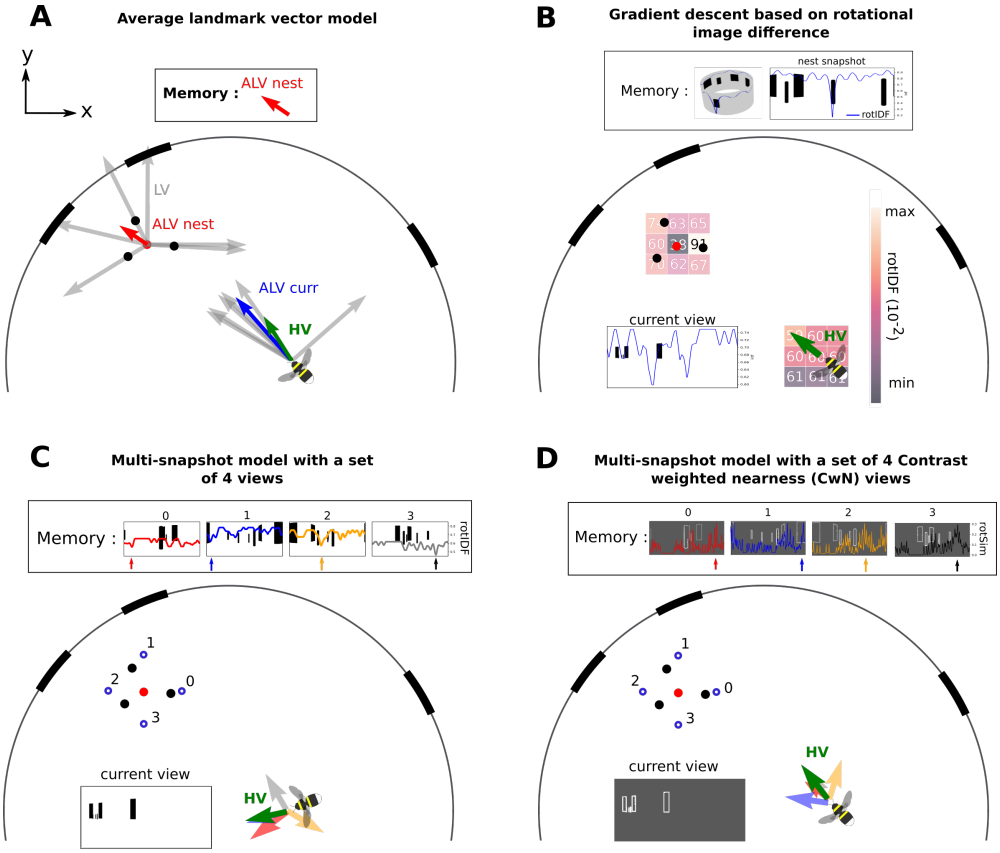

(Legend on previous page)

Models need to rely on a memory encoding for visual information linked to the home location to perform visual homing. In addition, they also need a method to compare this memory with the actual surroundings when returning home. This method leads to a home vector encoding for the home direction (argument) and its certainty (magnitude). We calculated the homing vector at each grid location to know the agent direction anywhere in the arena. Consequently, each model yields a vector field in the arena. In the following paragraphs, we describe the different models investigated in this study.

The Average Landmark Vector

To accomplish homing, the agent used as visual information the bearing of visual landmarks on its retina: in our case, each of the three cylinders and each of the three stripes. Each bearing led to a unit vector, thus, not encoding for distance information, called a landmark vector ($\vec{LV}$) (Fig 2.3A). From these 6 $\vec{LV}s$ the agent calculated their average: the average landmark vector ($\vec{ALV}$). The $\vec{ALV}$ at the nest location was the vector kept in memory by the agent. The home vector ($\vec{HV}$) was the difference between its current average landmark vector at its location ($\vec{ALV}_{curr}$) and the memorized one ($\vec{ALV}_{nest}$). This model requires an external compass to perform meaningful vectors calculations based on an x-y coordinate system. Thus, for the simulation, a perfect compass aligned with the grid indicating for the x and y-axis was used.

Gradient descent based on Rotational Image Difference function (rotIDF)

For this model (Fig 2.3B), the agent used the brightness contained in panoramic views as visual information. These views were segmented in pixels but are not subject to additional segmentation; thus, the agent used the environment as a whole (i.e., holistic [203]). The agent memorized a panoramic view taken at the goal location to later home. Then, the agent used the difference between its current view and the memory to compute the home vector at all grid locations. But, determining the image difference is not an easy task; for example, two panoramic images acquired in different orientations but at the same location yield high differences. However, to solve this issue, one can rotate the first image against the other until the difference is null. Consequently, the two images are now aligned. Therefore, in a compass-free environment like ours, an agent not

knowing its orientation could rotate to minimize the difference between its current view and the memorized view; this is the minimum of the rotational image difference function (rotIDF). This could relate in nature to ants stopping and scanning the environment on the spot before deciding where to go [200].

The minimum rotIDF, described by equation (1) is the minimum of the square root of the average difference between the rotated current view ($I_{x,y}$ of axis u azimuth and v, elevation) for different azimuthal orientations, α, and the nest snapshot (I_N). This calculation is also called the root mean squared difference (r.m.s) [203] (2.1). This formula needed to be adjusted due to the distortion on the views caused by the reprojection of the environment from a uniformly sampled 3D sphere, mimicking a bee's view, back to 2D equirectangular images. This distortion creates an oversampling at the poles. Consequently, a different weight, w, is applied to the image depending on the pixels' retinal position along elevation. This weight is given by a sine function along the image y-axis with a wavelength $2N_v$, resulting in a weight of 1 at the equator, and 0 at the pole as described in equation (2.2) [56]. In this way, the pixels' values close to the poles have less weight for the computation. We add this weighting function (2.2) to the rotIDF formula (2.1).

Therefore, the agent could now descent the gradient forming a vector field of home vectors, derived from the potential encoding the minimum rotIDF between the current view and the memorized view (Fig 2.3B).

$$d_{x,y} = \min_\alpha \sqrt{\frac{\sum_{u,v} w(v)(I_{x,y}(u+\alpha,v)-I_N(u,v))^2}{N_u \sum_v w(v)}} \tag{2.1}$$

$$w(v) = \sin(\pi(v+0.5)/N_v) \tag{2.2}$$

Brightness Multi-snapshot model

The agent used the brightness of panoramic views as visual information. It memorized several panoramic snapshots s_i, constituting a set of view $S = \{s_0; s_1; \ldots; s_n\}$, located around the nest location. In the model, each snapshot was oriented toward the entrance. In nature, ground-nesting insects perform a learning choreography around their nest-hole, during which they may collect views oriented towards the nest thanks to path integration [69, 124], or the ability to visually track the nest-hole at short distances [146]. When returning to its nest, the agent followed a homing vector calculated from the four rotIDFs between its actual view s_{curr} and each memorized view in S. Therefore, a different heading direction at each grid location x, y was determined for each snapshot Eq. (2.3) based on the rotIDF. These headings were then weighted by the ratio between the minimum rotIDF (as computed in (2.1)) of all snapshots s_i in S_{dmin} (2.4) and the rotIDF of this one, d_{s_i}, as described in Eq. (2.5). Finally, the homing vector $\vec{HV}$ was the weighted circular mean of the different heading directions h_{s_i},(2.6). The homing vector depends on the set of memorized views; for example, the number of views in S or their locations may affect the homing performance [55]. Therefore, we used different sets of views S. The different sets consisted of either 4 or 8 equally spaced views taken at two distances from the nest-hole; at 5 cm (inside the cylinders constellation) or 15 cm (outside the cylinders constellation) (Fig 2.3C).

$$h_{s_i,x,y} = \text{argmin}(\text{rotIDF}(I_{x,y}, s_i)) \tag{2.3}$$

$$S_{dmin} = \min_{S}(d_{s_i,x,y}) \tag{2.4}$$

$$w_{s_i} = \frac{S_{dmin}}{d_{s_i,x,y}} \tag{2.5}$$

$$\vec{HV} = \arg\left(\sum_{S} w_{s_i}.exp(h_{s_i,x,y}).i\right) \tag{2.6}$$

Gradient ascent based on Contrast-weighted Nearness (CwN)

The agent used views encoding for the depth and contrast of the environment to perform its homing: contrast-weighted nearness views (CwN) (Fig 2.1E & Fig 2.3D). The CwN map is calculated based on the Michelson contrast, i.e. the ratio of the luminance-amplitude ($I_{max} - I_{min}$) and luminance-background ($I_{max} + I_{min}$) within a 3x3 pixel window on the view. Then, the contrast was weighted by the inverse of the distance (nearness), obtained from the environment's spatial layout. Similar to the brightness-based model, the agent memorized the panoramic CwN view at the nest location. When returning home, the agent ascended the gradient of homing vectors following the maximum similarity between the CwN view at each grid point and the memory.

The CwN map encodes distance information. In nature, an insect gains distance information during translational movements through the array of elementary movement detectors (EMDs, for review [61]). The CwN acts as an approximation of the response profile of the insect's retiniotopic arrays of EMDs, as suggested by simulations [149, 102]. We applied the formula described by Dittmar et al. 2010 on each CwN grid-views (x, y) to calculate the rotational similarity function (rotSimF) be-

tween the current CwN view and the memory (2.7). The similarity is the correlation coefficient between the nest view (I_N) and the current view ($I_{x,y}$). As for the rotIDF, we assumed the agent to be able to internally rotate its current view to compute the best similarity value.

$$\mathrm{sim}_{x,y} = \max_{\alpha} \frac{\sum_{u,v} w(v)(I_{x,y}(u+s,v)).I_{\mathrm{N}}(u,v))}{\sqrt{\sum_{u,v} w(v)\mathrm{I}_{x,y}(u,v)^2}\sqrt{\sum_{u,v} w(v)\mathrm{I}_{\mathrm{N}}(u,v)^2}} \tag{2.7}$$

Contrast-weighted Nearness multi-snapshot model

The multi-snapshot model based on brightness views, as described above, was adapted here for CwN views and the rotSimF, hence, the memory was a set of CwN views $S = \{s_0; s_1; ..; s_n\}$, where $s_i = CwN(x_i, y_i)$. Here, the agent followed an homing vector at each grid point computed by the weighted circular means of each headings of the CwN views in S (Fig 2.2D).

2.3.5 Description of the Homing algorithm behaviour using the Helmholtz-Hodge decomposition

From the vector fields (gradient) obtained by the different homing models, we wanted to infer where the agent was most likely to end its journey, this can be found by studying where the vectors converge. We obtained the convergence of the vector field by decomposing this one into two components using the Helmholtz-Hodge Decomposition. The component of interest here is the curl-free component, i.e. the divergence of a potential ϕ [11, 2]. This potential can be seen as basins, valleys, and summits: thus, we can conceive the agent as a fluid flowing from summits down to basins

Visually based homing models List					
Model name	Requires compass	Holistic	Memory	Visual cues	Comparison method
ALV	yes	no	one vector	landmark bearing	vector substraction
Gradient descent (brightness)	yes	yes	panoramic snapshot	brightness values	rotIDF
Gradient ascent (CwN)	yes	yes	panoramic CwN snapshot	distance and contrast	rotSimF
Brightness multi-snapshot	no	yes	several panoramic snapshots	brightness values	rotIDF
CwN multi-snapshot	no	yes	several panoramic snapshots	distance and contrast	rotSimF

Table 2.1: Main criteria distinguishing the different tested models: the need for a compass, the type of cue, its holistic nature, the memory and the mechanism used for comparison between the current visual information and the memory. CwN stands for the contrast of the image weighted by the nearness, rotIDF for the rotational image difference function and the rotSimF for the rotational similarity function.

(Fig 2.5A). We described the agent's homing behaviour for each model by the topology of its potential, following this analogy the landscape was split along the z-axis at different levels, i.e. isohypses. The different isohypses are shown with overlaid contour lines on (Fig 2.5A). The highest isohypse surrounds a summit and the lowest a basin. Basins correspond to areas where the agent is homing. The creation of basins gives additional information like the size of the region of convergence; thus, by using the Helmholtz-Hodge Decomposition, we could directly compare search areas, where the bees spent most of the time looking for their nest, with the basins' locations and shapes (Fig 2.6).

We ran the Helmholtz-Hodge Decomposition on each vector field for all homing models and then scaled the obtained potential between 0 and 1 (Fig 2.5A).

2.3.6 Quantifying the models predictions

The models gave predictions on where the animal may search for its nest, i.e. the basins' locations. Thus, we need to compare the basins' locations to the behaviour of the bees, i.e. the search areas.

We defined search areas as regions where the probability density distribution of the bumblebees' location was above a certain threshold. This behavioural threshold was set at a third of the the probability density function's maximum for each condition, splitting the areas between high probabilities and low probabilities of observing a search. Similarly, the homing landscape was split between values above and below 0.15, where the models are more likely to converge, corresponding to a basin. The homing landscape was split between search prediction and non-search prediction (respectively, the behaviour was split between search behaviour

and non-search behaviour). From these predictions and observations we built a confusion matrix (Table 4.2). From the confusion matrix, we calculated an accuracy measurement, the F1-score, of each model prediction Eq. (2.8 to 2.10). The F1-score gives a good metric to check the accuracy of the models without ignoring the costly impact of false positives and negatives. Indeed, we consider false positives (fp) costly since the agent searches at a wrong location, which could theoretically impair its homing, besides, false negatives (fn) show that the prediction fails to describe the full behaviour.

The isohypse used to define the prediction areas is an important parameter, indeed, the lower the isohypse is set, the smaller the predicted search area gets. Consequently, we systematically varied this one between 0.1 and 0.29, and studied its impact on the F1-score (F1-score when varying the model prediction isohypse). We compared the different models' F1-score over a varying threshold for each condition using a Kruskal-Wallis test (because our data are not normally distributed), followed by a pairwise comparisons using Dunn's test for multiple comparisons of independent samples. Finally, all p-values were adjusted by a Bonferroni correction.

$$precision = \frac{\mathrm{tp}}{\mathrm{tp} + \mathrm{fp}} \tag{2.8}$$

$$recall = \frac{\mathrm{tp}}{\mathrm{tp} + \mathrm{fn}} \tag{2.9}$$

$$F1_{score} = 2.\frac{\mathrm{precision.recall}}{\mathrm{precision} + \mathrm{recall}} \tag{2.10}$$

		Model prediction		
		Search prediction	Non-search prediction	Total
Behaviour	Search	true positives	false negatives	$tp + fn$
	no-search	false positives	true negatives	$fp + tn$
	Total	$tp + fp$	$fn + tn$	N

Table 2.2: The confusion matrix

2.4 Results

2.4.1 Behavioural analysis

Bees fly straight back home in the familiar non-conflict situation (see examples Fig 2.4A). Thus, how do they search for their home when visual cues surrounding their nest have been brought into conflict?

After the two cue constellations formed by the stripes and the cylinders have been moved (i.e. visual conflict), bumblebees entering the flight arena from the feeding chamber, fly towards the ground and start searching for the nest-hole. Their dedication to go back home is reflected in the flights' height distribution in the arena (Fig 2.2). Interestingly, most bumblebees do not continuously search for their nest-hole during the entire 5 minutes intervals. They sometimes fly at higher altitudes or against the transparent ceiling of the arena.

Where do bumblebees look for their nest when the different cue constellations indicate two different nest entrances? For a given condition

most trajectories show similar search locations, but some variability is visible (Trajectories examples and illustration of the behavioural variability). This variability is expressed by the time spent searching, and the area of the search. Therefore, to account for these differences, and to get an idea on the overall behaviour under the different conflict conditions, we looked at the probability distribution of the bumblebees' location in the arena (Fig 2.4). The bumblebees spend most time in restricted areas around the different fictive nest-holes locations, corresponding to the two types of cues. In a few cases, we observe that they fly in the direction of the third stripe. (Fig 2.S.1 45/-135). For all conditions, bumblebees search at the stripes' fictive nest location. But, when the conflict between the cue is small, they mostly search at the cylinders' fictive nest (e.g. conditions for 45° and -45° conflict, Fig 2.4B). Thus, the probability density distribution seems to be influenced by the placement of the cues relative to each other.

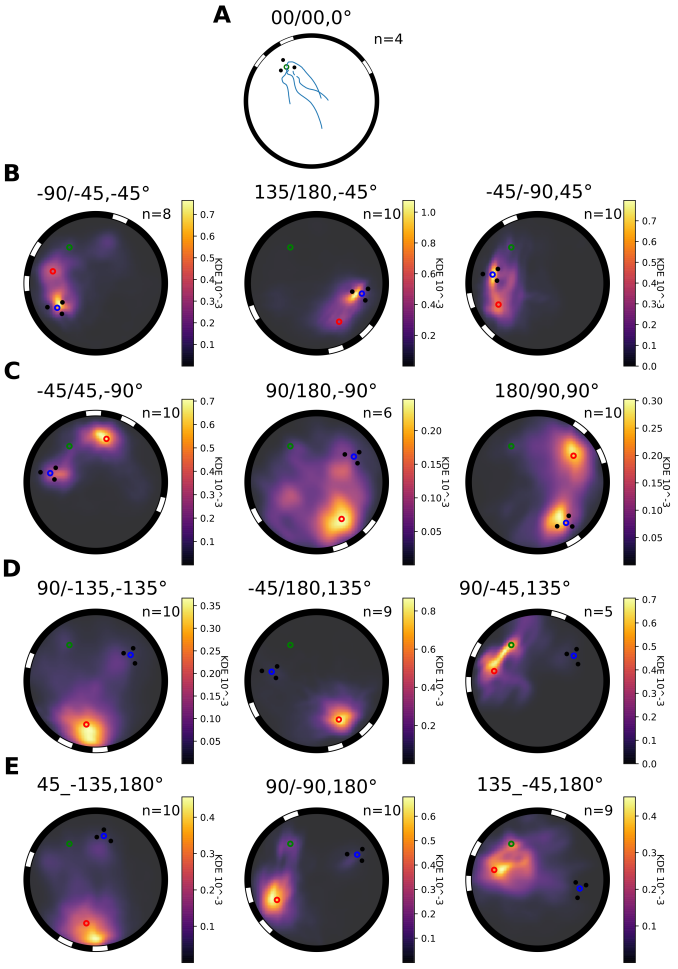

Figure 2.4: Probability distribution of bumblebees' search location in the arena during conflict situations. Each subplot represents the arena with the different cues; the three stripes and the three cylinders, and the corresponding fictive nest entrance; red and blue. The real nest-hole is represented by a green dot. A: the trajectories of bumblebees during non-conflict situation (n=4). For all the other subplots, the colormap represents the normalized KDE of the flights distribution from low density (black) to higher (yellow). The number of flights in each condition is indicated in the corresponding subfigures. Each sub-titles numbers informs about the tested condition: the first number describes the angle between the real nest-hole and the cylinders fictive nest-hole from the center of the arena, the second number informs of the bars' fictive nest-hole location. Finally, the last number describes the directed visual conflict angle between the two cues. B: 45° absolute visual-conflict conditions, C: 90°, D: 135°, E: 180°

2.4.2 Simulations of visually based homing under non-conflict condition

Various homing algorithms have been proposed to explain the behaviour of hymenopterans returning to their nest-hole (see Material and Methods). We investigate in the present study the homing success of these models in our environment (Fig 2.1BC).

Interestingly, not all the models, when looking at their potential derived from their field of homing vectors in the arena, succeed to account for homing during the non-conflict situation (Fig 2.5). Indeed, the lowest isohypse, indicating where the agent is led, does not always surround the nest location (Fig 2.5BCD). The two models (gradient descent based on brightness and gradient ascent based on CwN) using a single snapshot taken at the nest as a memory, show a very flat profile and several basins surrounding locations different from the nest-hole. The only models fitting the non-conflict situation are the ALV and the models using more than one snapshot as memory.

The multi-snapshot model using a brightness based set of views (Fig 2.5C) leads to successful homing only when the snapshots are taken outside of the cylinder constellation. In addition, when this model uses only four views, the lowest isohypse surrounds the centre of the arena, but this one disappears when eight views are stored in memory; therefore, the agent will be driven in the middle of the arena if only four snapshots are used (Fig 2.5AC). Also, when the views are collected inside the cylinder constellation, a basin is formed in the centre of the arena. This basin is still present when a larger number of snapshots are used; thus, the agent will be driven in the middle of the arena in both situations (4 or 8 snapshots) when the views are taken within the cylinder constellation.

Similar observations can be made for the multi-snapshot model based on CwN views (Fig 2.5D). However, four views taken outside of the cylinder constellation were sufficient to produce a basin at the nest location. Oppositely, when the views are taken inside the cylinders constellation, homing vectors drive the agent away from the nest. It suggests that the number of snapshots kept in memory and the cue they encode (brightness or CwN) are crucial parameters for the homing success of the model.

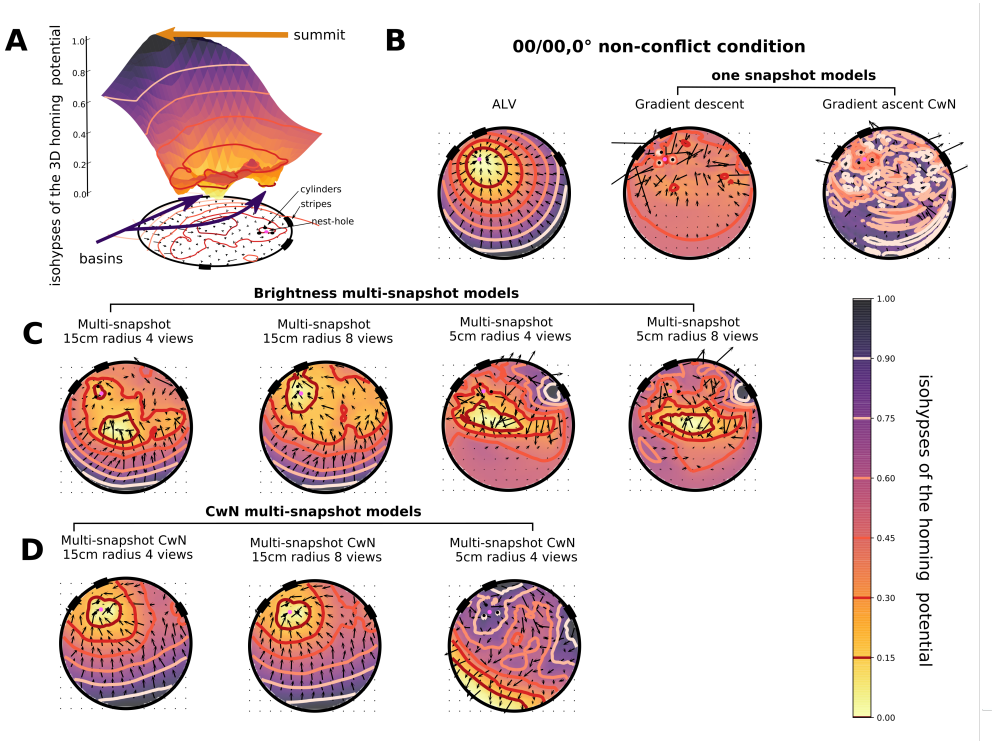

Figure 2.5: Model homing potential during non-conflict situation (condition 00/00,0). A: Helmholtz-Hodge Decomposition 3D profile of the Multi-snapshot brightness model, coloured along the z-axis, from yellow, basins, to black, summits, overlaid with contour lines indicating the different isohypes of the profile. Levels are projected on the ground with the schematic of the arena at the 00/00 condition. The nest-hole is represented by a pink circle. In addition, the vector field from which the homing potential is derived is plotted. B: Performance of the ALV model homing potential and one-snapshot models (the type of model used is indicated above the individual plots), are described by the colormap and the isohypes, overlaid with a vector field encoding for the homing vectors at each grid points. The performance of each model is plotted in the same manner. The yellow of the colormap and the dark red of the contour indicates areas where the vector field is converging. C: Brightness multi-snapshot models, using a set of views constituted of 4 or 8 views taken at 15 cm or 5 cm from the nest(indicated above the plots). D: CwN Multi-snapshot models, based on 4 views taken at 15 cm from the nest, then 4 and 8 views taken at 5 cm from the nest.

The altitude at which the different homing models are tested also influence the homing. At 6cm altitude some of the multi-snapshot models could predict the homing behaviour correctly, but what happens at an altitude of 15cm (see Methods for details)? Only the model using four or more CwN snapshots predicts homing at the nest-hole location in the non-conflict situation (Fig 2.S.3). In contrast, the multi-snapshot model based on brightness images has several basins at a more central place in the arena. This result implies that the agent is likely to end in a location different from its nest.

Overall, the nature, number, spatial distribution and altitude of the views kept in memory does play a role in the homing success of multi-snapshot models during the non-conflict situation.

2.4.3 Bumblebees' homing behaviour versus model performance during visual conflict

We studied the performance of the different homing models during visual conflicts only for the models successful under the non-conflict condition at 6cm altitude, i.e. with a lowest isohypse surrounding the nest-hole.

We expect the different homing models to replicate the search behaviour of the bumblebees during a condition of visual conflict. If bumblebees use similar visual strategies, these models should guide the agent to the locations where the bumblebees search for their nest. All models behave differently to each other during conflict situations. The ALV systematically leads the agent between the two fictive nests, as shown by the vector field of homing vectors and its potential (Fig 2.6B). Hence, it roughly predicts an area surrounding the search location of the bee when the distance between the two fictive nests is small. But in details, during

small cue conflict, the model leads the agent to a location in between both fictive nests, while the bees search primarily at the cylinders' fictive nest and secondly at the stripes' fictive nest. Finally, the ALV model visibly fails to predict the search behaviour when the conflict between the two visual cues is larger than 45°.

For the multi-snapshot model, based on a brightness set of views taken outside the cylinders constellation, (Fig 2.6C) basins form at locations where bumblebees search for their nest. The broad basin located at the stripes' fictive nest fits the behaviour of the bumblebees. However, the predicted basin at the cylinders is not always seen in the behaviour (e.g., -45/180). This result is reflected by an average F1-score close to 0.5 (0.45±0.17) (Fig 2.7). This intermediate F1-score is mostly due to a large number of false-positives predictions (Fig 2.S.5) at the cylinders' fictive nest (e.g., -45/180), or due to the prediction of too large search areas (e.g., -45/45).

Fig 2.6D shows the results for the multi-snapshot models based on a CwN set of views. This model has basins at the two fictive nest-holes. Basins at the stripes' locations are where the bumblebees appear to spend most time Fig 2.6D. In addition, the model does not create too many false-positive search predictions at locations different from the fictive nest locations (Fig 2.S.5). The average F1-score for all conditions, of 0.52±0.15; thus, reflects a slightly better performance than the previous models (Fig 2.7).

We finally wanted to test the robustness of the calculated F1-score by investigating if the selected isohypse, defining the search area of the model prediction, has an impact on this one. For the different conditions and models, it appears that a higher isohypse, thus larger predicted areas, is in general associated with a worst F1-score, except for some conditions

in the ALV model (90/-135, -45/180). In contrast, a lower isohypse, thus, smaller predicted search areas, improves the score of the multi-snapshot brightness model. The impact of this variation on the CwN multi-snapshot model is minor, thus, conclusions about its F1-score are robust to the variation of this parameter.

The quantitative analysis of the performance of the different models versus the bumblebees' search locations, based on varying the isohypse on which the model prediction was selected (Fig 2.S.4), shows a tendency for the CwN multi-snapshots model to give a better prediction of the results for some conditions. Nevertheless, in most cases, this difference is not significant (three significant conditions out of seven: -45/45, 180/90, 90/-15, -45/180: $p>0.5$; 135/180, -45/-90: $p<0.001$, 90/-90 : $p<0.05$, Kruskal-Wallis posthoc Dunn's test, with Bonferroni correction for multiple comparisons).

In conclusion, the ALV does not predict the behaviour, and the two multi-snapshots almost perform similarly; the accuracy of the CwN multi-snapshot model is slightly better in specific conditions.

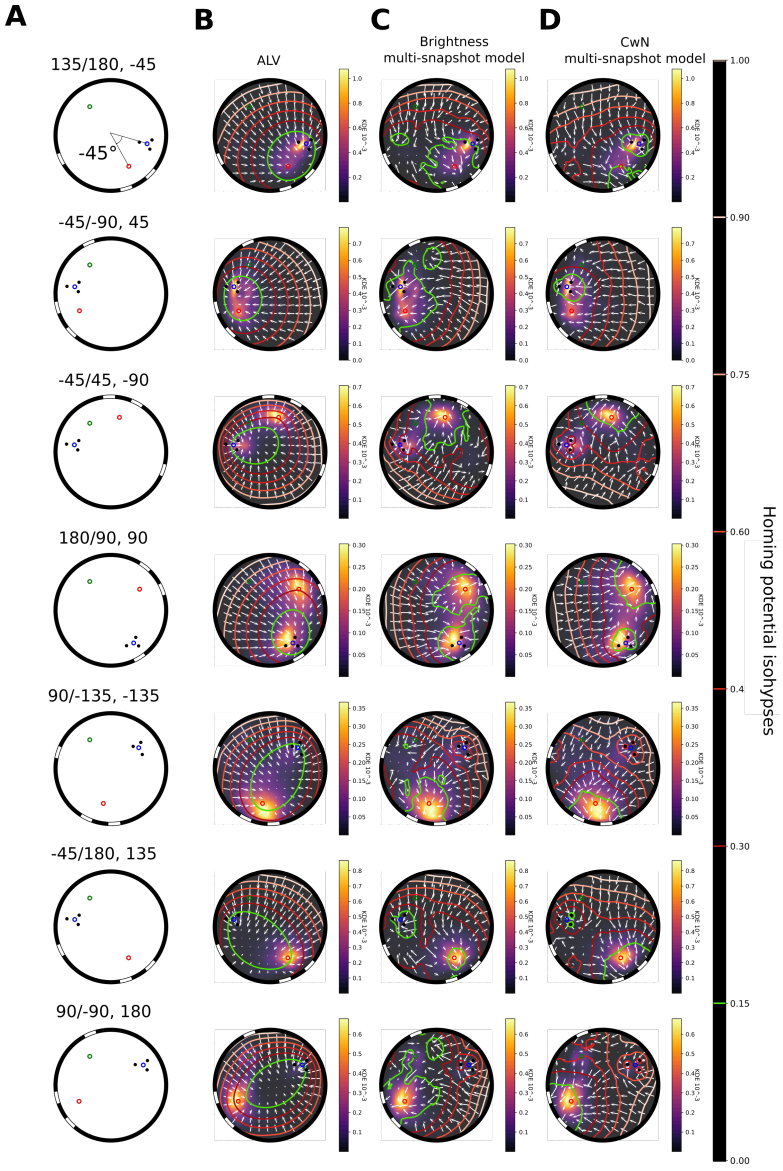

Figure 2.6: Qualitative models and behaviour comparison for different conflict conditions. A: Schematic of the set-up for the different conflict conditions.Columns BCD, The behaviour in the arena along the x and y axis of the arena is represented as a colour coded KDE from dark to yellow. The vector fields of homing vectors for each model is represented on a 8-times downsampled grid by white arrows. Models results are expressed by an homing potential obtain from the Helmholtz-Hodge decomposition represented as contour lines or isohypses. The isohypse at 0.15 is coloured in green then the upper ones are coloured from dark red to white ("summit"). B: The ALV model for the 7 conditions, C: the 8 views Multi-Snapshot brightness model, D: The CwN 4 views Multi-snapshot model.

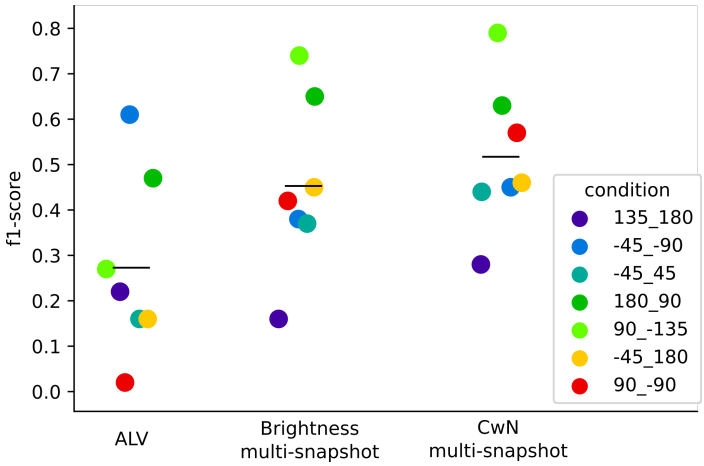

Figure 2.7: Quantitative models and behaviour comparison during conflict situations. Distribution of F1-scores indicating the accuracy of the models prediction for each conditions describe with a colour code. The horizontal black bars represent the mean of the F1-score per model.

2.5 Discussion

Returning home after a foraging trip is, in addition to an innate aspiration for survival, a duty to ensure the colony growth [72]. Therefore, bumblebee foragers are excellent navigators and show astonishing homing abilities. In our study, bumblebees learned to fly back home in an artificial visual environment providing them two constellations of visual cues: small cylinders in the nest vicinity, and a stripe pattern on the arena wall. Our experiments clearly show this dedication to fly back home. During training, our bumblebees flew straight back to the nest. However, after the environment has been visually altered the bees obstinately search for

their home at the fictive nest entrances indicated by the different visual cues. This directed behaviour confirms the critical role of vision in the context of local homing.

During conditions of large degree of visual conflict between the stripes and cylinders constellations, bumblebees mostly searched at the stripes' fictive nest (Fig 2.4), while they often ignored the cylinders. Oppositely, during a small conflict, the bumblebees spent most time searching at the cylinders' fictive nest, but still spent some time at the stripes' fictive nest. The degree of conflict between the two visual cues clearly affects the overall decision to search at one or the other cue; thus, the weight accorded to the stripes and cylinders is not immutable. Therefore, the two cues might not be treated differently by the bumblebees. Indeed, if the stripes and cylinders would be classified upon learning depending on parameters like the nest distance, their retinal size or their number of dimensions (2D or 3D objects) [31, 202, 42], their weight should not vary with the conflict angle. Consequently, a strategy based on cue segregation and integration might require too complicated tunnings to account for the variation in search location during visual conflict. Alternatively, a holistic and more straight forward approach, similarly treating the two cues, could explain this variation in cue preference. Furthermore, holistic models do not require a high level of processing and can describe a large variety of behaviour [195].

Aside from the non-successful ALV model based on the integration of each visual landmarks, we tested four different holistic models, based on brightness values or depth and contrast information. These models' rely on memories of one or several panoramic views taken at the nest location or in its vicinity. In non-conflict experiments, the two models using only one snapshot were unable to form a basin of attraction at the nest location (Fig 2.5). Their homing potential, derived from the vector field

of homing vectors, is shallow, which would trigger a random endless trajectory rarely leading to the nest (Fig 2.5). Eventually, both models are still able to guide the agent home but only in the extreme vicinity of the nest, i.e. when inside the cylinder constellation. The model based on one brightness snapshot has been mostly described as a strategy to explain homing in outdoor scenarios [203]. Contrarily, the visual environment in our arena is simple; this could explain the failure of the model due to the lack of visual disparity and sufficient information. In addition, our results are contingent to previous indoor studies where models based on an image difference function could not fully predict the animal foraging or homing behaviour [101, 109]. We hypothesize that the CwN one-snapshot model partly fails for a similar reason. Finally, there might be a geometrical reason why one snapshot is insufficient to replicate the homing success of bumblebees in our set-up: the third stripe is visually occluded on the memorized snapshot at the nest location (Fig 2.1D), making one key element of the environment missing in the memory. Accordingly, several snapshots should reduce the likelihood of landmark occlusions, especially in simplistic environments or in cluttered ones, a solution many times proposed [87, 75, 94, 55].

Consequently, we investigated such models using different sets of snapshots surrounding the nest location. For these different models, we asked what properties of the set of views impact the homing results. From our results, one feature had a clear impact on the homing success of these models: the location of the views in relation to the nest-hole and the closest landmarks (i.e. the cylinders). Models based on views taken inside the cylinder constellation failed to predict a successful homing, there might be several reasons explaining this observation. First, when the snapshots are taken too close to each other, inside the cylinder constellation, the disparity between images may be too small to guide the agent home (Fig 2.S.2, Fig 2.5). This disparity originates from the three cylinders occupying a

large proportion the visual field (Fig 2.S.2) and being periodically placed around the nest, thus, the four views share almost the same information. Impact of view disparity has been already discussed in the study of Dewar et al. 2014, from a systematic analysis of sets of views properties, they observed that the homing performance was slightly affected by the level of disparity. Finally, the location of the views inside the cylinder constellation may as well lead to the occlusion of the stripes which would impair the impact of the distant objects, here the stripes, to guide the agent home (Fig 2.S.2).

A second aspect showing an impact on our results is the number of views stored in memory. Dewar et al. 2014 in their simulation showed that four snapshots taken at optimal positioning were efficient to home. For the non-conflict situation, the brightness multi-snapshot model needed eight views to keep only the basin at the nest-hole and nowhere else (Fig 2.5), while, the CwN-based multi-snapshot model required solely four views to create a unique basin around the nest. From these results and the study of Dewar et al. 2014, we conclude that a larger number of views can sometimes improve homing success. There is scarce evidence on the number of views an insect can store in its memory, Ardin et al. 2015 [4], using a biologically constrained model, suggested that more than a hundred views could be stored. Nevertheless, fewer images make a model preferable since the memory of an insect might also be filled with en route snapshots. Therefore, the model based on four CwN views is computationally more parsimonious than the model based on eight brightness views.

The CwN multi-snapshot model distinguishes itself from the brightness based multi-snapshot model in other aspects. It predicts slightly better the behaviour during visual conflict, i.e. showing the preference of the bumblebees for the stripes fictive nest and mostly ignoring the

cylinders during large conflicts (Fig 2.6D). Unfortunately, this result is not evoked by the metric used for quantitative comparisons of the models. Indeed, the F1-scores of the multi-snapshot models at the condition 45/180 are similar while the predictions are quite different (Fig 2.S.5). The brightness multi-snapshot model predicts search at the cylinders and the stripes' fictive nest while the CwN model predicts a large search area around the stripes. The CwN model is sanctioned for its too large areas but ignores the cylinders like the bumblebees. Finally, the CwN is more robust to changes in altitude; only this model has a single basin at the nest location for both tested heights (see Method for details) during the non-conflict situation. This makes this model ecologically relevant as robustness against altitude is a crucial qualification for flying insects which perform learning flights at different heights and home by gradually lowering their altitude [107].

The ability of the CwN multi-snapshot model to partly predict the search location during visual conflict, and its homing ability for the non-conflict condition, could be due to its encoding of distance information. This result is following many studies suggesting the importance of distance information, derived from the optical flow, for homing [202, 46, 56, 178, 107, 141, 15]. Additionally, CwN images because of their encoding of contrast, highlight the edges of the different landmarks (Fig 2.1E, Fig 2.3C). Along, this property is likely to underlie diverse insects' behaviours, like the use of edges for pattern recognition and learning in bees [27, 158]. A close look at the homing vector directions for the CwN snapshot model shows that the agent would be drawn to the edges of the stripes (Fig 2.8): this behaviour was observed in our experiments (personal observation). This strong edge attraction implies that this model cannot be the only one in play at the extreme vicinity of the nest, as the agent is driven to the edges of the stripes. Thus, the use of brightness might give a more accurate home direction very close to the nest. Although, it would

be of interest to compare the present study with experiments performed in natural visual surroundings, where contrast and edge detection might be more challenging. Hence, we may assess if the model performance is robust to a higher degree of visual complexity.

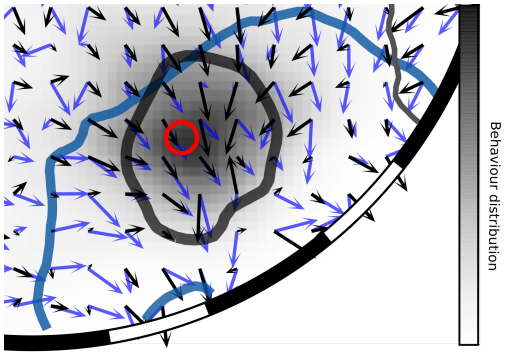

Figure 2.8: Details of the field of homing vectors for the CwN multi-snapshot model and for the Brightness multi-snapshot model The CwN multi-snapshot model vector field is represented in blue, with the lowest isohypse of its derived potential in dark blue. The brightness multi-snapshots vector field is in black with the lowest isohypse of its potential in black. The distribution of the behavior is represented by a black gradient from white to black. The red circle indicates the location of the stripes' fictive nest.

2.6 Conclusion

Overall, we have been able to find features easing the success of visually based homing models: like storing multiple snapshots outside a constellation of local landmarks and encoding information about the 3D layout of the environment. The multi-snapshot model based on views

encoding distance information derived from the optical flow, does apply these characteristics and is a biologically plausible model partly explaining the behaviour of the bumblebees, contingent on the degree of visual conflict. Thus, this model brings a simple explanation to an apparently complex behaviour. Eventually, this model could easily be implemented on an agent using biologically inspired artificial motion perception system for navigation, without requiring additional equipment.

2.7 Supporting informations

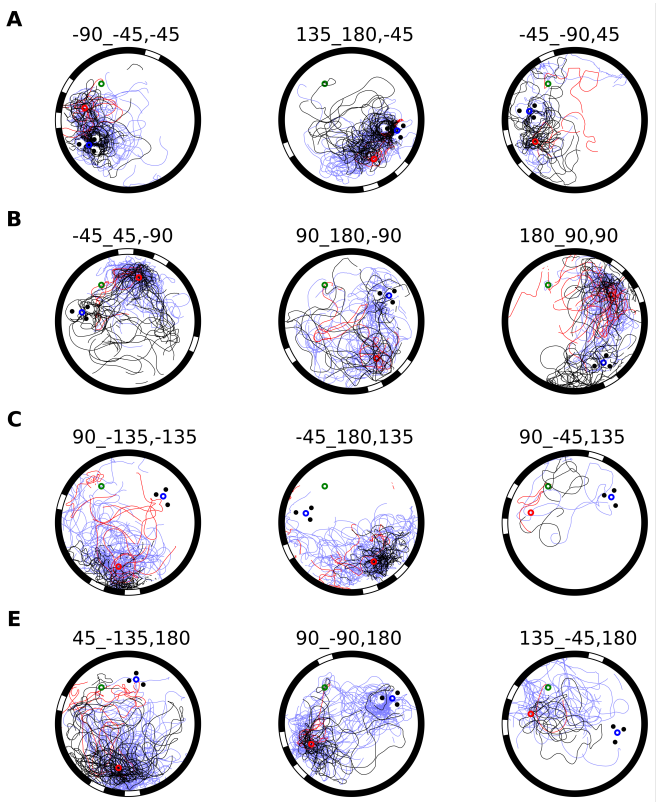

Figure 2.S.1: Trajectories examples and illustration of the behavioural variability:For each condition, we represented 3 trajectories examples. The examples were selected based on the amount of time the bees spend searching. Each trajectory is colour coded as follow: The bumblebee which spend the most time in blue, the less time in red and the bumblebee spending the average amount of time in black.

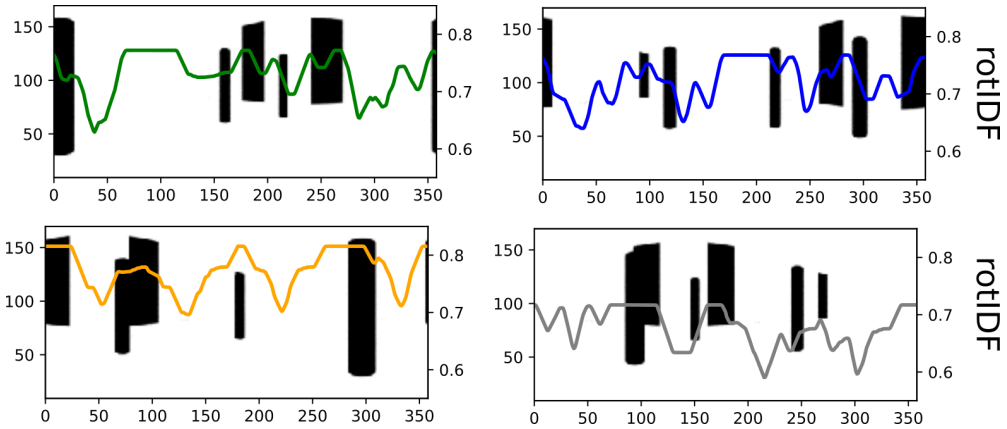

Figure 2.S.2: The set of views S for the multi-snapshot brightness model taken at 5cm from nest-hole. The 4 views are represented as an equirectangular projection constituting the set of view, and are overlaid with their own rotIDF function with the current view as in Fig 2B.

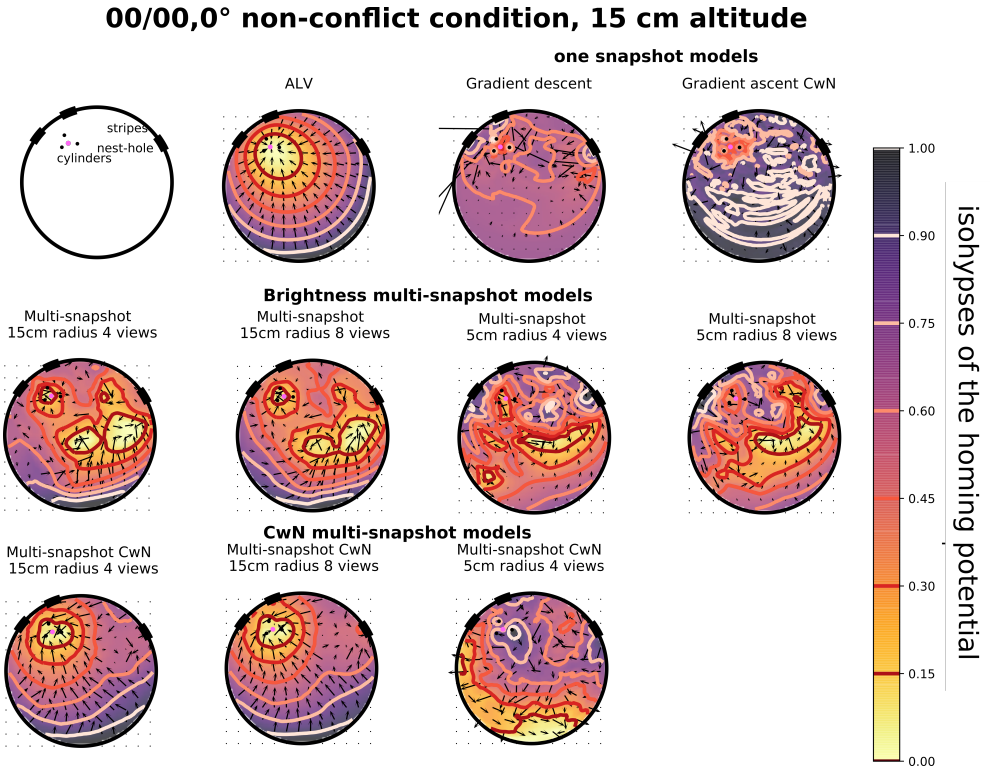

Figure 2.S.3: Homing potential of all different models during non-conflict situation at 15cm elevation. The ALV model is not affected by the change in altitude since this one use the exact position of the cues in the 2D plane.

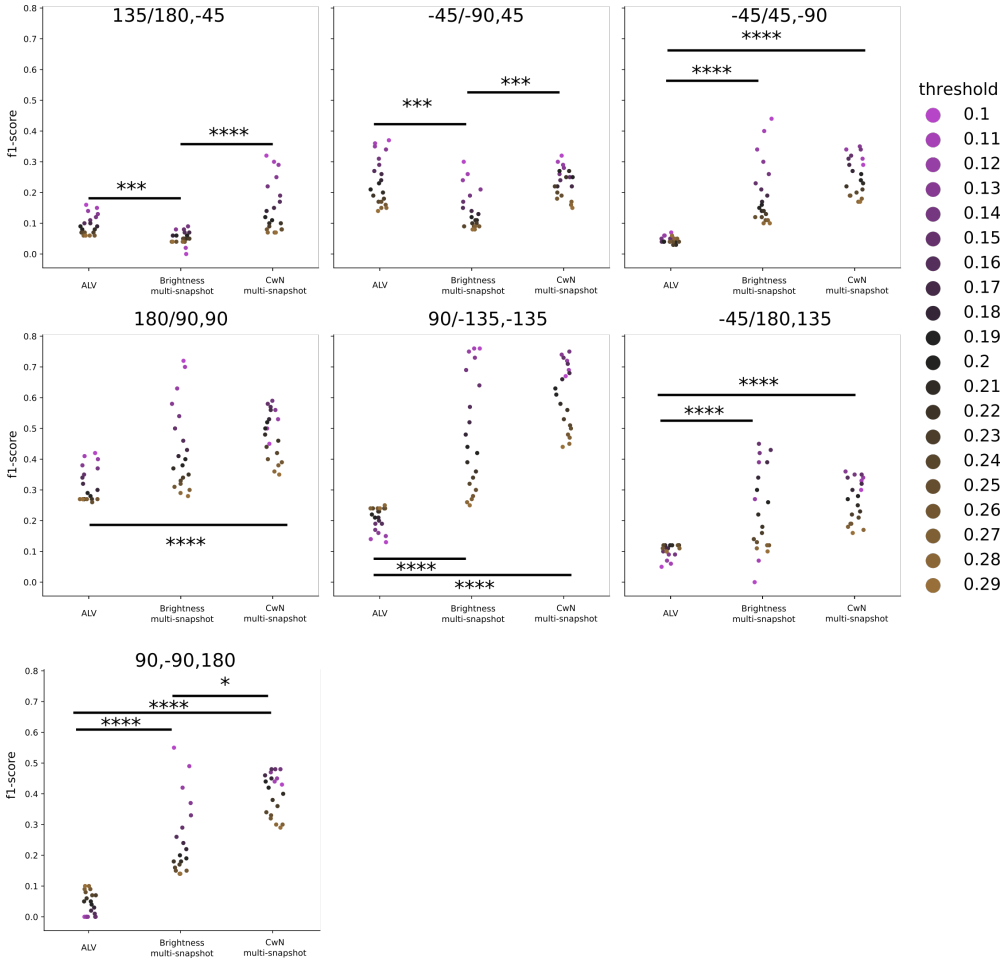

Figure 2.S.4: F1-score when varying the model prediction isohypse. Each plots represents for each condition the F1-score depending on the selected isohypse from 0.1, pink, to 0.29 ,light brown. A Dunn's Post-hoc test following the Kruskall-wallis test was perform on each conditions: the adjusted significance values are represented when significant. The significance levels are coded as follow: p<0.5 *, p<0.1 **, p<0.01 **,p<0.001 ***, p<0.0001 ****.

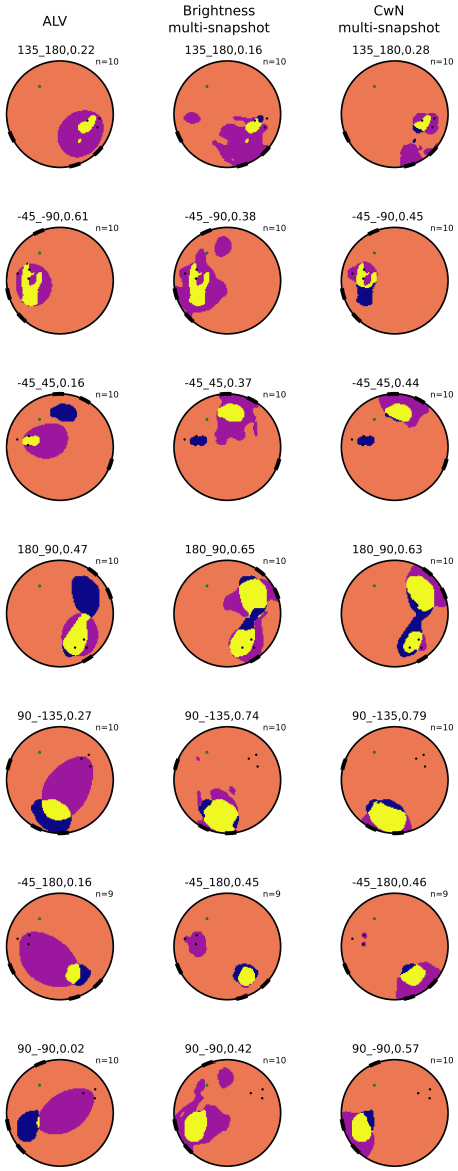

Figure 2.S.5: 2D representation of the confusion matrix values for each conflict conditions. 2D representation of the confusion matrix values for each conflict conditions. Each subplots represents the confusion matrix output for each model during tested conflict conditions, from left to right, first column ALV, second column Brightness multi-snapshot model, and third column the CwN multi-snapshot. Each title informs the tested condition followed by its F1-score. The colours describe the correct predictions: the true negatives in orange and the True positives in yellow while the failure of the models prediction are: false positives in purple and the false negatives in dark blue.

3 Bumblebees behavioural patterns while homing in a visual conflict situation

3.1 Introduction

GOING BACK HOME seems to be a trivial exercise that humans succeed in their daily routine, no matter how far they travel. In the modern world, our visual environment is very reliable because it is rarely subject to many changes, which allows us to serenely use the landmarks associated with our home when returning to it. But, on the scale of an insect, this statement cannot be made so quickly. Indeed, much of the visual environment around an insect's home can suffer from harsh weather conditions, such as wind, but also anthropogenic changes. As a result, the visual environment of an insect nest can change rapidly, and therefore it could differs from the previous experience. Do insects adopt a specific behaviour in such situations, and how can they find their home despite these changes? After a foraging trip, social Hymenopterans such as bumblebees or wasps rely on vision to find the entrance to their nest, which is often inconspicuous [170, 142, 201]. They can use the available visual information in different ways, either by exploiting the visual environment as a whole (holistic approach, see Chapter 2 and [195,

203]) or by using distinct visual cues, i.e. landmarks [31, 202, 42]. The latter approach implies that the cues are represented in the insect brain as separate and labelled as landmarks (visual landmarks are defined here as distinct objects or features in the environment that can be individually noticed and memorised [119]). According to these two types of homing mechanisms, when the visual environment is consistent with the previous experience, the insect is directed without problem towards its home. On the other hand, when the visual environment has been modified; for example, by changing the location of specific visual cues, there is ambiguity concerning where the nest entrance should be. It is therefore interesting to analyse how bumblebees may react to this situation and what behaviour they adopt to deal with this ambiguity.

This study is based on experiments in which bumblebees had to find their home in a situation of visual conflict after becoming accustomed to flying in an arena containing cues indicating their nest-entrance (see Chapter 2). In these experiments, the bumblebees could learn the location of their nest by using two constellations of visual cues. During the tests, the two constellations conflicted. As a result, when the bumblebees returned home, they were challenged by this altered environment. The visual conflict between the two cue constellations was quantitatively modified by changing the angle between them relative to the centre of the arena, which led to several test conditions (see Chapter 2). In an earlier analysis (see Chapter 2), we compared the locations where bumblebees searched for their nest with predictions provided by different models of visually-based homing strategies. Behavioural results show that bumblebees were pushed towards the positions indicated by the two cue constellations, but to a different extent depending on the degree of conflict between the cues. This analysis concluded that a holistic visual homing strategy could partially replicate these complex experimental results.

In Chapter 2, we focused on the overall performance of the bumblebee population tested, including where bumblebees sought entry to their home for each condition. The previous report did not characterize the individual behaviours adopted in visual conflict situations, nor did it study several aspects of the bumblebee flight such as changes in altitude or the time spent in the arena before finding the nest. Therefore, the present study uses the same data as in Chapter 2 to study in detail the behavioural flexibility of bumblebees and their performance during local homing in different visual conflict situations. For this purpose, trajectories are classified through a cluster analysis, resulting in a catalogue of behaviours performed in this challenging environment. Next, we provide a detailed analysis of the search behaviour to determine whether other variables in addition to the angle of conflicts, such as the distance between the nest entrance and the two constellations of landmarks, could indeed influence the search behaviour. Finally, we take a closer look at the development in time of what we describe here as "switch behaviour", which occurs if the bumblebee, in a conflict situation, does not seek a compromise location but switches between the fictive nest locations defined by one or the other of the two cue constellations. From this analysis, we try to explain the finality of the different behaviours adopted by bumblebees during this difficult situation, and how these behaviours can fit into the framework of visually-based local homing strategies as defined in the previous chapter.

3.2 Materials and Methods

In this study, we used the 3D-flight trajectories of bumblebees during return flights obtained by the method as described in Chapter 2 of this thesis.

The set-up enabled us to create a visual conflict between two visual cue constellations provided to the bumblebees upon learning which are: a constellation of three small cylinders around the nest-hole and a large stripe pattern on the wall (with two of the stripes placed behind the nest) (see chapter 2 for details,& Fig 3.1). In a conflict situation, each cue indicates to the bumblebees a fictive nest location. However, the variable geometrical arrangement between the two cue constellations as well as their location with respect to the real nest-hole in the arena-floor could also affect the bumblebees' behaviour. The spatial variables potentially affecting homing behaviour are, thus, the following: the angle between the two fictive nests as seen from the arena centre, the absolute angle between them (i.e. the absolute conflict angle), and finally the angle between the real nest-hole and each of the fictive nest locations (Fig 3.1). In total these four variables may impact the search locations. The fictive nest-hole location associated to the stripe patterns or to the cylinders, respectively, are later referred as the stripe-associated nest-hole, SAN, and the cylinder-associated nest-hole, CAN, respectively.

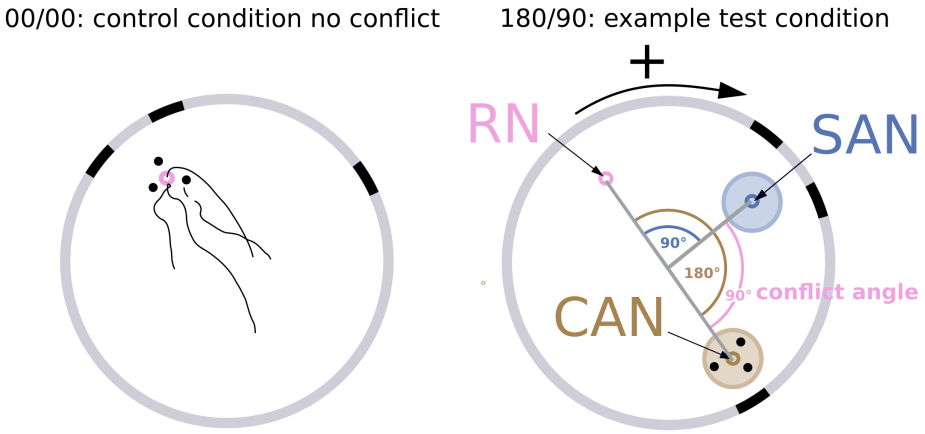

Figure 3.1: The different spatial variables based on the cues' fictive nest and real nest location. Top view of the flight arena with the walls in grey and the visual cues in black. The entrance to the hive, also called the real nest-hole (RN) is represented by a pink circle. The left scheme represents the training condition with the two black stripes behind the RN and the three cylinders around it. In addition, example flight trajectories of homing bumblebees recorded under the control condition are shown as thin black lines. The right Figure represents a conflict situation where the stripe-associated nest-hole (SAN) is at 90° from the RN, blue circle, and the cylinder-associated nest-hole (CAN) at 180° from the RN, brown circle. The conflict angle can be expressed as absolute or directed angle, with a clockwise movement from the RN as a positive angle. The second spatial variable indicates the absolute angle, thus the angular distance, between the SAN and the RN, and between the CAN and the RN.

3.2.1 Analysis of Influential factors on the bumblebees performance

After having entered the flight arena from the foraging chamber, the bumblebees had 5 minutes to return to their nest in this challenging situation. Two results are therefore possible: they return home within the allotted

time or they do not. Therefore, we wanted to evaluate how the spatial organisation of the cues can affect this performance; i.e. when, and if they find their nest. To study this performance, we followed an analysis scheme similar to the one used in medical biology, where scientists want to know the probability of death in response to a disease and compare groups under a specific treatment [35]. Following this analogy, the event of death is, in our context, "finding the nest", whereas the treatments would be the different angles of each variable studied. We fitted for each group (e.g. one group combines the return time of the bumblebees tested with the CAN at 45° from the RN) a so-called survival or Kaplan Meier curve. This curve is an estimate of the probability function of experiencing an event over time, in our context the event is finding the nest. This probability is defined as a constant between times of events, thus the probability is constant until the moment a bumblebee finds the nest, creating a new step after an individual of the population find home. Therefore, this estimate is a step function (for more details on survival curves, see [35]). Analyses are limited to 5 minutes; any bumblebees that required more time to find the nest-hole were "censored", which is a standard procedure of survival analysis to deal with “missing data” (for details see [35]). Not censoring the data would give a poor prognosis of the probability of "survival". The estimation of the statistical differences between the survival probability curves is obtained with a non-parametric test, the log-rank test [133]. Each survival curve also indicates the percentage of the population "at risk": it indicates the proportion of the population at time t still having a chance to find the nest or, in other words, still searching in the arena.

Finally, to estimate the impact of the different cue arrangements on the performance, we applied a "Cox's proportional hazard regression model" [17], which gives an indication of the probability of survival of one group relative to another group. For example, group A is twice as likely to

experience event as group B. This indication is called the "hazard-ratio", which is a measure of the relative survival experience between two groups.

3.2.2 Analysis of Influential factors on the search location

In chapter 2, the behaviour of bumblebees was characterised solely by the 2D distribution of the locations of the bees in the arena, highlighting the areas where the bumblebees spent most of their time searching for their nest between 0 and 20.63 cm. Here we want to examine variables that could affect the location bumblebees searched, in addition to the obvious influence of the conflict angle.

For each flight, we quantified the proportion of time spent in a cylindrical volume centred at each fictive nest (18 cm radius and 20.63 cm height from the ground). To select the spatial variables that can best predict the search time in these defined volumes, we applied a linear regression analysis called Lasso analysis (least absolute shrinkage and selection operator) from the Python library Scikit.learn [150]: the selection of the explanatory variables is based on the Akaike information criterion indicating the quality of a statistical model [1]. The lasso is advantageous because it is not necessary for the model to make assumptions about the dependency between variables, in addition the model tries to nullify some effects of the variables, thus limiting the number of explanatory variables.

3.2.3 Trajectories classification

Global descriptors of the trajectories

Since each flight is different Fig 3.2 and it is not yet clear what characteristics really characterize them and how these different flights may be similar to each other, we decided to classify those by a clustering procedure. This clustering will be based on a wide range of different characteristics that are behaviourally relevant. A total of 9 characteristics called "global descriptors" have been selected to describe each trajectory. We have selected descriptors that allow us to study aspects that are not considered in the previous chapter, such as time and height. Indeed, among all the recorded trajectories, there can be many variations along these two dimensions, such as the time to return and height of flight.

The first three global descriptors describe trajectories as a function of flight altitude, because in the previous analysis, only the behaviour up to a height of 20.63 cm above the arena floor was taken into account. Each of these three altitude descriptors corresponds to the time spent in a specific slice of the arena as a proportion of the total flight duration. The lower slice extends from the arena floor to 20.63 cm, being the section where most of the behaviour took place and where the bumblebees are searching for their nest. The middle slice ranges from 20.63 to 80 cm; the upper edge is chosen because it corresponds to the height of the stripe pattern on the arena wall. Finally, the top edge ranges between 80 cm and the roof of the arena (100 cm).

Where and how the bumblebees search for their nest is one of the major aspects addressed in this chapter. Consequently, the other global descriptors focus on the search behaviour associated with the two cue constellations. The cylindrical space defined around each cue-associated

nest-hole (18cm radius and 20,63cm height) is defined as cue-space, hence the space defined by the stripes is called "stripes-space", and the cylinders, "cylinders-space". For each of them stripes and cylinders-space, four types of measurements were done:

- The number of visits to the different cue-space: highlighting the flexibility of the search during the flight, by describing the number of times the bumblebee enters a cue-space.
- The overall share of time spent in the different cue-spaces, thus the search time associated to each cue.
- The average duration of a cue-space´s s visit, referred as visit-duration: To highlight the temporal attention given to a cue and to describe how long the bumblebee search continuously at this one.
- The maximum visit-duration in each cue-space. This measure represents the outliers in visit-duration in case most of the search happens in a single long visit.

Finally, the last global descriptor is the time at which the bumblebee found the nest after entering the flight arena from the foraging chamber; this time is called the return-time. A prior to classifying the trajectories based on these descriptors, and because the descriptors might be drawn from different distributions, their values need to be scaled. Each value is returned as its z-score. The z-score is calculated by subtracting the average value of the investigated descriptor and then dividing this difference by the standard deviation. Thus, a z-score of 0 indicates a data-point to be equal to the mean score, while a z-score of 1.0 indicates the value to be one standard deviation from the mean.

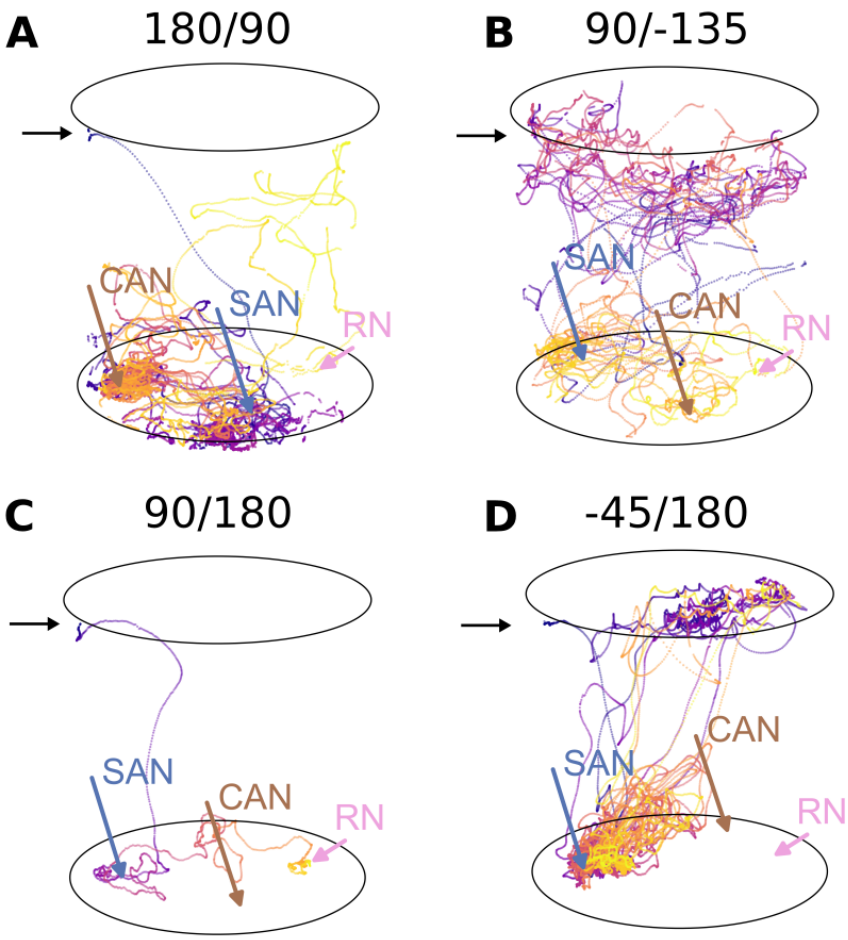

Figure 3.2: Trajectories examples. 3D Representation of trajectories example showing the variability of behaviours after the bees entered the flight arena through an entry hole (black arrow) close to its upper edge searching for its nest-hole. Each flight is time coded from dark purple, the start, to yellow, the end. Locations of the fictive nest-holes and the real nest-hole are represented by a pointing arrow, brown for the CAN, blue for the SAN and pink for the RN. The lower circle represents the arena floor and the upper one the ceiling. Each of the name is given after the tested condition it represents: the first number corresponds to the placement of the CAN relative to the RN and the second one the SAN relative to the RN. A: example of a trajectory representing Cluster 1, B: Cluster 2, C: Cluster 3, and D: Cluster 4.

M3C: Selecting the number of cluster

After reducing the flight trajectories to the set of the above-described descriptors, we can perform a clustering analysis to classify them in different groups. The clustering analysis requires to pre-set the number of clusters we expect to find. Since we do not have *a priori* knowledge about this number, we used a method called the M3C, or Monte Carlo reference-based consensus clustering, to constrain the choice of clusters numbers [86]. This method was implemented in the software R and used to assess the number of clusters that can be formed from the data. This method is preferred over alternative methods as it statistically tests for the hypothesis of having only one cluster or, in other words, the null-hypothesis that no clusters can be formed at all. This null-hypothesis is not tested by other procedure which may then, consequently, lead to a bias towards a high number of clusters as was, indeed, often found with alternative methods (for details see [86]. The results of the M3C inform about several measures to select the optimal number of clusters for example: the Relative Cluster Stability Index (RCSI), indicating the stability of the clusters for different iterations of the calculations and the p-value. We used the M3C method to estimate the most appropriate number of clusters when using a PAM clustering analysis (also called partitioning-around-medoids [89]). PAM analysis attempt to minimize the distance in the multi-dimensional space between points of the same cluster. It differs from k-means since it uses centroids detected from the input data to form clusters [89] and is not based on means, i.e. the average between points of a cluster. Hence, PAM is supposed to be more robust to outliers.

Tsne: validation of the clusters

The different clusters are defined in a multidimensional space depending on the number of parameters included in the clustering analysis. In our case this space has 12 dimensions corresponding to the 12 global descriptors (see previous paragraph). To represent these clusters in an understandable and picturable way, they are reduced to a two-dimensional space by using the t-SNE algorithm (the t-Stochastic Neighbouring Embedding algorithm) [175]. This algorithm relies on a single parameter, the perplexity, which is why t-SNE is called an unsupervised mapping algorithm [171]. When reduced to the 2D space all points representing each trajectory are expected to form clusters similar to the one found by the PAM clustering analysis.

Statistical analysis of the global descriptors

To statistically analyse differences between clusters we compare the different descriptors between all trajectories. Firstly, we test for normality with a shapiro-wilk test. Following the result of the shapiro-test either an ANOVA or a Kruskal-Wallis analysis (when samples are not normal), are used to compare the descriptors' z-scores between all clusters. When the null hypothesis is rejected, Kruskall wallis is followed by a Dunn-test and ANOVA by a Tukey-test to compare all clusters with one another. Each p-value is adjusted by a Holm-Bonferroni correction to account for the problem of multiple comparisons.

3.3 Results

When bumblebees are confronted with a change in their environment they behave in different ways Fig 3.2. Nevertheless, most of them direct their search to those spaces indicated by the two constellations of visual cues. They do not look for a compromise between the two constellations, but focus very precisely on these two places. On the other hand, the time spent at these cues is largely variable according to the conditions and sometimes even within one condition. Moreover, in spite of their behaviour mainly directed towards visual cues, they sometimes find the real entrance to their home. Therefore, we will first investigate the potential effect of different arrangements of the visual allothetic cues (i.e. cues external to the animal) in the arena to explain the variations in behaviour.

3.3.1 Bumblebees performance

The tested Bumblebees have in total 5 minutes to find their nest in all different visual conflict situations. The performance of the bumblebees is quite variable among the different flights: in many cases, bumblebees were able to retrieve their nest before the imposed time-limit; however, in others they did not manage to do so. Thus, we investigated how the cues arrangement (see material and methods Fig 3.1) is influencing their performance. A curve representing the probability to not find the nest over time is obtained for each group of bumblebees tested under a specific value of the investigated spatial variable . Differences between the probability to not find the nest over time can be visually interpreted from

the different curves' shapes: overlapping curves indicate that they do not differ from each other's (Fig 3.3). This visual impression is supported by statistical testing using the log-rank test.

Figure 3.3: Kaplan Meier curves for the different spatial variables. A: Curves representing the probability to not find the nest along time for the data grouped depending on the directed conflict angle between the two cue-associated fictive nest-holes; each group or angle corresponds to one colour. Censored data are represented by a cross. Below, a table of the population at risk for the different groups over time. B: Grouped survival curves based on the absolute conflict angle, C: based on the absolute angle between the SAN and RN, D: based on the CAN and RN absolute angle.

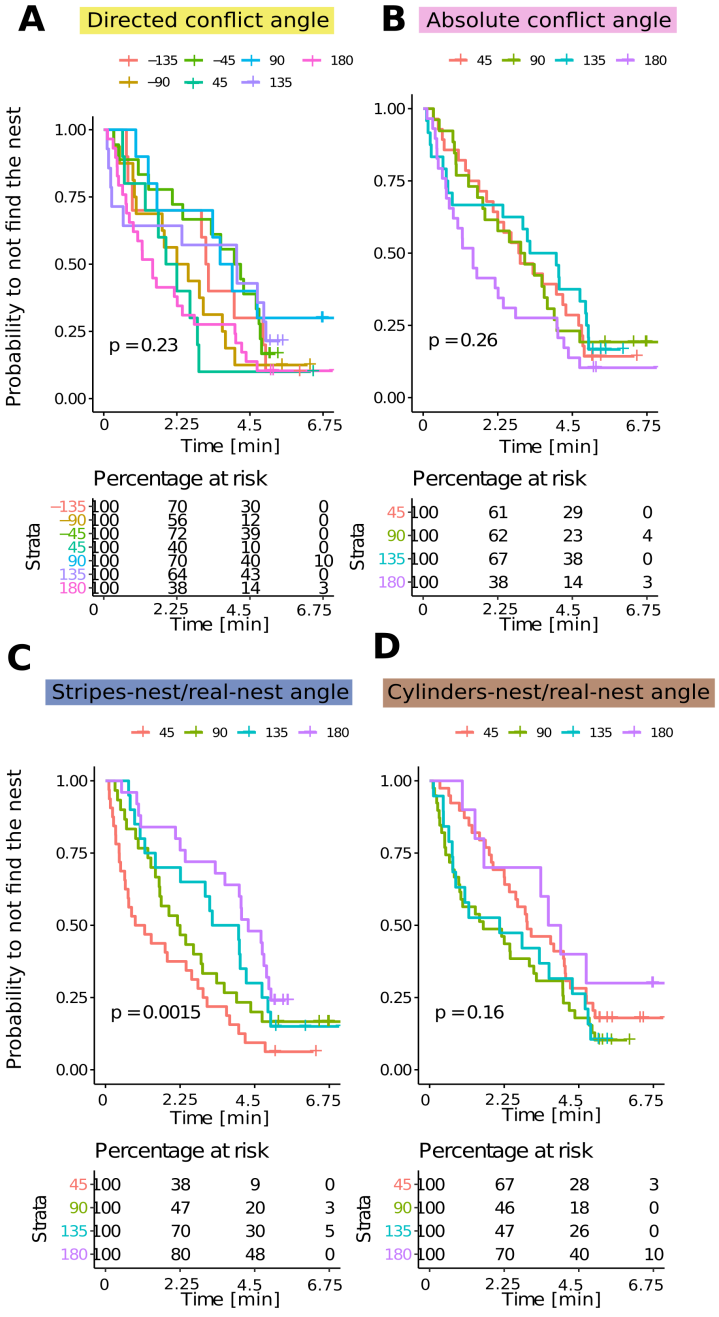

(Legend on previous page)

For the different conflict angles between the two fictive nests, directed or absolute, the probability to not find the nest over time does not differ significantly between groups. Indeed, the log-rank test p-value is for both larger than 0.05, and the survival curves for each angle overlap with each other. Similarly, the angular distance of the CAN to the RN does not have an effect on the probability to not find the nest ($p>0.05$). Therefore, the return-time does not significantly depend on the angular distance between the CAN and the RN. However, groups corresponding to the different spacing between the SAN and RN show survival curves significantly different from each other ($p<0.01$). In detail, the curves clearly split already after 3.5 minutes of the flight, with a percentage of population at risk (population which is still searching for the nest) differing by 10% for the different angles. In addition, the population at risk differs by almost 50% between the two extreme angles: for an angular distance of 180° between the RN and the SAN, half of the bumblebees are still in the arena at 4 minutes, while at the same time, for the smallest distance, almost all bees have found the RN (percentage at risk is only 9%)(Fig 3.3). Finally, the hazard-ratio calculated for the smallest spacing as a reference group, i.e 45°, decreases with the angular distance between the SAN and the RN; thus revealing a reduction in the hazard-ratio with an increasing angular distance (Fig 3.4). Indeed, the hazard-ratio is reduced by 66% when the SAN is located by 180° away relative to the RN in comparison to the value at a 45° angle. In conclusion, there is a tremendous effect of the placement of the SAN relative to the RN on the return-time: bumblebees need little time to reach their home entrance when the SAN is in vicinity of the RN, and the probability to find the nest decreases by more than a factor of 1/2 when the SAN is opposite to the RN.

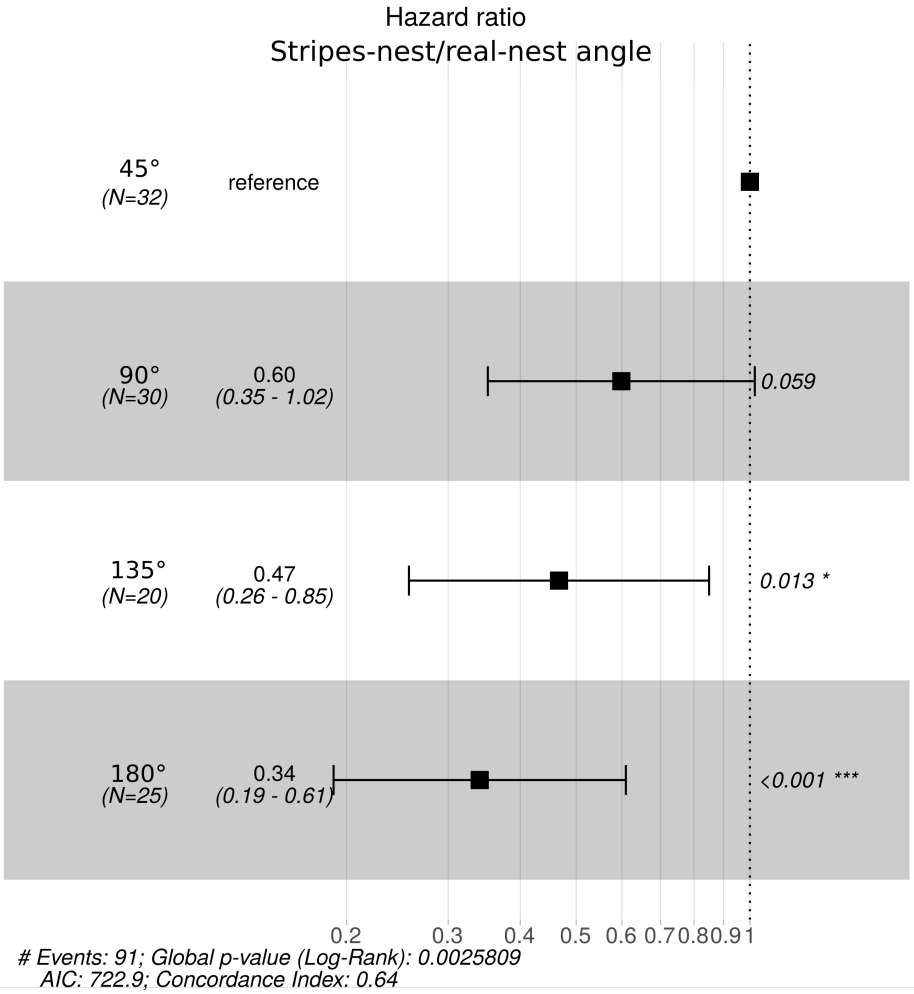

Figure 3.4: Cox linear regression model for distance variation between the stripe-associated fictive nest and the real nest. Representation of the hazard ratio calculated from a univariate fit of a Cox's model. The reference group is bees under the condition with the SAN at an angular distance of 45° from the RN. Each value of the hazard ratio shown as a black square is represented with its confidence interval (black whiskers). Hazard ratios before the dotted vertical black line, or <1, indicate a diminution in hazard.

Finally, for the different conflict conditions (see Chapter 2), there

might be confounding effects between all the different variables. Therefore, to investigate possible interactions between all covariates, we performed a multivariate analysis by fitting a Cox-proportional hazard model (Table 4.1). However, for simplification, we removed the directed conflict angle from the analysis. Firstly, the validity of the fit was tested with three different tests (likelihood, Wald, and score) all giving a significant p-value, indicating that the model is well-fitting ($p<0.0001$, $df=3$) and that the results of this model can be trusted.

Based on this model, we observe that the variation of the angular distance between the SAN and the RN is the covariate that has the strongest relationship with a decreased chance of finding the nest (Table 4.1). By contrast to the univariate investigation, the variations of the absolute conflict angle between the SAN and CAN have a significant impact on the chance to find the nest. However, the hazard-ratio of 1.006 indicates only a slight increase of the likelihood to find the nest when the distance between the CAN and the SAN increases. In conclusion, these results show that the angular distance between the SAN and the RN influences the probability over time of finding the RN even when confounding effects of different variables are included: the closer the stripes are to the real nest-hole, the sooner the bumblebees will find the RN.

Table 3.1: Multivariate Cox-proportional Hazard model

Covariate	Hazard-ratio	p-value
absolute conflict	1.005	0.01 *
stripes-nest/real-nest	0.98	2.1e-05 ***
cylinders-nest/real-nest	1.004	0.28

3.3.2 Search location

The search in the cylinders-space and the stripes-space has been characterised by qualitative analysis to depend largely on the degree of visual conflict between the two cue constellations (see Chapter 2). Here, we show the results of a systematic quantitative analysis of the proportion of time spent at these locations, depending on the different conflict situations (Fig 3.1). Results of the present analysis are shown in Fig 3.5. Overall, the proportion of time spent in the stripes-space, regardless of the different variables variations, is always between 20 and 30%. This observation of a relatively stable search at the stripes-space can be quantified by a Lasso analysis. A Lasso analysis is a regression procedure which selects features or variables to explain the data (for details see Methods). The fitted Lasso model has a low R-squared (R^2=0.10), thus, the model could not well predict the proportion of search in the stripes-space based on the variation of the different variables. In other words, independent on how the cues are placed in relation to each other or to the RN, there are no significant changes in the proportion of search at the stripes-space.

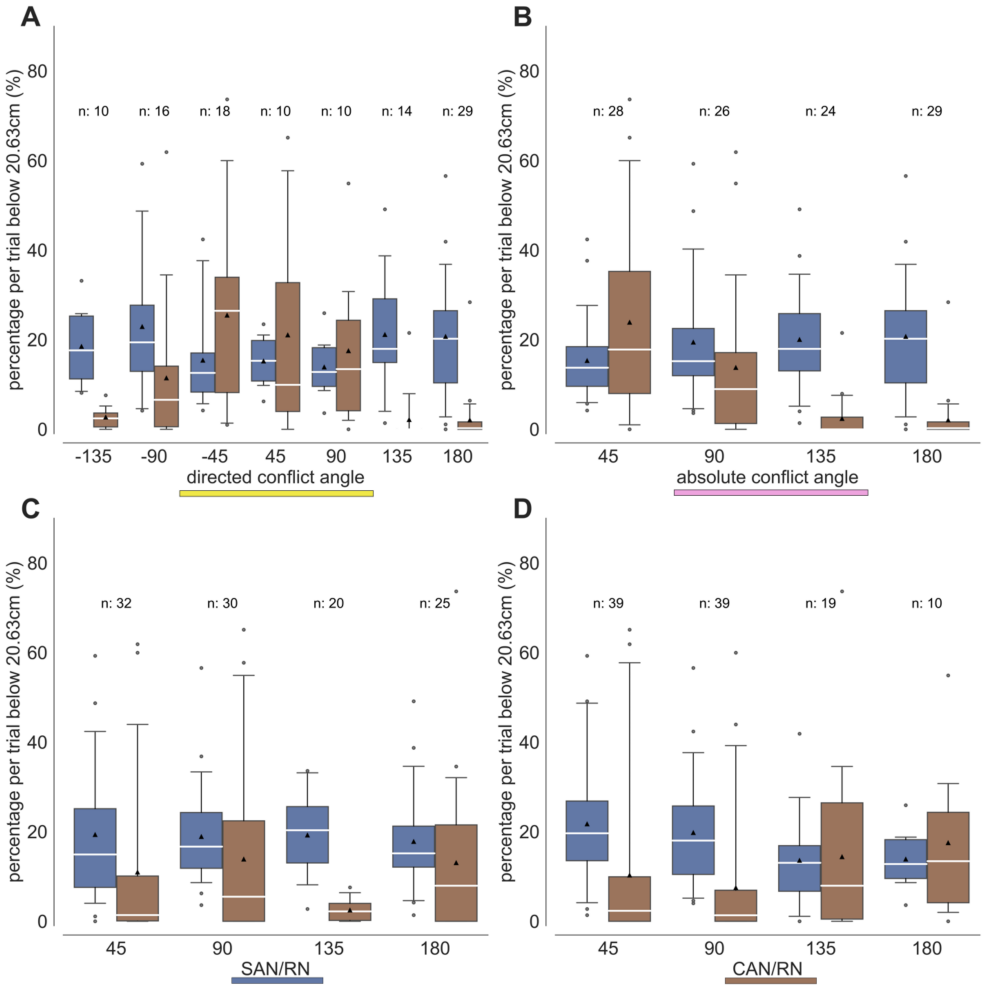

Figure 3.5: Boxplots of the time proportion [%] at the different fictive nest-holes, i.e. at the CAN and the SAN, depending on the different spatial variables. A: boxplots of the time proportion at the SAN (blue) and the CAN (brown) depending on the directed conflict angle between the two fictive cue-associated nest-holes; the median is represented in white, the box represents the first to the third quartile, and the whiskers of the boxplot show the 5% and 95% of the distribution. The other panels represent in a similar way the time proportion spent by the bees at the CAN and SAN, respectively, for the other spatial variables: B: the absolute conflict angle C: the SAN/RN angle D: the CAN/RN angle.

In contrast, the proportion of time invested in the cylinders-space is not constant when the data are grouped according to the different investigated variables (Fig 3.1). For example, the time spent in the cylinders-space appears to be negatively correlated with the absolute angular distance between the two cue constellations. Therefore, we also conducted a Lasso analysis on these results. Here, the Lasso model fitted to the time spent in the volume around the CAN has a larger R-squared than the lasso model fitted on the search proportion in the stripes-space(R^2=0.425). The model selects two variables predicting the proportion of time spent in the cylinders-space. These variables are the conflict angle (coef=-0.78) and the proportion of flight in the stripes-space (coef=-0.24). In conclusion, the quantitative analysis reveals that the bumblebees invested the same amount of time searching in the stripes-space independent of the condition, while the time they invested at the cylinders-space is mostly driven by the absolute angle between the two visual cue constellations. In addition, when bees search in the space defined by the stripes, they find their nest faster if the nest is close by (45° of the stripes).

3.3.3 Number of clusters and validation

Bumblebees that return to their nest have quite variable performance and behaviour. Some aspects of this variability have already been described above and in Chapter 2, however, one important aspect has not yet been taken into account, namely the fact that bees, although they search for a long time for the nest-hole relatively close to the ground, they also change their altitude over the whole vertical extent of the flying arena (see Fig. 2). To analyse these flight trajectories in relation to their full three-dimensional extent, we firstly had to classify them according to several global descriptors, including the altitude and temporality of the trajectories (see list in Method section). At first, to do this classification

we must defined *a priori* the number of clusters that can be formed out of the different trajectories expressed by those different descriptors.

When applied to our flight trajectories, the M3C method leads to an optimal number of four clusters (Fig 3.6). Indeed, the Relative Cluster Stability Index (RCSI), indicating the stability of the clusters for different iterations of the calculations, is the highest and the p-value given by the M3C method is significant when four clusters are selected (Fig 3.6). Since four to seven clusters could have been chosen on the basis of the PAM analysis, because they are associated with a relatively large RCSI (Fig 3.6B), we nevertheless decided to focus our analysis on the largest RCSI value given by this method.

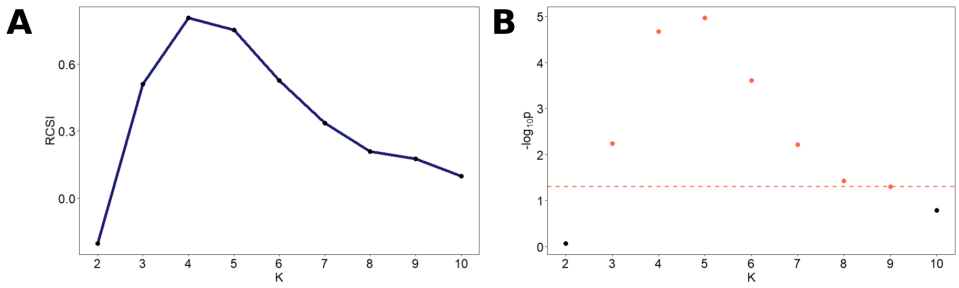

Figure 3.6: Results of the reference-based consensus clustering, PAM, of the recorded flight trajectories. A: the RCSI is shown for each number of clusters 'K' determined by the M3C method. The largest RCSI value is obtained for a number of four clusters. B: The p-value in logarithmic scale indicating the statistical validity of the clusters number is shown for each number of clusters 'K'. The red dotted line represents the threshold of significance, any points above this line correspond to numbers of clusters showing a significant p-value (red dots).

To check if this number of clusters is legitimate, we have represented each trajectory reduced to the values of the descriptors on a 2D representation using a t-SNE algorithm. On this representation Fig 3.7, for

different levels of perplexity, we can see that the points are grouped in four locations. This observation is similar to looking at the estimated distribution of these points by a Kernel Density Estimation (KDE) algorithm. Indeed, there are 4 maxima where the distribution of the points, representing each trajectory, is the most important (the yellow on the coloured map). Finally, the groups formed with t-SNE (i.e. 4 groups at the 4 maxima of the KDE) correspond to the clusters found with our clustering method (each cluster assigned to a trajectory is given by a colour on the points) Fig 3.7.

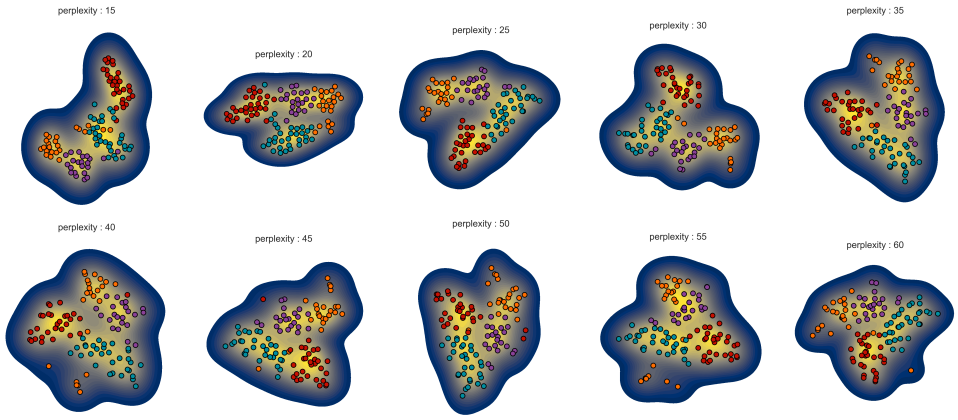

Figure 3.7: Mapping of the 4 clusters in the 12-dimensional space defined by the global descriptors into a 2D space. t-SNE mapping of the data points representing each trajectory for different levels of perplexity. The density of the data points is approximated with a KDE, colour coded from low density dark blue to higher density yellow. Each data point is colour coded with the assigned cluster. Cluster 1 orange, cluster 2 red, cluster 3 turquoise, cluster 4 purple.

Behavioural classification of trajectories

The cluster analysis identified four clusters based on the different descriptors. They are described in detail below.

Cluster 1 (Fig 3.2A): In the selected trajectory example (Fig 3.2A), the bumblebee switches between the CAN and the SAN after searching for some time in one or the other of these areas. Cluster 1 differs from the other groups in that it includes flight trajectories where the bees visit the CAN more often and for longer periods than the other trajectories (average and maximum duration of visit). Nevertheless, these trajectories also show a significant number of visits in the stripes-space, but the bumblebees do not spend much time there, as indicated by the time allotted to scratching and the average length of visit (Fig 3.9). In this respect, Cluster 1 also differs significantly from Clusters 2 and 3. Flights characterized as belonging to group 1 occur most often if the angle of conflict is low (Fig 3.8). This result corresponds to our finding that the time allocated to cylinder-space increases for small visual conflicts.

Cluster 2 (Fig 3.2B): it groups together flights where the bumblebees spent significantly more time above 80>cm, i.e. just below the ceiling of the arena. Therefore, compared to the other groups, bees spend significantly less time flying below 20.63 cm, where they are considered to be searching for their nest (Fig 3.9). In the example (Fig 3.2B), although looking for the SAN, the bumblebee spends a lot of time flying at high altitude, sometimes even bumping against the Perspex ceiling (Fig 3.2B). So it seems that this bee switch from one state to another: it searches and does not search.

Cluster 3 (Fig 3.2C): Trajectories corresponding to cluster 3 are shorter than those corresponding to the other clusters ($p<0.001$), as seen

in the trajectory example (Fig.2C). This example shows a bumblebee flying in the stripes-area before quickly reaching the RN. During these short flights, the proportion of time spent at the stripes-area is relatively large (larger than cluster 1 and 2 $p<0.01$) Fig 3.9. Finally, against all trajectories making up the other clusters, Cluster 3's trajectories show longer visit in the space around the SAN in proportion to the entire flight length $p<0.001$.

Cluster 4 (Fig 3.2D): This cluster comprises trajectories where the bumblebees search often and relatively long in the vicinity of the SAN (Fig 3.2D). The maximum visit duration in the stripes-space (3.84%,± 2.77%) does not differ significantly from that of the flights corresponding to cluster 3 (9.05%,±7.31%), but differs in this regard from clusters 2 and 1 (Fig 3.9). These results show that the bumblebees spent long visits to the stripes in proportion to the overall time spent in the arena. However, in comparison to the shorter trajectories the relative visit duration is not different. The selected trajectory example (Fig 3.2D) shows that most of the flight is condensed in the vicinity of the SAN and that the bumblebee sometimes interrupts its search there attempting to fly out of the arena and, thus, bumping into the translucent Perspex ceiling. Apparently, it switches between searching and not-searching. Flights corresponding to cluster 4 do not occur often if the conflict angle is small, but frequently in all the other conflict situations >35%. The incidence of the four clusters for the different conflict angles is summarized in Fig 3.8. Some clusters are not equally frequent for the different angles: this is especially true for cluster 1 and 4 $p<0.0001$ (chi-square): trajectories belonging to Cluster 1 are more present for small degrees of conflict and less represented for larger conflicts, while the flights belonging to cluster 4 are more frequent for larger conflict angles. Overall it appears that no cluster is clearly prevalent ($> 50\%$) for any of the conflict angles. Thus, their incidence may not only depend on the conflict angle.

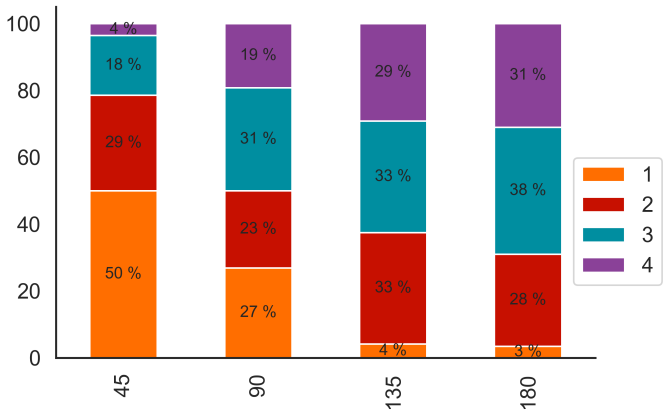

Figure 3.8: Clusters frequency [%] for the different visual conflict angles. The colour code is given by the inset. The x-axis represents the different absolute conflict angle, and the y-axis the frequency in percentage.

Figure 3.9: Distribution of non-normalised descriptors of the four clusters. Each subplot represents one of the global descriptors. Each cluster is represented as a boxplot of the distribution of the investigated descriptor. The statistical annotations indicate the level of significance of differences between the different clusters. such as ****, p<0,0001, *** p<0,001, ** p<0,01, * p<0,05, n.s p>0,05.

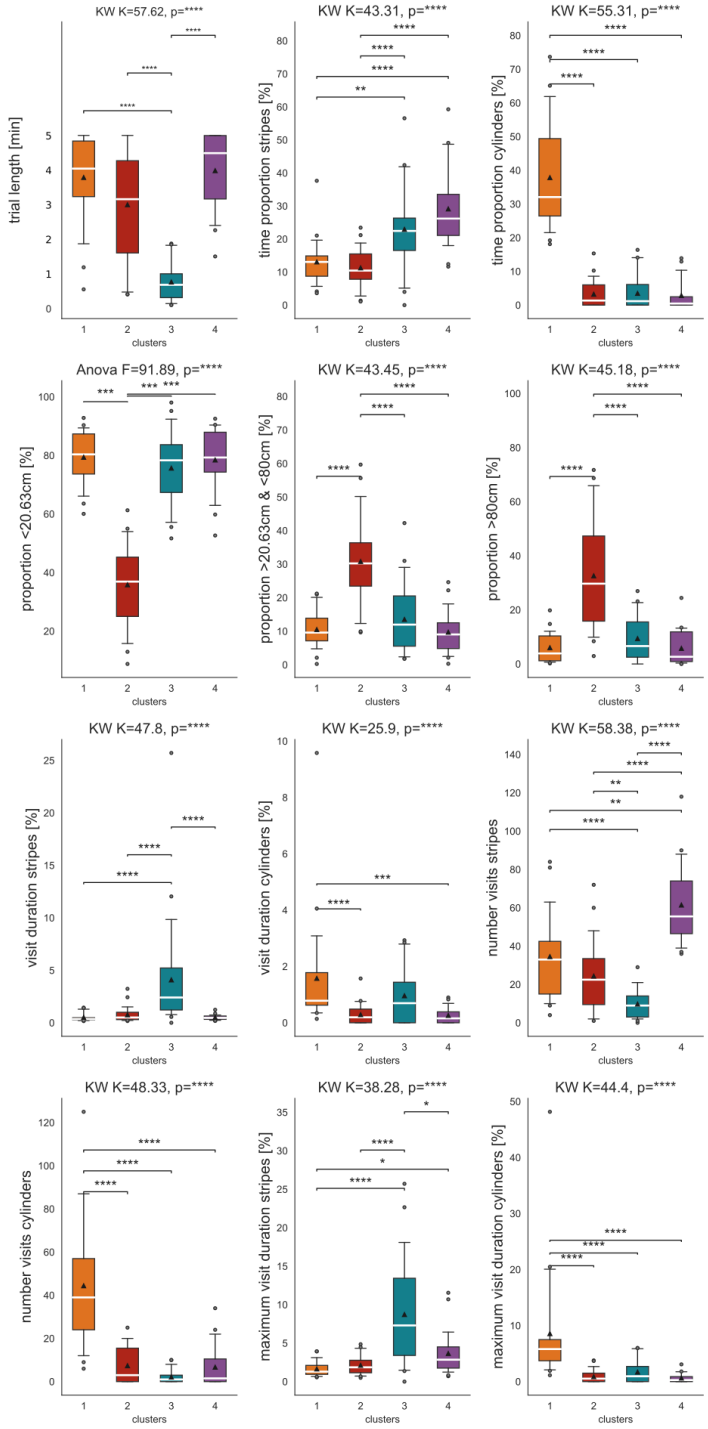

(Legend on previous page)

Because clusters 2 and 3 were equally frequent for the different conflict angles (Fig 3.8), we analysed if their incidence depends on the spatial arrangement of the cue constellations relative to the RN (Fig 3.10). Flights under conditions where the SAN is close to the RN (53 %) were mostly classified as belonging to cluster 3. This observation is congruent with the above-described result that bumblebees found the nest faster when the stripes are close to the real nest. Cluster-2-flights, are equally frequent for all angular distances between the SAN and the RN as well as the CAN and the RN (for both chi-square p-value >0.05).
Finally, despite the fact that the stripes are placed opposite to the original condition, 16% of the flights belong to Cluster 4. This placement in maximum conflict with the RN and the original position does not change the response of the bumblebees to the stripes: the bumblebees devote a large part of their behaviour to it. Overall, the bumblebee behaviour does not appear to be influenced in any obvious way by the locations of the visual cues relative to the real nest-hole except when the stripes are close to it; then, the flights are much shorter, because the real nest-hole is then found easily.

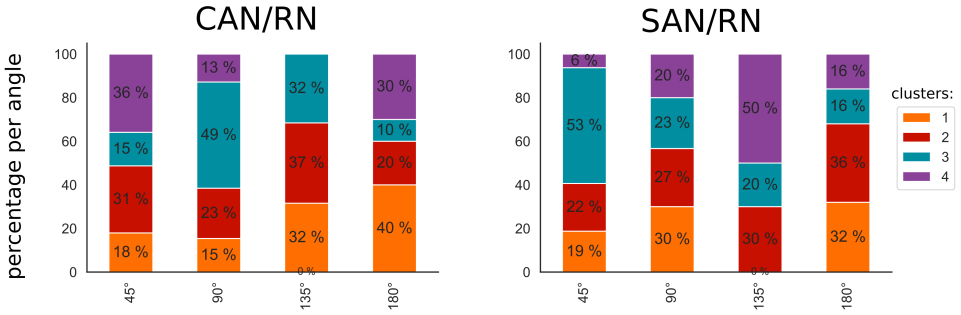

Figure 3.10: Clusters frequency [%] depending of cues spatial arrangement

3.3.4 Switching between the fictive nest-holes and states, study of Cluster 1

Cluster 1 is characterized by flight paths where bumblebees often move from one fictive nest to another, a behaviour called in the following lines "switching behaviour". In the following, we characterize the temporal structure of this behaviour for the trajectories belonging to this cluster.

The figure Fig 3.12 represents for each flight the moments when the bees are in the area of one of the dummy nests, i.e. the stripes-pace or cylinders-space, respectively. In addition, we investigated two types of events: (1) when the bumblebee moves from one marker to the other and (2) when the bumblebee crosses a defined altitude level (20.63 cm above the arena floor) between the bottom and the middle of the flying arena. The crossing of this altitude level between the bottom and the top of the arena was only considered as switching behaviour if a visit above this level lasted longer than one second (which corresponds to approximately the lowest 25% of the visit duration above the 20.63 cm limit). Each of the event occurrences is represented on Fig 3.12. In addition, since three of the flights in cluster 1 are relatively short (less than 2 minutes), we discard them for the later time analysis.

To statistically investigate the temporality of this behaviours, we had to normalize the duration of each flight between 0 and 1, with 0 corresponding to the beginning and 1 to the end of the flight; thus, the time of each event had a value between 0 and 1. For each trajectory, we determined the proportion of switching between the fictive nest associated space on the one hand, and the height levels on the other, occurring either in the first or in the second half of the flight. Thus, on the normalized time scale, the proportion of time of events less than 0.5 or greater than 0.5, respectively (Fig 3.11). For both types of events, most switching occurs in

the first half of flights. This observation is consolidated by the use of the Wilcoxon test between paired samples: for switching between fictitious nesting areas, p-value=0.003 (W=22); for switching between altitude levels, p-value=0.006 (W=32). Switching between altitude levels was also studied for trajectories belonging to group 4 after their normalization over time. For these, there is only a tendency to reduce the number of switches in comparison to the first half, but the result is not significant (p=0.08, W=52).

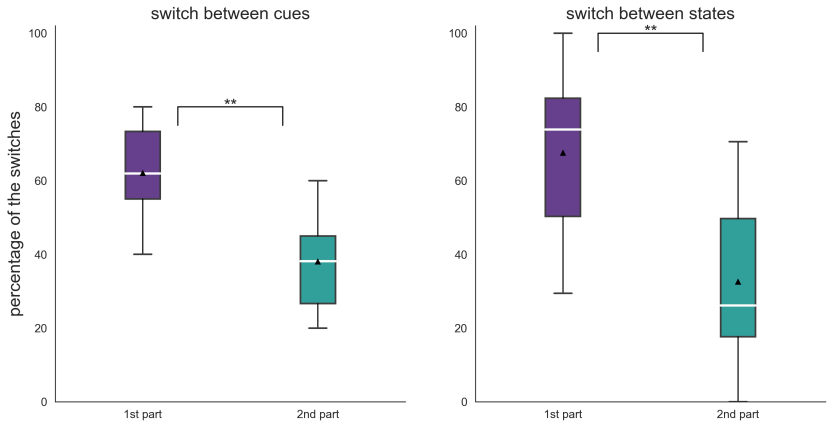

Figure 3.11: Percentage of behavioural switches count during flight trajectories belonging to Cluster 1. A: Distribution of the proportion of switches across flights between the two fictive nest-holes during the first half (purple box) and during the second half of the flights (green box). Black triangle represents the mean and the white line the median B: Distribution of the proportion of switches across flights between the two height levels in the first and the second half of the flights. In both cases there is a significant difference between the two halves of the flights with p<0.01 (Wilcoxon paired signed-rank test).

Figure 3.12: Event-plot of the trajectories belonging to Cluster 1. Each horizontal subplot corresponds to a trajectory represented along time in minutes. Vertical brown and blue bars indicated the time when the bumblebees is in the SAN area or the CAN area, respectively. The pink triangles at the upper margin of each subplot indicate the time when the bumblebee goes from one fictive nest to the other. The yellow triangles at the bottom margin of each subplot indicate the switching times between the lower and the upper part of the arena.

3.4 Discussion

Hymenopteran insects, such as bumblebees, wasps or ants, which arrive near their nests after a foraging trip, rely on the visual landscape around the nest to find its entrance, which is usually not very visible. Scientists suggest that these insects memorise their visual environment in the form of one or more panoramic snapshots containing information about surrounding visual landmarks (see Chapter 2 and [55, 203, 27]). What happens when the visual landscape when they return home, differs from the one previously memorised on their first trips outside? In the wild, insects have a wide range of options available to them. They are certainly not dependent on a single mechanism, as visual guidance is part of a broader set of tools used to perform navigational tasks. For example, insects can respond to this challenge by using non-visual cues, such as smell, or by following the direction determined from the integration of direction and distance of their outbound flight. However, path-integration (PI) can be prone to error, and visual cues are often weighted more heavily when present [196, 43]. Besides, several environmental factors could prevent the insect to confidently using these alternatives: a cloudy day, preventing the sky's polarised light from being used as a directional cue for the PI [58], or wind blowing away potential odour clues from the nest.

We, therefore, studied, in an experimenter-defined lab setting, how bumblebees face situations of visual conflict between two constellations of landmarks (small cylinders around the nest-hole and a pattern of asymmetrical stripes on the wall of the flight arena). We designed experiments in a way that the bumblebees could not use other cues; for example, the structures carrying the cameras above the arena were hidden as they could have been used as a compass, and the floor was covered with wood chips

that were shaken after each recording session, displacing any chemical cues marking the nest entrance.

Did our installation meet the requirement that no other cues, apart from those specified by the experimenter, could be used by the bees for guidance?

After foraging, when the bees entered the flight arena and the cues were displaced, we observed strongly directed search behaviour in the vicinity of the fictive nest-holes, as defined by the two constellations of visual cues. This behaviour was consistent irrespective of the location of the associated nest (CAN and SAN) relative to the location of the real nest (Fig 3.5). Indeed, when the two benchmark constellations were largely displaced from their initial position, the proportion of time spent at them was not affected by it. It is therefore unlikely that the bumblebees used other cues, such as a compass or an odour that could evaporate from the actual nest. Nevertheless, bumblebees were able to return to their nest on many occasions within the allotted time (Fig 3.3); consequently, to reach their nest entrance, they had to first leave the area around the fictive nest-hole as defined by the cue constellations.

When and how did the bumblebees find their real nest?

First of all, we observed a relationship between bumblebee nest finding performance over time and the location of the SAN relative to the RN. This relationship is plausible since bumblebees have focused their search on the location of the SAN and are therefore more likely to accidentally encounter their actual nest if it is close to their search area. Nevertheless, even though the return time increased with the distance between the SAN and the RN, bumblebees found their nests in many other situations. Ignoring flights with the SAN close to the RN (45° angle to the real nest), bumblebees found the nest on average (in all other conflict condi-

tions) after 2 minutes and 49 seconds (±1:56). It is therefore evident that bumblebees could leave the area around the fictitious nest-holes if they managed to return to their nest.

What strategy did the bumblebees use to successfully leave the fictive nest areas as defined by the visual cues?

When animals are lost and unable to find the goal they are heading towards, they usually adopt what is called a search behaviour. Search behaviour has been described for many species, including social hymenopterans such as ants [147, 187]. In the case of ants living in a dry salt pan, which is a visually barren habitat, when ants do not find their nest, they immediately engage in a systematic search focused on the location given by their path-integration [148]. This search consists of walking in a spiral around the starting point of the search while increasing its radius. This behaviour could prove to be optimal, as there is no time to lose when you are an easy prey for predators or the victim of the burning sun. However, when searching in a visually richer habitat or by adding visual cues in the desert, the behavioural pattern is different. The ant does not progressively increase its distance from the search starting point; in fact, the search is much more condensed towards it. This observation is similar to the behaviour observed for our bumblebees, which reveal dense clumps of search at the supposed nest location indicated by the visual cues (Fig 3.12). For flying insects, another study has shown that after being captured in their hive and released further, bees engage in a strategy called optimal looping levy-flight strategy [140]. This type of search involves a random component that shapes the behaviour. This random component has been interpreted as a consequence of an inaccurate navigation system and the bees' inability to recognise an area already visited. On the basis of our analysis, we cannot draw conclusions in this respect, as it was found that the search of our bumblebees was strongly deter-

mined by the location of the visual cues. Since the study by Reynolds et al. 2007 did not take into account an essential aspect of bee flight, namely its third dimension, the results obtained in this study cannot be directly linked to the 3D search model we characterised for bumblebees. Overall, bumblebees showed a very different search pattern from a levy-flight. Therefore, they are likely to use another strategy to return home in our study.

The question remains, therefore, what behaviour do bumblebees adopt when confronted with visual ambiguities about the location of their nest?

It should first be possible to establish groups for which the trajectories would be globally similar. Unfortunately, we cannot only group them according to the degree of conflict. Indeed, in situations of visual conflict, bumblebees showed a wide variety of behaviours that were not always related to the spatial arrangement of the cues in the arena. For these reasons, a clustering analysis was carried out to assess whether these different return flights could be separated into distinct behavioural classes. This classification was based on behavioural characteristics related to the spatial and temporal structure of the flight (e.g. search duration). The clustering analysis found four classes of trajectories; two of them were studied in more detail. Of the two groups not included in the analysis, the first includes most short flights because the behaviour stopped abruptly when the bee found the nest-hole. Therefore, these trajectories cannot be easily compared with the longer trajectories. We also excluded for this analysis those flights where the bumblebees spent a large part of their time flying against the translucent ceiling while trying to leave the flying arena. This behaviour is remarkable and could be due to a lack of motivation or a desire to escape; however, to assess the reasons for such behaviour, further experimental analysis would have been necessary.

In this detailed analysis, we focused on flight trajectories exhibiting mostly genuine search for the nest entrance, for example, by analysing trajectories where bumblebees alternate their search between the two fictive nest-holes. To understand this behaviour, we need to return to the studies of visually based homing strategies done in Chapter 2. Bumblebees on their return journey follow the indication, i.e. the homing vector, given by one, or a combination of visual guidance. Finally, all homing vectors in the same plane of the arena are integrated to form a potential, indicating where the bumblebee is steered. As a result, the area around the nest in which the homing vectors indicates the goal, thus where the bumblebee can return home, i.e. the catchment-area, may vary in shape depending on the visual strategy used. The catchment-area is highly correlated with the position of the visual cues. Indeed, we found that for the visual strategies that correctly predict the location of the bumblebee in conflict situations, catchment-areas were formed at the locations indicated by the two constellations. In the centre of these areas, the visual environment may be similar to the memory, or at least more alike than the surrounding points; i.e. a local-minima. When the bumblebee is at a local-minima indicated by the chosen homing strategy, if not using other strategies in parallel, this one is unable to leave its position. However, because we observe the bumblebee changing between the two fictive nest entrances, it implies that they can escape a local-minima. A second relevant observation is the changes in altitude during the return flights. The bumblebees did not continuously search in the fictive nest areas defined by the cues. They often interrupted this search by flying in the upper part of the arena. Because of the location of the nest in the ground, it seems warranted to consider the flight sections near the arena floor as "search behaviour", whereas the flight sections in the upper part of the arena probably do not reflect this search behaviour. However, this categorisation should be reconsidered.

Would there be any functional importance of gaining height while the nest is located in the ground?

Intuitively, gaining altitude is something we may have experienced and try ourselves when we are lost in a forest, for example. From a higher vantage point, we can see a larger area of the surroundings and can find known landmarks that were not previously visible at a lower altitude. In our arena, the bumblebees may as well try to get a better view of the landmark constellations by gaining height, if they cannot find their nest. Indeed, the cylinders are quite small and hardly visible to the bumblebees when flying on the other side of the arena, their angular size is not more than 1.15° when observed at a distance of one meter and therefore only perceptible by the front part of the bumblebee's eye [168]. Furthermore, the catchment-area corresponding to either of the fictive nest-holes is not only two-dimensional but extends along the elevation of the flight arena forming a catchment-volume. Nevertheless, depending on the visual tracking strategy used, the resulting potential can be noisy and create many local minima at positions quite different from the areas defined by the constellations. Therefore, these minima may also appear or disappear with changes in altitude [126]. Consequently, gaining height could be a way for bumblebees to escape a local-minima, and in our current design, to pass from the catchment volumes defined by the stripes to the one defined by the cylinders. Indeed, the size of catchment-volume may increase with altitude, allowing a transition between them as suggested in a study by Murray et al. 2017. In our observations, many bees gain in height and leave the lower part of the arena before switching to the space defined by the other landmark constellation (Fig 3.12). Finally, according to this hypothesis and because the SAN attracts most of the search behaviour, we can assume that the catchment-volume of the CAN is rather small compared to the one of the SAN. As a result, bumblebees may be unable to leave the capture volume of the SAN in many cases, such as in the

trajectories forming cluster 4. In conclusion, the altitude changes during return flights can be interpreted as a switch between a "visual matching" performed at ground level, where bees try to match their memory to the real scene, to a second process being more of a "gradient evaluation" done at a higher altitude.

Finally, the frequency of passages between the fictive nests and the lower and upper parts of the flying arena decreases during the test, suggesting that bumblebees reduce their energy costs or that they are more confident about the selected fictive nest. Although these observations are mostly correct, there is still some behavioural variability, and a more detailed temporal analysis is undoubtedly required.

3.5 Conclusion

The behavioural repertoire exhibited by homing bumblebees when confronted with a visual conflict situation is not yet fully understood, although this study provided some new insight on the possibility that switching between different behavioural modules may play a role during search for the goal. Therefore, tools such as unsupervised classification analysis came in handy to classify and quantify behaviours and to conduct meaningful comparisons. However, this approach may have dismissed important aspects of the temporal variability of behaviour.

Nevertheless, some behavioural modules could be pinpointed to some extent. Bumblebees are suggested by our analysis to switch between the

catchment areas defined by the different cue constellations and are hypothesized to use a changes in elevation to redirect their search. This hypothesis gives some perspective to design insect-inspired visually guided homing models involving two additional dimensions: elevation and time.

4 Learning while flying: how do bumblebees stabilised their head during the initial phase of learning flights?

4.1 Introduction

When leaving a relevant location for the first times, such as the nest or a food source, many flying hymenopterans perform complex aerobatic manoeuvres called learning or orientation flights (honeybees [181, 24, 25], wasps [201, 42], bumblebees [107]). The insect starts this routine by leaving its inconspicuous nest-hole in the ground or a tree; then it turns back to face its nest entrance while moving away from it with an increasing altitude. All learning flights of hymenopterans appear at first similar, but, there is some variation across species. For example, solitary wasps fly in arcs with ever-increasing radii [201, 40], whereas bumblebees loop around their nest-hole in a less structured manner [107, 134].

Despite these differences, all learning flights are thought to be the basis for the visual acquisition of the nest surroundings, as first shown in early experiments where pine cones, located around a nest-hole of digger

wasps were displaced and led to false returns [169]. Many experiments also revealed the ability of bees to learn artificial visual landmarks to find back home or a food source [99, 26, 57]. Nevertheless, which exact properties of the visual cues are learned is still unknown. One way to answer this question is to look at the learning flight choreography. Indeed, learning flights are supposedly the reflection of an active vision strategy to collect useful visual information for later returns [165, 68]. Accordingly, the learning of visual information does not only depend on but also shapes the way the insects fly [60, 100].

For example, while flying, the pattern of apparent motion of the surrounding scenery on the animal's retina, called the optic-flow (OF), is an important visual cue providing information about self-motion and the 3D layout of the environment, easing navigation since it even allows to decamouflage textured objects against a similarly textured background [56]. In theory, distance information can be derived from the OF solely during translational movements ("motion-parallax"), i.e. when the flow field on the eyes is dominated by its translational component [176]. Accordingly, many flying animals adopt an active vision strategy to segregate translational movements from rotations. This one is called a saccadic flight and gaze strategy. In essence, the animals show periods of constant gaze by stabilising their head orientation, interrupted by fast head rotations mainly around the vertical-axis (blowfly [176], *Drosophila* [122]; honeybees: [13], birds [59, 143]). During pure rotations, the amplitude of image displacements is independent of the spatial arrangement of objects; thus, it does not carry information about the distance to objects and depends only on the dynamics of self-motion.

This saccadic flight and gaze strategy has been described for a variety of flying insects. Indeed, saccades are easily detectable as rapid and relatively large changes in head direction. In comparison to saccades,

the rotations during intersaccadic intervals are much smaller. This poses the problem that it is methodologically much more difficult to unravel to what extent the relatively small residual rotations can be regarded as noise, or still have a systematic directional component. These rotations may even hint at a different functional significance of the intersaccadic OF and may be actively controlled [141, 15]. In contrast to motion-parallax, the OF resulting from these rotations would lead to some pivoting around a so-called 'pivoting point', thus, providing spatial information relative to this point in space ('pivoting-parallax'). The difficulty of assessing the intersaccadic head movements and, accordingly, the corresponding OF is the consequence of considerable technological limitations to get a precise estimation of the head orientation. Consequently, a detailed analysis of head orientation, especially during intersaccadic intervals is usually missing, while this issue might be the key to understanding what information is provided by the visual input during learning flights allowing to find out the basis of a successful return home.

In this study, we tracked at unprecedented precision the head orientation of bumblebees, *Bombus terrrestris*, during learning flights, and characterise its dynamics around all three axes of rotations (x,y and z-axis). On this basis, we could unravel the consequences of head dynamics on the visual input and its consequence for the OF experienced especially during intersaccades. We investigated the plausibility of bumblebees performing either motion-parallax or pivoting-parallax during intersaccadic intervals, thus, potentially extracting distance information relative to themselves or to a pivoting point, respectively. We do this by a systematic analysis based on signal-to-noise-ratio calculations for both active vision strategies. Furthermore, we scrutinized to some extent at the idiosyncrasies of head movements during the initial phase of learning flights.

4.2 Materials and Methods

4.2.1 Experimental set-up

We used a hive of *Bombus terrestris* with a small number of individuals provided by Koppert B.V., The Netherlands. Bumblebees had access to pollen ad libitum in their hive. The hive was placed in a Perspex box connected by transparent tubing to a flight arena (Fig 4.1). The bumblebees entered the metallic cylindrical flight arena (diameter: 70cm, height: 50 cm) through a 1 cm hole in the middle of its floor. In the arena centre, a circular area of the floor of 3.5 cm diameter was elevated by five millimetres. To allow the lighting of the set-up and recording of learning flights, the arena was covered with a transparent Perspex lid. The walls and floor of the arena were covered by a random white and red pattern that was spatially low-pass filtered leading to a pattern with a 1/f frequency distribution (pink noise) providing the bumblebees with enough contrast to use the OF. We did not introduce artificial landmarks, in the hope that the head movements will not be biased by the animal looking at prominent landmarks in the environment. Indeed, such landmarks might drive the attention of the bumblebees during learning [128]; thus, impairing the investigation about a potential pivoting-parallax performed around the nest-hole. After completing their learning flights, bumblebees were able to leave the flight arena via a hole of 10 cm diameter, the exit-hole, giving access to a transparent tube leading to a foraging chamber with an artificial feeder containing a sucrose solution (30% saccharose).

However, during our experiments no bumblebees with markers found its way to the foraging chamber. This exit-hole, in addition to the nest-hole itself, was the only distinct visual landmark which was in the height range where bumblebee would fly in our recordings (exit-hole centre located at 12 cm above the ground).

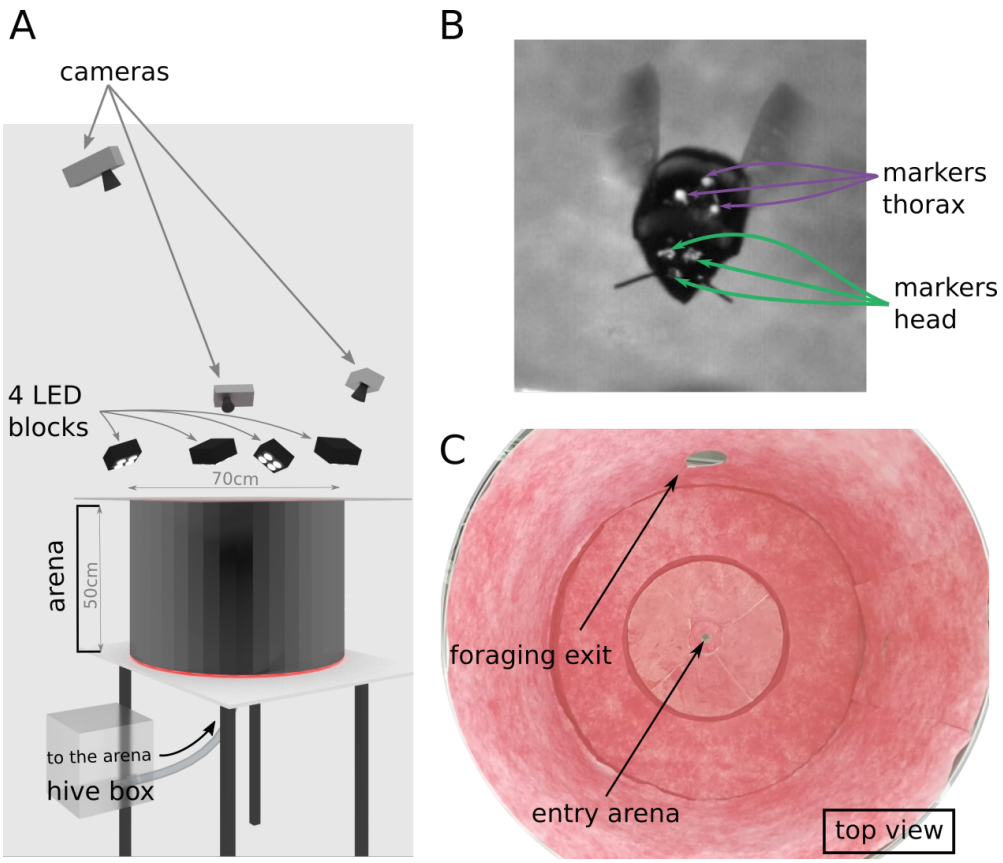

Figure 4.1: Experimental set-up. A: Representation of the experimental set-up recreated with Blender. The bumblebee enters the flight arena through the nest-hole connected by a tube to the hive. The bumblebee takes off from the center of the arena. Learning flights were recorded by 3 cameras from above the arena. The flight arena was illuminated by four blocks of four LEDs. The roof of the arena was a transparent Perspex plate. B: Single cropped frame from our footage showing a marked bumblebee during a learning flight; green arrows indicate the head markers and purple arrows point to the 3 thorax markers. C: Photograph of the inside texture of the arena as used during experiments, showing entry hole and exit to the foraging. Walls are covered with a red noise pattern.

4.2.2 Animal preparation

We caught several bumblebees from the hive to place head and thorax markers on them. The bees were kept under mechanical constraint to be marked without anaesthesia. We drew three small dots (approximately 1mm diameter each) of acrylic paint on the bee's head: one above each eye and the third in between the two eyes at the height of the antennae scape insertion point, similarly to Riabinina et al.(2014)[141]. During the marking procedure, attention was paid to not cover the ocelli and bumblebees' eyes (Fig 4.1B). We used an equilateral triangle (side length of 5mm) of black paper with a white pearl dot (1mm diameter) at each apex to mark the thorax (inspired from [138]). Thorax markers were fixed with a mixture of bee wax and tree sap centred between the two wings and in alignment with the longitudinal body axis. After marking, we placed the bumblebees back to the hive. To assess potential individual differences, or an experience-dependant impact on the head dynamics during the initial phase of learning flights, we post-identified the different individuals. A tag for identification could not be placed on the bumblebees as they would interfere with the automatic tracking of our markers. So, from a close look on the recordings, the tiny differences between the head markers' shape could be used for identification of the bumblebee. We conclude that 4 flights are performed by the individual named 'a' (flights id numbers 1,2,3,4 in chronological order), and flight 5 and 6 being learning flights of two different individuals b and c, thus; leading to 3 individuals and 6 recordings.

4.2.3 Tracking of head and thorax markers

We recorded the flights via three high-speed cameras (Optronis CR3000x2) with a resolution of 1710*1696 pixels. The three cameras placed above the arena at different positions and viewing directions, recorded a volume of approximately 10*10*10 cm^3 around the nest-hole (Fig 4.1A). The recording area was restricted to just a small part of the arena to allow monitoring the head and thorax orientation at a sufficiently high resolution. The recording volume was illuminated by four blocks of four LEDs each (HIB Multihead LED, HS vision GmbH, Germany)(Fig 4.1A). When a bee entered the arena from the nest-hole, we started the recording as soon as the bumblebee took-off to perform a learning flight. Recordings were made at a shutter speed of 1/2000s, a frame rate of 500 frames per second, and for approximately 11 seconds. The three cameras were calibrated with the Matlab toolbox dltdv5 (Hedrick 2008). We tracked the head and thorax markers with a custom-made Python script, based on open CV. The videos were then manually reviewed with the software IVtrace (`https://opensource.cit-ec.de/projects/ivtools`); in case of tracking errors, the marker positions could be manually set. Finally, the markers' positions in 3D space were reconstructed (Hedrick, 2008). After each learning flight, the recorded bumblebee returned to the hive without visiting the foraging chamber. This finding can be explained due to the experiments being performed only over 5 days, so most bumblebees did not have enough time to learn the location of the foraging chamber and because there was maybe enough food stored in the honey pots already present upon delivery. In this manner, our recorded bumblebees (a,b and c) could be considered as "novices". For example, ants novices are thought to perform learning walks of a similar structure until they accidentally discover a food source [66]. This

observation, extended to our bumblebees, allows us to consider the multiple learning flights performed by individual 'a' in a similar way.

4.2.4 Head and thorax spatial orientation

To accurately monitor the movements and orientation of the animal's thorax and head, we reconstructed the head and thorax markers' positions. Indeed, head and thorax orientation are subject to different functional constraints and, thus, often not aligned with each other. For instance, the thorax executes large roll movements during curves or sideways translation to generate appropriate torque moments or forces, while the head compensates for these to a large extent [15, 14]. Therefore, head orientation and thus, gaze direction can only be inferred to a rather limited extent from the thorax orientation. Consequently, to reconstruct the head and thorax orientation we defined three coordinate systems: the reference frame of (1) the head- (HCS) and (2) the thorax-centred (TCS) coordinate systems as defined by the head or thorax markers, respectively, and (3) the world coordinate system (WCS) attached to the flight arena (Fig 4.2A&B). Head and thorax global orientations were determined as the angle required to align the HCS and TCS, respectively, with the world coordinate system. We determined for each captured frame the instantaneous yaw, pitch, roll (YPR) angles of head and thorax, respectively. Each angle was determined in the following order corresponding to Diebel's (2006) convention: first rotation along the animal's roll (x-axis); second, rotation along the pitch axis (y-axis); third, rotation along the yaw axis (z-axis). Similar methods have already been used to estimate instantaneous orientations in previous studies on a variety of flying animals [137, 132]. Each YPR angle was smoothed with a planar cubic spline function (Scipy.signal package) with smoothing parameter (lambda = 150) interpreted as the degree of freedom, and estimated by general-

ized cross-validation criterion (smooth.spline R function). Cubic splines are often used in biomechanics data filtering [191] due to its underlying cubic polynomial representation which gives continuous first and second derivatives (speed and acceleration respectively), necessary in our case for the saccade extraction. Examples of filtered time courses of the head and thorax YPR angles are shown in (Fig 4.2). Finally, from the YPR orientation, the respective angular velocities referred as w_x, w_y and w_z were expressed in the HCS and TCS, following Diebels et al. Equation 39-40 p9 , so velocities are expressed along the x,y and z axis of the corresponding body segment.

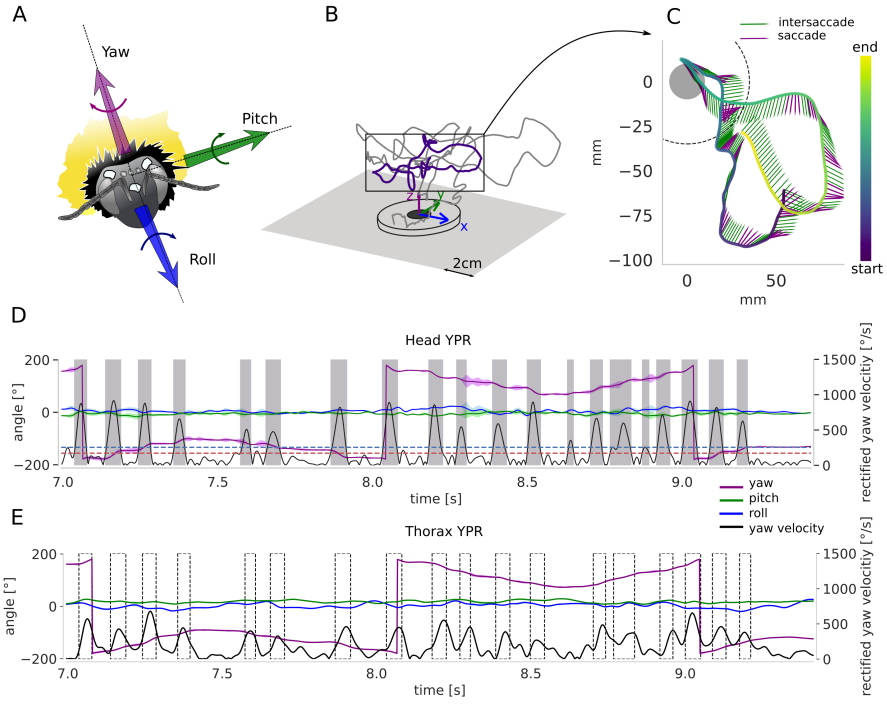

Figure 4.2: Head and thorax spatial orientation. A: The head coordinate-system: the bumblebee head with the three markers and the yaw pitch and roll axis. B: The world coordinate system: 3D representation of a learning flight's initial phase. C: Top-view of the learning flight section showing the downsampled yaw orientation. The head direction is indicated by the arrows' head. Time along the trajectory is indicated by the the arrow head colour, following the "colorbar" at the right. Purple arrows indicate saccades and green intersaccades. D: Filtered time courses of the head YPR orientation for the flight section shown in C, with yaw in purple, pitch in green, roll in blue. Each orientation is overlaid with its error in degrees. Rectified yaw velocity on the right axis (black). Grey shaded areas represents saccades determined by the two-thresholds method (see text): for the head, onset threshold (upper blue line) = $372.42°.s^{-1}$ and ending threshold 2 (lower red line) = $200.5\ °.s^{-1}$. E: Filtered time courses of the thorax YPR orientation (left-axis) and yaw-rectified velocity (right-axis) for the flight section shown in C, similar legends as in D. Saccades as defined on the basis of head velocity is indicated by dotted blocks.

4.2.5 Saccade extraction

Based on the rectified yaw velocity time courses (obtained from smoothed yaw angle time courses), we investigated the saccadic flight and gaze strategy. To do so, we determined head saccades as periods where yaw velocity exceeded a given threshold ($372.42°.s^{-1}$, as in [141]) and until it decreased below another threshold ($200.53°.s^{-1}$) (Fig 2). We applied this two-thresholds method automatically to all flights (Fig 4.2D).

4.2.6 Tracking error propagation

We propagated the error from the tracking to the YPR orientation at each time point for each trajectory. To estimate our tracking error, we calculated for each bee the deviation of each frame from the average distance between each pair of markers across all frames. This average distance is hypothesized to be the actual distance between the markers, which is in theory constant for each pair of markers. Therefore, any deviation from this value is the result of a tracking error. We kept the worst 'tracking error', $\varepsilon(t)$, from all the pairs to populate a co-variance matrix, σ measured (1). This covariance matrix is highly simplified, since the error is assumed to be the same for all markers along the different axes. The 'co-variance' components are not considered , i.e. the off-diagonals terms are simply 0

since the error of the different measures are considered uncorrelated [83] see (1).

$$\sigma_{measure} = \begin{matrix} x_0 & \cdots & z_2 \end{matrix} \begin{matrix} \\ \\ \\ \end{matrix} \begin{pmatrix} \epsilon(t) & \cdots & 0 \\ & \ddots & \\ 0 & \cdots & \epsilon(t) \end{pmatrix} \begin{matrix} x_0 \\ \vdots \\ z_2 \end{matrix} \tag{4.1}$$

The error propagation was calculated by applying the co-variance matrix to a numerically estimated Jacobian matrix (2) so $\sigma_{bee} = J\sigma_{measure}$. The Jacobian was numerically evaluated because of the high number of functions on which the expression of YPR of the head depends, this one derived from the three head markers' positions xyz_0, xyz_1, xyz_2 (3).

$$J = \begin{pmatrix} \frac{\partial f_x}{\partial x_0} & \frac{\partial f_x}{\partial y_0} & \frac{\partial f_x}{\partial z_0} & \cdots & \frac{\partial f_x}{\partial z_2} \\ \vdots & & & & \\ \frac{\partial f_{roll}}{\partial x_0} & \frac{\partial f_{roll}}{\partial y_0} & \frac{\partial f_{roll}}{\partial z_0} & \cdots & \frac{\partial f_{roll}}{\partial z_2} \end{pmatrix}$$

$$\frac{\partial f_x}{\partial x_0} = \frac{f(x_0 + h, y_0, \cdots, z_2) - f(x_0 - h, y_0, \cdots, z_2)}{2h} \tag{4.2}$$

where:

$$h = 10^{-6}$$

$$\begin{pmatrix} \mathrm{x_{bee}} \\ \mathrm{y_{bee}} \\ \mathrm{z_{bee}} \\ \mathrm{yaw_{bee}} \\ \mathrm{pitch_{bee}} \\ \mathrm{roll_{bee}} \end{pmatrix} = f(x_{m0}, y_{m0}, z_{m0}, ...x_{m2}, y_{m2}, z_{m2})$$

$$\begin{pmatrix} \mathrm{x_{bee}} \\ \mathrm{y_{bee}} \\ \mathrm{z_{bee}} \\ \mathrm{yaw_{bee}} \\ \mathrm{pitch_{bee}} \\ \mathrm{roll_{bee}} \end{pmatrix} = \begin{pmatrix} f_x(x_0, ..., z_2) \\ f_y(x_0, ..., z_2) \\ f_z(x_0, ..., z_2) \\ f_{yaw}(x_0, ..., z_2) \\ f_{pitch}(x_0, ..., z_2) \\ f_{roll}(x_0, ..., z_2) \end{pmatrix} \tag{4.3}$$

The angular error calculated by this method along the YPR for each time course is overlaid on the YPR orientation in Fig 2.

4.2.7 Analysis of head and thorax rotations

The frequency spectrum of head and thorax YPR changes along time, were characterized by applying a Fast Fourier transform using Welch's method similar to Kern et al. 2006 [90]. In detail, yaw, pitch and roll angular velocities were split into data segments of 388 frames (=0.7s), being the median length of continuous recording sequences without missing values, while too short continuous recordings,<388 frames, were discarded. By picking the median length of the data sequence, the trade-off between high-resolution and discarding data was optimized. Finally, Welch's method divides the continuous sequence into overlapping segments of the chosen length (when possible, i.e. >388 frames); here we choose an overlap of 50% (i.e. the recommended value for the method). For each seg-

ment a periodogram was calculated and then averaged leading to a new periodogram: This method reduces the variance of the estimated power-spectra density [161]. We obtained the power-spectra for each w_x, w_y, w_z and compared them depending on the studied body-segment. Later, density distribution of angular velocities during the saccadic and inter-saccadic intervals were characterized separately.

4.2.8 Retinal projection

To analyse how the nest and exit-hole are displaced on the retina during learning flights, their coordinates were transformed from the Cartesian WCS in x,y and z, to the spherical HCS in azimuth and elevation. This was done first, with the real YPR orientation and then by considering a stabilised roll (roll =0°) and a constant pitch (pitch equals to the median pitch).

4.2.9 OF analysis

The OF calculation

From the head orientation and position we computed for each flight trajectory the experienced OF induced by the head motion at equally spaced sampling points around the nest-hole (on a 10cm^2 grid centred at the nest-hole) and one point at the exit-hole's centre. For each projected point, the translational and rotational component of the OF averaged along the intersaccadic interval was determined following the equations given by Koenderink 1987 [92]. From the formula describing the displacement of a point (at the positions Q_i) along time relative to the vantage point of

an eye (4.4), the geometrical optical flow is the time derivative of the change in the direction of this point, see equation (4.5). To ease computation Eq. (4.5) is a simplification, since a dimensionless combination is formed from the speed and nearness (i.e; the product between speed and real nearness). From this product, nearness can be expressed as the 'reduced nearness' (or also known as 'time-to-contact'). By doing so, the speed does not longer play a role allowing the resolution of the equation to find the geometrical OF by reducing the number of unknown components (such as the unknown 3 rotational components, for detail see Koenderink 1987). In equation 2, t is a vector representing the direction of the translation, d_i is the viewing direction of the point, μ_i is the reduced nearness. Finally (4.5) is written, such as in eq. (4.6), where A_i represents the 'apparent rotation' due to a translation. Thus, Eq (4.6) separates the translational (A_i) and rotational component (R_i) of the flow field. This equation is expressed in a Cartesian coordinate system where the OF is a vector with the components OFx, OFy and OFz along x, y and z, respectively. It needs to be converted to a spherical coordinate system to match the OF experienced by a spherical eye, following the method described in Bertrand et al. 2014 [9].

$$\Delta \mathrm{Q_i} = -(T + R \times Q_i)\delta \mathrm{t} \tag{4.4}$$

$$\mathrm{OF_g} = \mu_i(t - (t \times d_i)d_i) - R \times d_i \tag{4.5}$$

$$\mathrm{OF_g} = -(A_i + R) \times d_i \tag{4.6}$$

Assessment of the signal-to-noise-ratio for two active vision strategies

We wanted to investigate how much distance information a bumblebee could gain during intersaccadic intervals. This information is contained by the OF pattern on the eye. Depending on the active vision strategy used, motion-parallax vs. pivoting-parallax, during intersaccades the resulting OF pattern and, thus, the available distance information, would be different. Therefore, the OF pattern must be read accordingly to the use strategy.

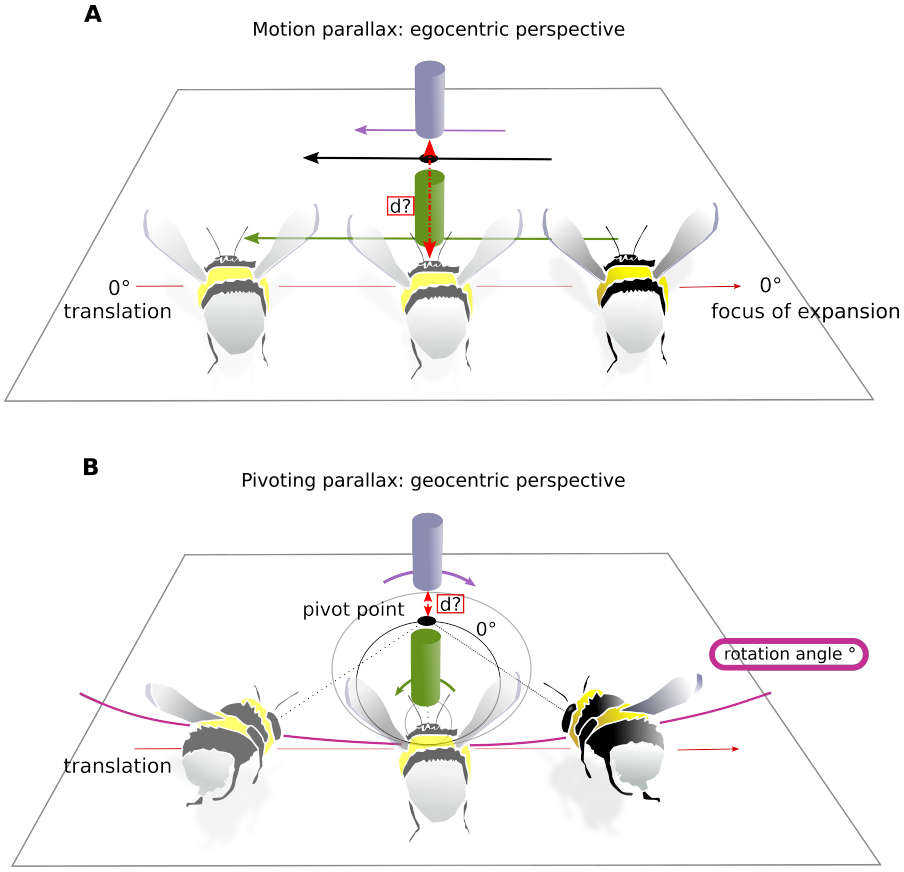

Figure 4.3: Two active vision strategies A: Motion-parallax. As a consequence of translation the bumblebee gains distance information about the landmarks relative to its own current position. Here the purple landmark moves slower on the bumblebee's eye than the green landmark. Thus, the purple object is more distant to the bumblebee. B: Pivoting-parallax. The bumblebee pivot around a point, the pivot-point, by a certain rotation angle while translating. By doing so the bumblebee gains distance information relative to the pivot point. Here, the purple landmark moves in the opposite direction on the retinae to the green landmark, because the latter is placed in between the pivot point and the bumblebee. The black circle represents the zero-horopter (as named in Zeil et al; 1993[201]), this one separates areas of image motion with opposite sign: inside the horopter, the green landmark follow the rotation of the bumblebee and outside, the purple landmark moves in the opposite direction.

SNR for motion-parallax Firstly, we assumed the bumblebee to use an active vision strategy based on pure motion-parallax to extract distance information from the OF (Fig 4.3A). During motion-parallax, the head is stabilised along the YPR axis. Then, only translational movements of the head affect the OF. During this translation, the nearest objects move faster on the retina, and the furthest ones slower. Therefore, from their apparent movement distance from an egocentric perspective can be derived. To investigate how much information can be extracted from the real OF by employing such a strategy we computed a signal-to-noise ratio (Fig 4.4). The signal is obtained from an ideal trajectory setting the intersaccadic head rotations to zero, leading to a perfect motion-parallax. To compute this ideal trajectory we simulated a trajectory based on the real x,y and z coordinates of the bumblebee's head during each intersaccade but set its yaw, pitch and roll orientation constant during this interval (average value over the intersaccade). From this simulated trajectory we obtain the theoretical OF. Then, we calculated the norm of the average theoretical OF over the intersaccade for two different projected points on the retina : the exit-hole and the nest-hole (and 100 points around the latter), because the nest-hole and the exit-hole are the only behaviourally immediately relevant and visually distinct locations in the flight arena. The resulting value at each point for each intersaccade is our signal. The noise is then the difference between the average measured OF norm obtained from our original trajectory and the theoretical OF norm (our signal) (Fig 4.4). A $\log_{10}$ SNR below 0 indicates the noise to be larger than the signal, thus, distance extraction from the OF to be compromised.

SNR for pivoting-parallax We also determined the signal-to-noise to assess the plausibility of the animals using pivoting-parallax during intersaccadic intervals to gain distance information, implying that the residual

intersaccadic rotations cannot be regarded as noise, but are of functional significance. During pivoting, uni-directional rotations around the yaw axis yield the retinal fixation of a specific point in space (Fig 4.4). In this way, distances could be estimated relative to this pivoting point (geocentric perspective) [for details see [201, 45] and Fig 4.3B] and not from an egocentric perspective as during motion-parallax (Fig 4.3A&B). To assess this possibility, we simulated an ideal trajectory based on the measured one where the overall intersaccadic rotations are assumed to be the basis of a pivoting-parallax. To do so, we assumed a uni-directional drift of yaw orientation, which yields to a pivoting. This drift was obtained by fitting a linear regression to the measured time-dependent yaw orientation during each intersaccade. Similarly to motion-parallax, we define the SNR from the nest-hole's apparent-motion during our trajectory: the SNR is the ratio between the signal (i.e. the norm of the OF averages from the theoretical trajectory) and the noise (i.e. the difference between our measured OF norm and the signal).

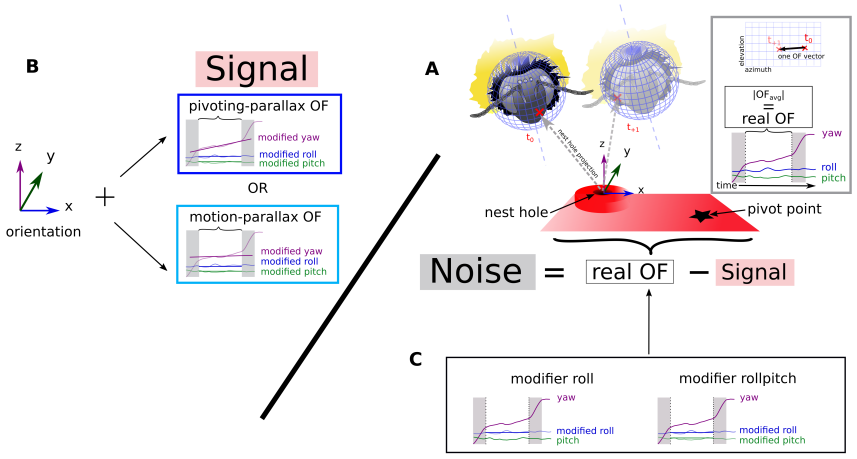

Figure 4.4: Calculation of the signal-to-noise ratio for the nest-hole projection during one intersaccade. From the x,y,z head coordinates and the YPR orientation of the head during an intersaccade, an OF vector at the nest retinal projection is computed for each time point and all are averaged over the intersaccade, the norm of the average OF vector is our real OF (A). Then, from this value a signal is subtracted to calculate the noise. The signal is calculated in a way depending of the tested strategy, pivoting or motion-parallax (B). For the pivoting-parallax, a linear regression is fitted to the value of intersaccadic yaw orientation. For the motion-parallax, the yaw orientation is held constant over the course of the intersaccade. For both signals roll and pitch are kept constant (median value). Then, as before, the averages of the OF norm of the projected nest gives a theoretical OF, i.e. the signal, which is either the pivoting or motion-parallax OF. Finally, we can apply two different modifiers on the real YPR orientation to calculate the SNR from a more stabilised head (C). The roll modifier, where the roll orientation is held constant and the roll-pitch modifier where roll and pitch orientations are held constant.

Both active vision strategies, aside a different control of the yaw, imply head stabilization along the pitch and roll axes. Thus, residual rotations along these axes should impair the SNR. To test if our SNR is affected by remaining pitch and roll rotations, or is mainly the consequence of head displacements along the yaw axis, we studied for both

extreme scenarios, pivoting or pure motion-parallax, the impact on the SNR of the roll and pitch rotations by keeping these constant or not. In this way, three theoretical trajectories are simulated for each scenario (1) roll and pitch are the measured ones and only the yaw is adapted, (2) roll is kept constant and pitch varies as for the real trajectory, (3) both roll and pitch are held constant, so only the yaw orientation will affect the signal-to-noise ratio. These changes on the pitch and roll rotations are later referred to as modifiers (Fig 4.4)C.

Statistical analyses are performed to investigate the differences of the SNR distribution between pivoting, motion-parallax and for the different modifiers with a one-way ANOVA due to the normality of our data (qualitative estimation with qqplot, not shown), then followed by a multiple paired t-test. All p-values were adjusted following Holm's correction for multiple hypotheses [81].

Determining pivoting points

For each intersaccade and their corresponding rotational drift angle (Fig 4.5), we calculated in two dimensions the location of the pivoting point. The z-axis was ignored as there is relatively small variation on this one, and to ease computation. During pure motion-parallax characterised by a rotational drift of 0°, there is no pivoting point as the heading directions at the start and end of the intersaccade are parallel to each other and so cross at infinity. With a rotational drift different from 0° it is possible to calculate the pivoting point coordinates of an intersaccade of drift θ and length l following Eq. 4. In this way, the pivoting point is in the heading direction of the bee if $\theta > 0$, and behind the bee (tail direction) if $\theta < 0$ (Fig 4.5A&B).

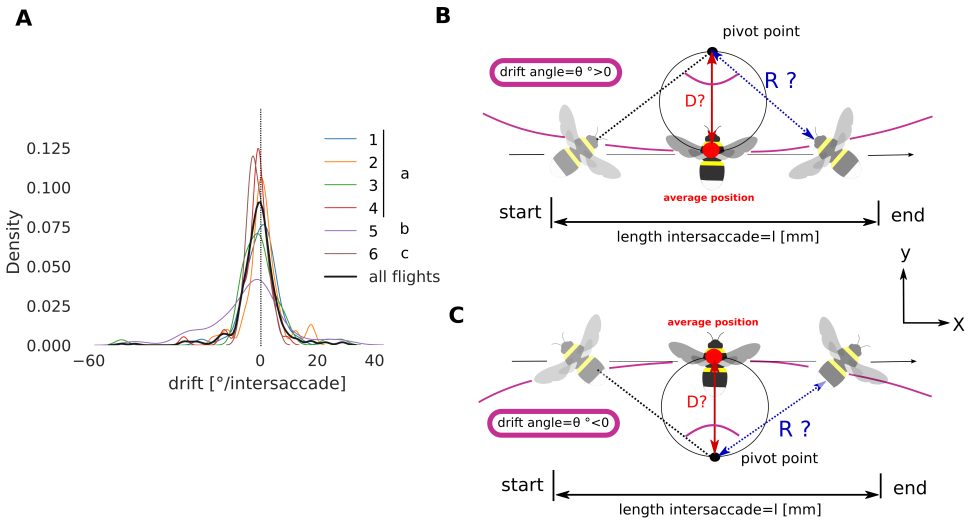

Figure 4.5: Intersaccade yaw drift and pivoting points location. A: Kernel density estimation of the yaw drift during intersaccades expressed in degrees per intersaccade. KDE for all flights (thick black line) and for each flight (coloured lines, see legend). B: Method for estimating the pivot point location. With a positive drift angle the pivot point lies in the heading direction of the bee. C: Negative drift angle, the pivot point lies behind the heading direction.

4.3 Results

4.3.1 Description of head and thorax movements

Yaw saccadic structure

The saccadic flight and gaze structure is clearly visible for the time-dependant head and thorax yaw orientation. We can observe a sharp saccadic structure of the head's yaw rotations and a smoother one for the thorax's yaw orientation (Fig 4.2 D&E). In the shown example, the thorax saccadic structure fits temporally the head's saccadic structure but with apparently slower saccades and less stabilised yaw orientation during the intersaccadic intervals. Furthermore, for a time window centred at the head saccades' velocity peak (time=0ms) (Fig 4.6 C&D), we can see that the thorax initiates the saccadic yaw turns, and this for all flights. Nevertheless, despite the thorax initiating the saccade, both segments reach their velocity peaks at the same time because the thorax turns more slowly (Fig 4.6D). This observation must be interpreted with care as it results from an overall average. Indeed, in Fig 4.2E, there are several examples of the thorax yaw velocity peak being reached later than the head's velocity peak, or on the contrary, in much rarer cases earlier than the head's peak. Overall, the thorax in general performs a longer and slower saccade centred with the head saccade's velocity peak. This observation is congruent with the idea of an active vision strategy where the body would initiate the saccade with the head following, confining head rotations to a

minimal time interval. Interestingly, the bee performing flight nb°5 shows an average yaw saccade of much smaller amplitude than the other ones (Fig 4.6D, thin purple line); this suggests inter-individual differences in the saccadic structure.

If bumblebees follow a saccadic gaze strategy, the yaw orientation is generally assumed to be stabilised during the intersaccade. In the shown example, the yaw orientation during the intersaccadic intervals appears mostly stabilised. During the intersaccade, the distribution of rectified yaw velocities mostly lie between 0 and $400°.s^{-1}$, while the rectified yaw velocity distribution during saccadic intervals spreads between 0 and 2000 $°.s^{-1}$ (Fig 4.3E). Then, we analysed if the remaining rotations are associated with low frequency unidirectional turns, later called drift. Fig 4.6 describes the distribution of angular amplitude of the yaw drift angles during intersaccades which follows a normal distribution (Agostino and Pearson: $p<0.001$) with a standard deviation of 7.7° per intersaccade. This corresponds to a median absolute yaw-drift of 2.9° per intersaccade.

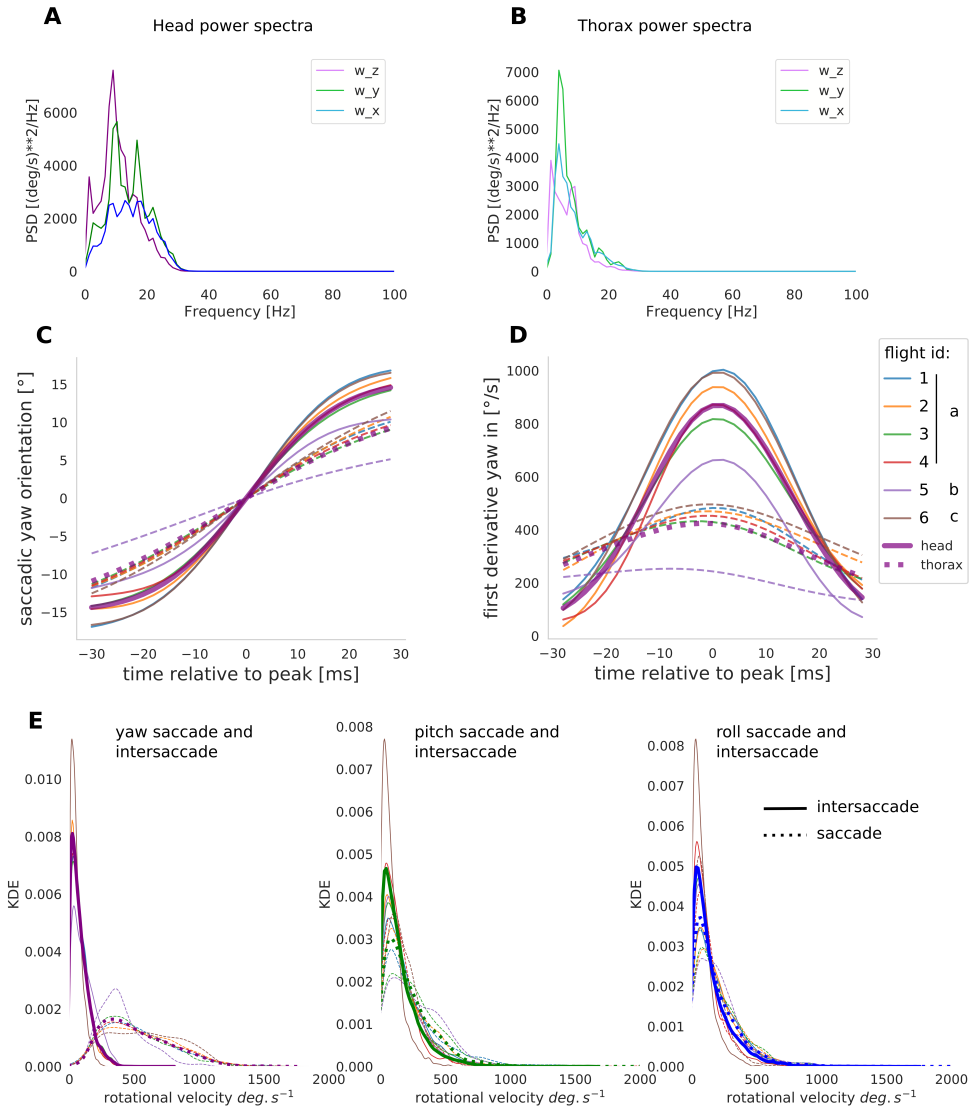

Figure 4.6: Analysis of head and thorax rotations. A: Fourrier analysis of the head YPR velocities, with the average yaw power spectra in purple, pitch in green and roll in blue, N=3, n=6. B: Fourrier analysis of the thorax YPR velocities C: Yaw orientation during saccades: head's yaw average purple line, thorax' s yaw-average dotted line, the different flights are individually coloured (blue,orange green and red (same bee 'a'), red and purple). D: Average Yaw rectified velocity during saccades. E: From left to right, distribution of yaw, pitch and roll angular velocities (w_z, w_y,w_x, respectively) during saccades (dotted line) and intersaccades (continuous line).

Roll and pitch rotations

For the sample time course shown in Fig 4.2, but also for all flights (Fig 4.11, YPR time courses are not shown for all flights), the roll orientation varies around 0° for both head and thorax. For the head, the power spectra of the roll and pitch velocities show that most fluctuations happen at frequencies around 10 and 20 hertz (Fig 4.6A). For the thorax the most prevalent frequencies are lower, i.e. below 10 hertz for the pitch velocity and 5 Hz for the roll velocity (Fig 4.6B). Predictably, the thorax rotates at lower frequencies than the head. For the yaw velocity, we also observed lower frequencies for the thorax than for the head according to the saccadic structure of learning flights. On the whole, the yaw, pitch and roll velocites of head an thorax vary at similar frequencies suggesting fluctuations around the different axes to happen at the same frequencies. By comparing intersaccades with saccades we can see that the roll and pitch angular velocity distributions are similar during both intervals (intersaccades and saccades) ranging from 0 to $1000°.s^{-1}$, but with less slow rotations during saccades (Fig 4.6E).

4.3.2 Consequences of the head movements on the visual input

Nest-hole and exit-hole retinal projection

During the analysed learning flights, the nest projection on the retina is kept for most of the time within a very broad frontal area of the eye: below 0° elevation and mostly between –75° and +75° azimuth (Fig 4.7A). Thus, bumblebees fixate their nest-hole during learning flights mostly in this eye region. In contrast, the exit-hole is moving on the retina all along

the azimuth but at a constant elevation of 0°. These observations suggest an active control of the flight to keep the nest-hole in the frontal visual field, while the other points in space move broadly on the retina. From a more stabilised head, with pitch and roll held constant, the fixation was not qualitatively improved as the nest projection lay in the same elevation and azimuth range as when the head is not perfectly stable, hence roll and pitch rotations are not actively controlled to ease this fixation but neither impair this one (Fig 4.7B).

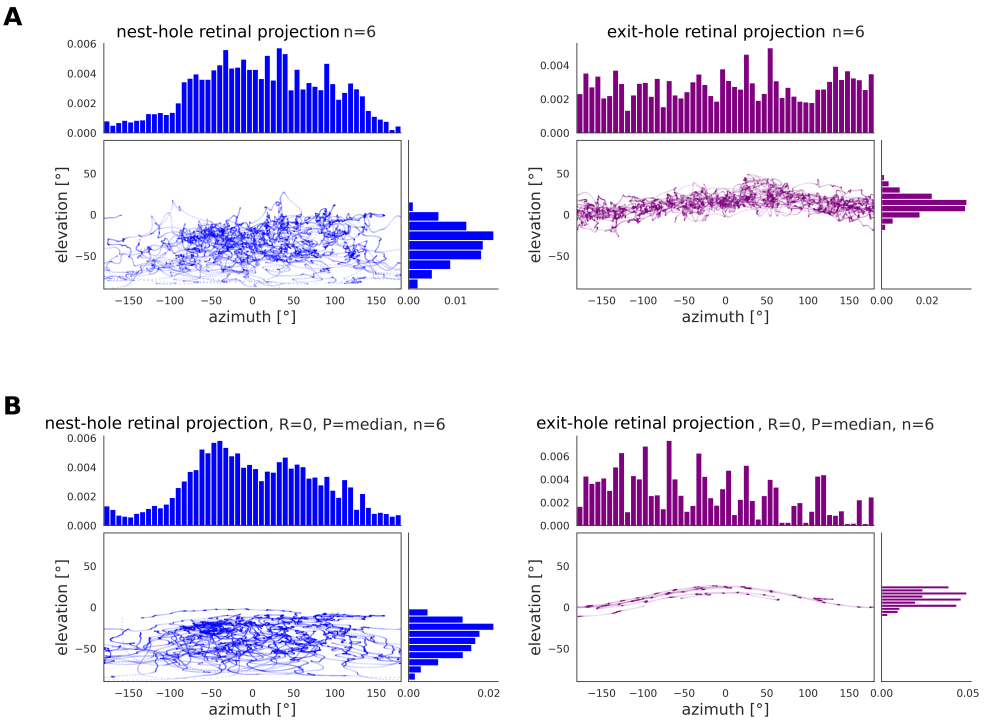

Figure 4.7: Nest-hole and exit-hole retinal projection. A: Left, scatter plot of the nest-hole retinal projection along azimuth and elevation during all 6 flights with non-modified head's YPR orientation. Azimuth and elevation location of the nest projection is marked by a single point, thus, highlighting phases of fixation. Distribution of the retinal projection of the nest and exit-hole, respectively along the elevation and azimuth are represented by an histogramm for each axis. Right, similarly plotted the retinal projection of the exit-hole B: Nest-hole retinal projection along azimuth and elevation during all 6 flights with roll held constant at 0° and the pitch at its median value. Right, retinal projection of the exit-hole with modified head orientation.

SNR derived from OF during pivoting and motion-parallax

Our previous results hint towards an active strategy slightly different to the flight and gaze strategy reported for other insects [176], where the head is kept stable along the yaw axis to perform motion-parallax. Indeed, our results shows unidirectional yaw rotations suggesting an active control in order to pivot around a point in space during the intersaccade (Fig 4.3B). Yet, it is important to know if those rotations are functional or not since the information encoded in the OF pattern will have a different signification. Therefore, to unravel which strategy is accomplished between the two, we investigate depending on the active strategy used during intersaccade the distance information that is encoded into the apparent motion about two meaningful points in the arena, the exit-hole and the nest-hole. Thus, depending on the strategy used the distance information about the nest-hole will or exit-hole will have a different signification (a) in the case of pivoting-parallax the information will indicate the distance between the nest or exit-hole and a pivot-point different at each intersaccade, while (b) in the case of motion-parallax, the distance between the bumblebee, which also change its position at each intersaccade, and the nest or exit-hole . From the simulated OF resulting from a pure motion-parallax or pivoting-parallax, with both encoding for some distance information, the SNR is derived from the apparent motion of the two points during the real trajectory. Then we analysed the impact of the roll and pitch rotations on the respective SNRs.

When looking at the SNR distribution for all intersaccades measured at the nest-hole retinal location, the results show no clear differences between the two strategies (Fig 4.8A). The signal-to-noise ratio distribution is better for the pivoting-parallax when the real experienced YPR orientation is used, with a median pivoting SNR of 4.10 and a median SNR of 1.59 motion-parallax. Yet, there is no overall statistical difference

when comparing the $\log_{10}$ transformed data of the intersacacdes SNR of the two strategies with the different modifiers (one-way ANOVA F=2.15, p>0.05). Nevertheless, a post-hoc paired t-test analysis reveals that the motion-parallax SNR without modifier is significantly smaller than the pivoting SNR (t-test< 0, corrected p-value< 0.05). A similar observation can be seen between the following pairs : SNR for stabilised roll during motion-parallax smaller to SNR for stabilised roll during pivoting, roll-pitch SNR for motion-parallax is smaller to roll SNR during pivoting. All statistics are reported table 1. A visualization of the pairwise comparison of the SNR during each intersaccade for both strategies also shows that for most intersaccades better results were obtained when considering a pivoting strategy: points lay above the bisection line towards the pivoting-parallax SNR axis (Fig 4.9A). This observation can be made for all bees and flights, suggesting no idiosyncratic nor experience differences. In conclusion, if the OF is read assuming a pivoting or a motion-parallax OF field, for both some spatial information about the nest-hole could be obtained.

A larger difference between the SNR for the different strategies and modifiers is found when looking at another behaviourally relevant location in the flight arena, i.e. the exit-hole to the feeding chamber (Fig 4.8B) (ANOVA, F=11.8, p-value<0.001). The paired t-test analysis revealed that most pivoting SNRs are significantly larger than the motion-parallax SNRs (table 4.2), except when the pivoting SNR without modifiers is compared to the motion-parallax SNR with a constant roll and pitch (p>0.05). Indeed the motion-parallax SNR based on the real YPR orientation is significantly smaller than the one obtained with the roll and pitch angle constant (t-test=-2.963 and p-value<0.05). For the pairwise comparison (Fig 4.9B), when the experienced YPR orientation is used, the OF has a better signal-to-noise ratio when the pivoting strategy is considered over a motion-parallax strategy. When the roll and pitch are

kept constant, the pairwise distribution does not show a clear alignment with the bisection line. Some points diverge towards pivoting and some towards motion-parallax, indicating that the SNR during some intersaccades is better when considering a pivoting strategy while for others this one is better when considering a motion-parallax strategy. These results suggest an advantage when using the pivoting-parallax strategy to extract distance information about the the exit-hole in relation to a pivot point. In addition, the pivoting SNR is not affected by a poor head stabilization along the roll and pitch axis.

Finally, we investigated the intersaccadic SNR in an area around the nest-hole. For the motion-parallax, the results are not uniform in this area: the SNR radially decreases with increasing distance from the nest-hole, from $\log_{10}$ 0.8 to 0.35 (Fig 4.8C). Oppositely, for the pivoting strategy, the SNR is almost uniform over the entire nest area. Thus, the information available from a pivoting-parallax is rather constant over a larger area, than the information derived from a motion-parallax. Finally, the SNR around the nest is not different from the previous results when roll and pitch are constant (Fig 4.8D).

The results indicate that both strategies lead to a good SNR (i.e. SNR motion-parallax all points=3.19, pivoting-parallax=4.10), indicating that the experienced OF could be used to gain some kind of distance information following one or the other strategy. Nevertheless, an active vision strategy based on pivoting-parallax perform slightly better. Following this conclusion, we looked at where the points of pivoting are located since the information derived from pivoting will always be relative to those points.

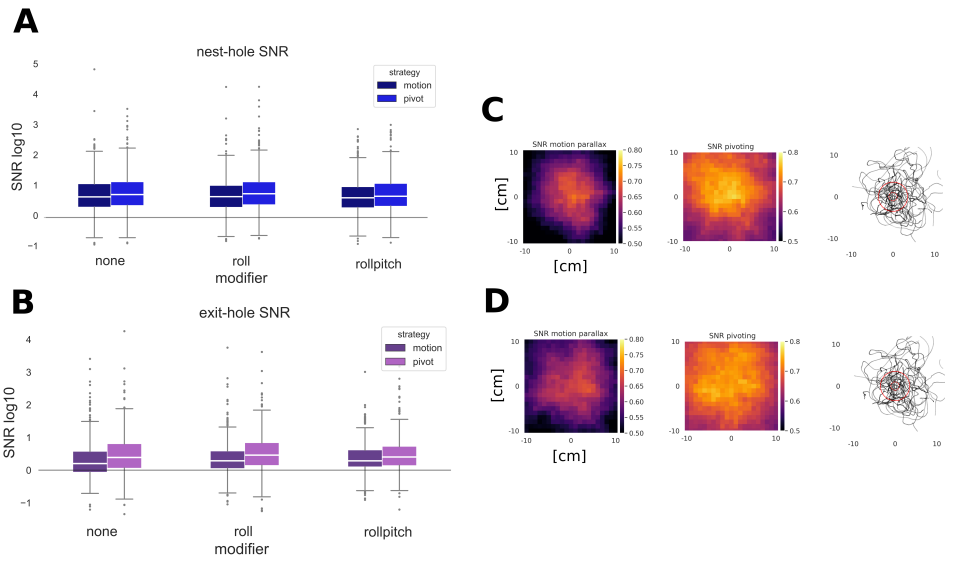

Figure 4.8: Signal-to-noise ratio during intersaccadic intervals. A: SNR distribution for the nest-hole retinal projection. For the motion-parallax strategy (Dark blue) and the pivoting-parallax (Light blue) with different modifiers: none, roll constant, and "rollpitch" i.e. roll and pitch constant. The median is represented by a white line. B: SNR distribution for the exit-hole retinal projection motion-parallax(purple), pivoting parallax (pink). C: SNR of the projected nest area (-10 cm +10 cm around the nest-hole) without modifiers, from left to right : motion-parallax, pivoting-parallax and finally all learning flights in this area. positive SNR from 0 white to 0.8 purple, and negative SNR from white to -0.4 black. D: SNR of the projected nest area with roll and pitch constant.

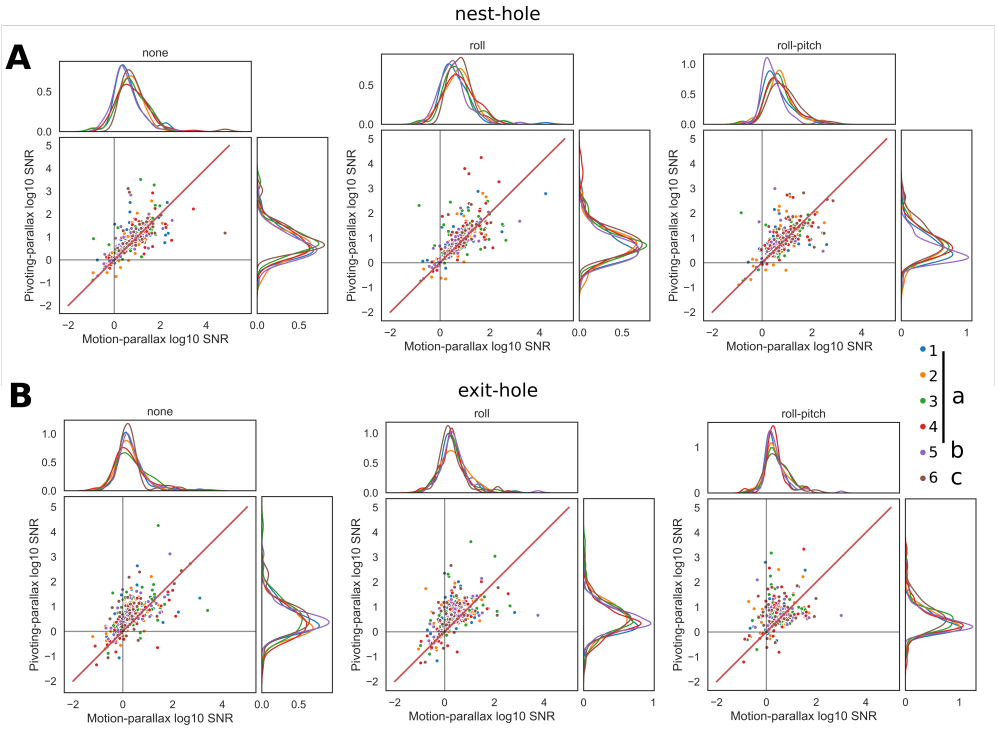

Figure 4.9: Pairwise comparison of the SNR for each intersaccadic intervals. A: Pairwise comparison of the SNR for the nest-hole for each flights (n=6) colour coded and with the different modifiers (none, roll constant, roll and pitch constant). The motion-parallax SNR is on the x-axis and pivoting-parallax SNR is on the y-axis, the bisection line is represented in red. B: same for the exit-hole SNR.

Table 4.1: Post-Hoc paired t-test multi-comparisons nest-hole SNR.

	stat	adj. p-value
none motion vs none pivot	-2.9897	0.0383
none motion vs roll motion	0.0197	1.0
none motion vs roll pivot	-2.6989	0.0867
none motion rollpitch motion	0.4613	1.0
none motion vs rollpitch pivot	-1.2005	1.0
none pivot vs roll motion	2.1603	0.2816
none pivot vs roll pivot	-0.6971	1.0
none pivot vs rollpitch motion	2.4505	0.1465
none pivot vs rollpitch pivot	0.7679	1.0
roll motion vs roll pivot	-3.9282	0.0015
roll motion vs rollpitch motion	0.5217	1.0
roll motion vs rollpitch pivot	-1.3443	1.0
roll pivot vs rollpitch motion	3.1781	0.0222
roll pivot vs rollpitch pivot	1.5473	0.9801
rollpitch motion vs rollpitch pivot	-2.6601	0.0891

Table 4.2: Post-Hoc paired t-test multi-comparisons exit-hole SNR.

	stat	adj. p-value
none motion vs none pivot	-7.449	0.0
none motion vs roll motion	-1.4361	0.6067
none motion vs roll pivot	-6.2424	0.0
none motion rollpitch motion	-2.963	0.0225
none motion vs rollpitch pivot	-5.4204	0.0
none pivot vs roll motion	4.1998	0.0003
none pivot vs roll pivot	-1.22711	0.6613
none pivot vs rollpitch motion	2.5552	0.0657
none pivot vs rollpitch pivot	-0.607	1.0
roll motion vs roll pivot	-6.8062	0.0
roll motion vs rollpitch motion	-1.9833	0.2398
roll motion vs rollpitch pivot	-4.6966	0.0
roll pivot vs rollpitch motion	3.9745	0.0007
roll pivot vs rollpitch pivot	0.503	1.0
rollpitch motion vs rollpitch pivot	-4.1969	0.0003

The pivoting points

Given that the nest-hole is kept in a broad frontal area of the visual field during learning flights, it is plausible that it is of functional significance for the bee. Therefore, it is suggested by the paper of Riabinina et al. 2014 that the pivoting points resulting from any intersaccade presenting an overall unidirectional rotation should be in the nest area [141], allowing the bumblebee to build a nest-area centred spatial view of its environment. However, when the pivot points would lie away from nest-hole they may lead to meaningless distance information.

When solely considering the yaw orientation in 2D, we could estimate the location of the pivoting point for each intersaccade and for each flight

(Fig 4.10). The distribution of the pivoting points in space is quite spread, but many of them cluster around the nest-hole, with 21.88% of them being within a radius of 10 cm around the nest-hole. In total, 35.35% of points fall outside the arena. In addition, we can observe that pivot points located closer to the nest-hole often correspond to a stronger rotational drift. Finally, it is important to note that pivoting points corresponding to a negative drift are located opposite to the heading direction (Fig 4.5C); this concerns 54.88% of the pivoting points.

For the flights 1, 2, 3 and 4 belonging to the same individual and chronologically numbered, there are no apparent changes in their placement due to experience (Fig 4.10). Otherwise, it seems that there is an individual difference as flight 5 differs largely from the others. Flight nb° 5 has well-clustered points around the nest-hole with intersaccades of strong drifts. All pivoting point locations calculated here are just an approximation, since the z-axis is ignored, and a small yaw error during intersaccades may still produce slight differences in location.

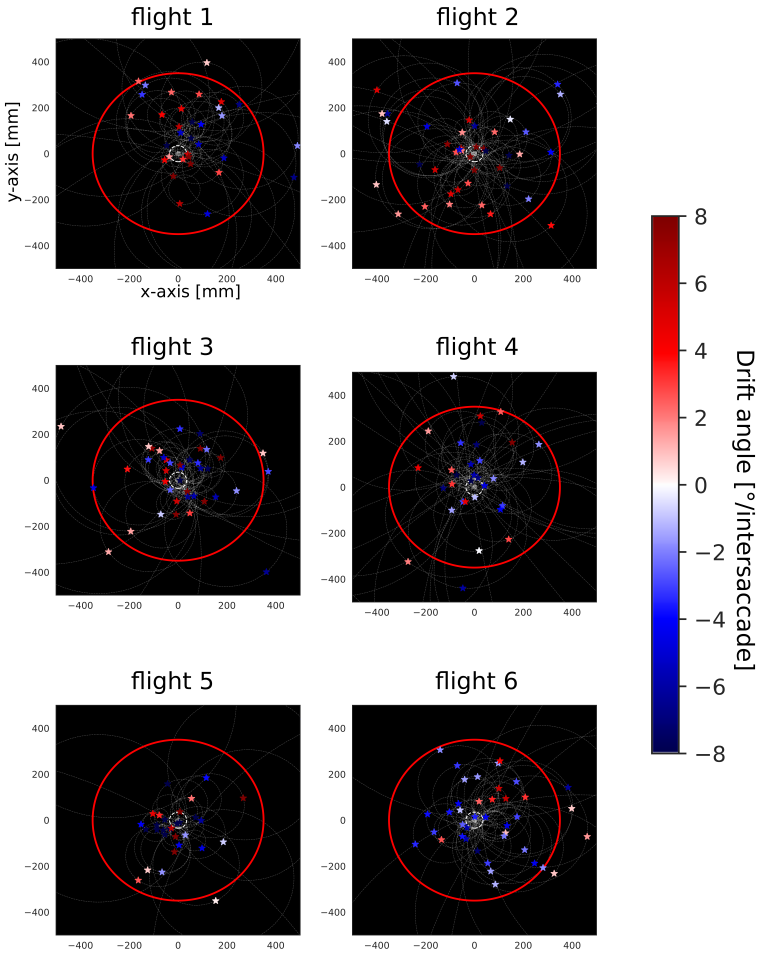

Figure 4.10: Pivoting points in the flight arena. Each subplot corresponds to one flight. Pivoting points are colour coded by a diverging colormap depending on the drift angle of the corresponding intersaccade i.e. Drift below 0, from white to blue; drift above 0 from white to red. Each pivot point is associated an horopoter represented by a thin dotted white line. The arena walls are shown by the red circle. the nest-hole and platform are represented by the white dot in the middle of the arena. The exit-hole is located at x=0 and y =-350.

4.4 Discussion

Head stabilization and gaze control are observed in many animal species and assumed to help reducing motion blur, extracting of distance information, or easing goal-directed behaviour [76]. For insects, the extraction of information about the spatial arrangement during phases of head stabilization, 'intersaccades', is of high importance. In fact, insects often fly in a quick manner. For example, when flying through a cluttered environment, they need to quickly avoid obstacles on their way and, thus require distance information. But, the information extracted from ego-movements during intersaccades might be also relevant in other contexts; for instance, bumblebees can use distance information about landmarks to retrieve a goal location [57, 202].

A recent paper has suggested that distance information about the visual surrounding of the nest location could be collected by bumblebees in the course of learning flights during the intersaccadic intervals by pivoting around their nest-hole in the ground [141]. Thus, the distances extracted would be in relation to this pivot point. However, by analysing the gaze strategies of bumblebees at unprecedented spatial and temporal resolution, we could show that at least in our experimental setting, bumblebees were not pivoting around their nest-hole in any systematic way. Their head often performed unidirectional yaw rotation's during interssaccades interval but these corresponded to pivot points largely spread in the environment and even behind the bumblebees' tail (Fig 4.5C). This finding has strong implications, since if it is the case, the distance information available in the OF pattern resulting from pivoting cannot be easily re-

lated to the location of the nest-hole. In addition, the head was neither perfectly stabilised for the roll and pitch during intersaccades, potentially inducing inoperable rotational flow on the retina. Therefore, questions arise about the potential functional consequences of such rotations for navigation during learning flights and for future homing trips.

From our systematic study of the bumblebees' head dynamic movements and its impacts on the visual input during learning flights, one major findings was how little roll and pitch rotations affect the distance information contained in the OF about the nest-hole. As a reminder, we obtained the signal-to-noise ratio measurement by considering our signal as the apparent motion derived from an ideal trajectory with a controlled YPR orientation (i.e. pitch and roll stabilised) and the noise being the deviation from this signal (for details see Method). In results, the obtained SNR of the real trajectories was large despite the remaining intersaccadic roll and pitch rotations.

Interestingly, the pitch and roll angles are commonly thought to be perfectly stabilised in insects because they may induce strong rotational component on the retina. This almost perfect head stabilization has been observed in free flying blowflies [176] where during intersaccades angular rotations along YPR are smaller than 100° per seconds, which is much littler than the corresponding rotational velocities we found for our bumblebees (Fig 4.5E). This difference could be explained by Dipterans possessing "halteres", organs acting like a gryoscope, which could facilitate through motor signals compensatory head movements [77]. However, the smaller body-size of the blowfly may induce less inertia in comparison to bumblebees, which may play a role in this context [15]. Despite observing large angular roll velocities even during intersaccades, the head roll orientation in the world coordinates was still stabilised to a large extent in the course of the flight in comparison to the thorax (Fig 4.11). In this

regard, our data are similar to other studies done on honeybees [14] and wasps [180]. In these investigations, the recorded flight choreographies were much simpler than the complex loops characteristic of a learning flight, i.e. mostly forward motion towards a vertical food source and thus without clear impact of the flight complexity on the head roll stabilization. In addition, the roll angle was as stabilised in our indoor set-up, as when wasps were recorded outdoor [180]: the head roll orientation in the study on wasps also ranged between +- 10 degrees. Thus, the absence of visual cues such as a light gradient or polarized light which could be process by the ocelli was not an obstacle to the roll stabilization in the world coordinate system [76, 180]. All-together, despite suffering from strong inertia, and a complex flight choreography our bumblebees efficiently minimized roll and pitch rotations so the OF-based distance information was not impair during intersaccades.

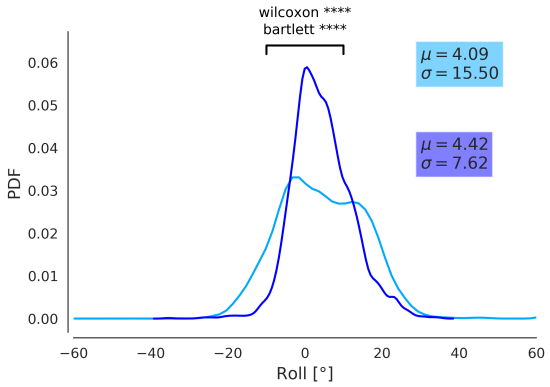

Figure 4.11: Distribution Roll angle for head and Thorax, n=6. The head roll angle probability density function and its variance, dark blue line, ($\mu = 4.09°$, $\sigma = 7.62°$) is statistically different from the Thorax roll, light blue line ($\mu = 4.42°$, $\sigma = 15.50°$). With p<0.001 for Wilocoxon and Bartlett test for variance.

Although roll and pitch do not have strong consequences for the distance information contained in the OF, it is not clear what are the

functional consequences of remaining yaw rotations during intersaccades. As described earlier, the yaw rotations are mostly limited but sometimes induce a residual unidirectional drift, which can lead to two different form of OF pattern, one giving distance information through an ego-perspective (motion-parallax) and the other through a geo-centric perspective (pivoting-parallax). From our analysis both strategies could co-exist during learning flights, as some intersaccades show extremely small drifts and other larger ones (Fig 4.6A and Fig 4.10), and both strategies could be used since the signal-to-noise ratio is good in both scenarios (Fig 4.8A&B). From the SNR results, the pivoting-parallax might be a slightly better strategy since its SNR is more robust to roll and pitch rotations and the SNR is better about further away points like the exit-hole in comparison to the motion-parallax. However, the existence of pivot points at the back of the bumblebee may raise questions about the real function of these rotations (Fig 4.10).

Therefore, how the distance information, if collected through the OF pattern of those intersaccades presenting a yaw drift, can later be used during homing?

Intuitively, this information should be set in relation with the nest-hole which would be the reference point. Hence, during motion-parallax the bumblebees need to have an idea about its own location relative to the nest in order to set the ego-centered acquired distance view in relation to the nest-hole, while, during pivoting, its the location of the pivoting point when not at the nest location which needs to be set in relation to the nest-hole. However, the knowledge of their own position in space or of another point (i.e. the pivot points) is surely imprecise due to their tortuous choreography [32], and moreover it would require that bumblebees are able to visually follow their nest [146, 144], and to deduce their own position in relation to this one. These conclusions interrogate the ability

for the bumblebees to easily use distance information contained in the OF for navigational purposes like local homing.

Yet, modelling analysis performed in Chapter 2 of this thesis showed that to enable a successful homing there is no need to know about the exact location in space of a visual memory conceptualized as a panoramic-snapshot, with those encoding partly distance information, to find back home [55]. In details, these models solely requires those memorized panoramic-snapshot, to be oriented towards the nest-hole. This orientation could be obtained by visually tracking the entrance to the nest, or thanks to some external compass cue [69, 146] . However, the head should be stabilised along the roll and pitch while gathering these memories. In fact, rotations along roll and pitch have been shown to make it impossible to use a brightness snapshot-based model (i.e. panoramic memory encoding brightness value), as described in the route following behaviour of ants (effects of roll [136], and pitch variations [3]). If such a strategy is used, it should be combined with homing models invariant against roll and pitch rotations [164, 162] or it would require a large number of snapshots to average the noise introduced by uncontrolled head rotations.

However, distance information might not be the only issue during the early phase of learning flight; the head might also be actively controlled to keep the nest-hole in the frontal acute region of the eye [168], giving the bumblebee a better picture of the close surrounding of the nest (Fig 4.7). In this way, while looping around the nest-hole, the bumblebee could precisely orient the collected memories, aspect which is required in the models described earlier. Finally, the detailed picture of the nest could also be used during local homing to precisely pinpoint the nest, indeed hymenopterans can show extremely precise return towards rather inconspicuous holes [144, 183].

Finally, our findings need to be put in perspective with the limitations of our method: our sample size is rather small and reconstruction error cannot be fully avoided. Indeed, the placement of markers is challenging due to the extremely small bumblebees' head, covered with thick hair, limiting the number of individuals keeping the appropriate amount of markers when placed back in the hive. In addition, the spatial resolution of any camera systems is limited. So small deviations on the frames may yield to large reconstruction errors. Finally, the positioning of markers would require to be precisely controlled, since their placement might impact the overall orientation, which might be the reason for saccades of smaller amplitude performed by individual 'b'(=flight nb°5). In consequence of these technical constraints, we could analyse the head orientation only during a small fragment of their flight in a limited indoor space, while those flights are known to be naturally much longer [53]. However, despite these limitations, we largely reduced the reconstruction error (mean yaw-error=4.1°, pitch=5° roll=4°, Fig 4.12) and our main conclusions were consistent across all flights and individuals: the head was not perfectly stabilised along the YPR during intersaccades and performed much faster rotations than the thorax. In consequence, using thorax orientation to estimate heading direction would only deliver a coarse estimate of the OF pattern experienced by the insect. Due to the limits imposed by head tracking, It would be of interest to find an algorithm, which from the less challenging measurements of thorax YPR's orientation could provide a good prediction about the head orientation [90].

In summary, there is no possibility to conclude that these remaining head rotations along the yaw axis are actively controlled to perform a pivoting strategy, the results of a poor execution of a motion-parallax strategy or even produced by chance due to methodological noise. But, from our analysis, we can neither infer if those rotations are a problem or

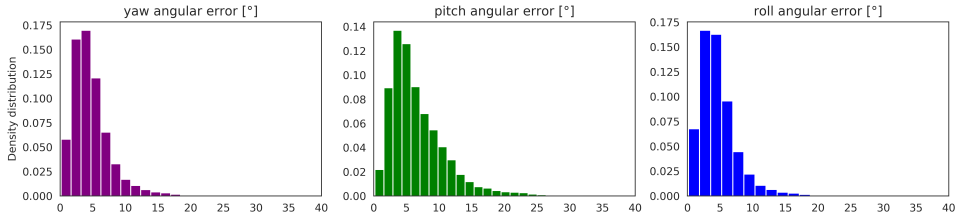

Figure 4.12: Propagated tracking error on the YPR head angles. From left ro tight the propagated error distribution in degrees for the yaw head orientation, then for the pitch and finally for the roll. All errors lay between 0 and 15°, n=6.

an advantage for the bee when performing local-homing. Unravelling the functional significance of the head-rotations might be extremely complex since there is still so much to learn about what information bumblebees are really using during this task. Nevertheless, over-all we could see that the head dynamic is not optimal, but this one might be efficiently controlled, so distance information can be gathered during intersaccadic intervals.

4.5 Supporting informations

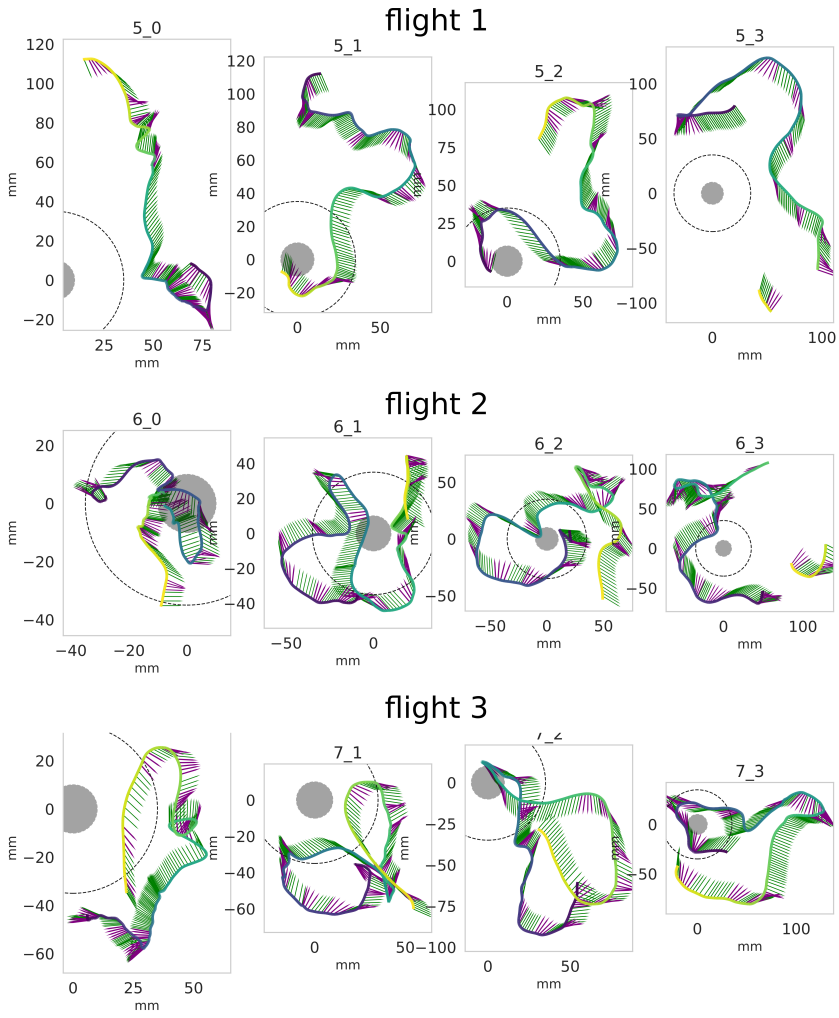

Figure 4.S.1: Learning flights trajectories: 1,2,3. All recorded learning flights consist of complex loops manoeuvrers around the nest-hole. All bumblebees during the initial phase of learning flights stay in the immediate surrounding of the nest-hole.Same legend as in Fig 4.2C. x,y,z positions and yaw orientation during learning flight

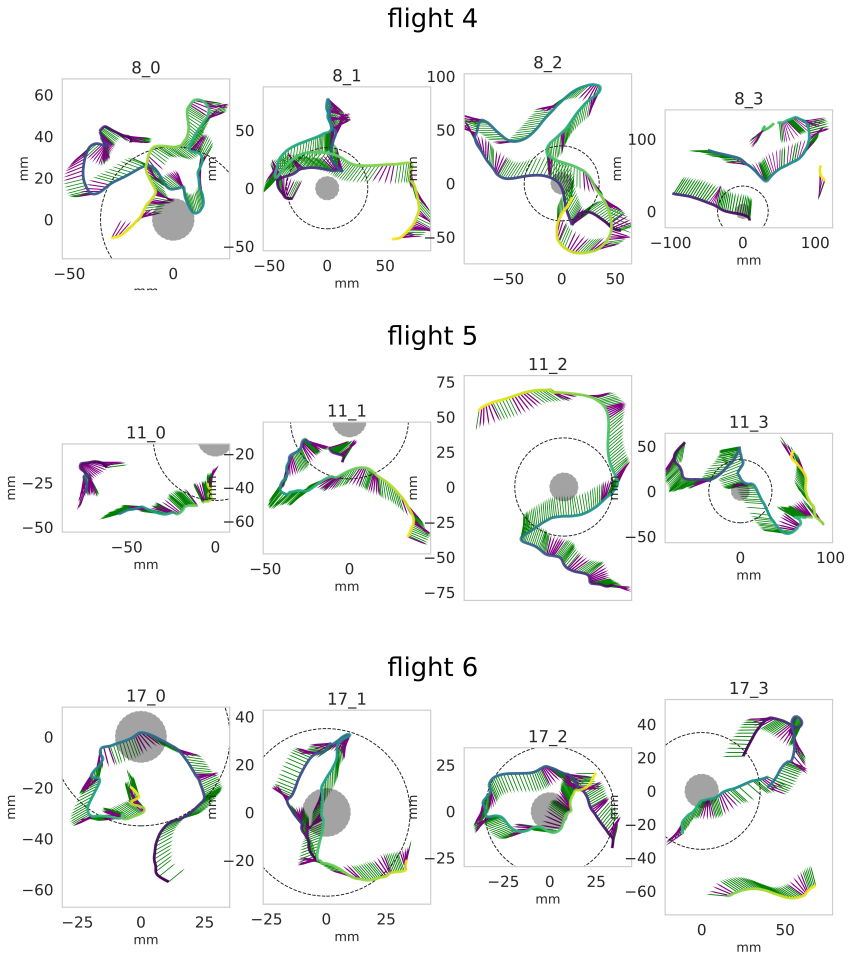

Figure 4.S.2: Learning flights trajectories: 4,5,6. x,y,z positions and yaw orientation during learning flight

5 Concluding remarks

5.1 Main conclusions

In order to return to a previously visited place, it is necessary to remember some significant characteristics of it. For example, a person who wishes to return to their[1] hotel room will most likely learn the floor and room number to which they have been assigned. Therefore, when returning from dinner, the person will follow the number on the door. Undoubtedly, this indication will probably be followed even though the hallway's carpet as now being changed to blue. However, insects cannot be expected to have such blind faith in numbers or other man-build indications, so how do they decide (1) what they need to learn in their visual environment to return home, and (2) how do they learn that information. These are two of the questions addressed in this thesis.

First of all, "deciding" to learn a cue would mean that the insect is able to dissociate meaningful information from non-significant information. However, in the case of bumblebees leaving their nest for the first time, they only have knowledge of the inside of their hive. Thus, their experience of the external visual world does not yet exist. This could mean that they may not have enough knowledge about the outside on their first foraging trip to "decide" what they need to learn to return home. Therefore, what and how bumblebees learn upon their first departure, can be

[1] Gender neutral pronoun

assumed to be an innate decision process, which proves to be usually successful, because it allows the return home.

Besides, it is difficult to decide how and what landmarks or visual cues in the environment might be stored and even prioritized by the small brain of insects. Therefore, scientists studying navigation have come up with a more intuitive and parsimonious alternative. In essence, insects could remember a whole pixel-based view of their perceivable visual environment. While this idea removes complex parameters that would have played a role when segmenting a visual environment between landmarks and others non-relevant cues, there is still a multitude of possibilities behind what is contained in a holistic view of the visual environment.

As mentioned in the introduction, navigation is a movement towards a goal by recognizing its direction but also distance. In the conclusion of this work, it appears that distance as an environmental feature is critical for local homing. Indeed, based on the experiments described in Chapter 2, a visually-based homing model using panoramic views stored in the insect's memory, with these ones encoding information about the depth-structure of the environment has partly reproduced bumblebees behaviour during a local homing exercise. In brief, this model guides the insect home based on the disparities between the stored memories, i.e. the panoramic views encoding distance, and the current view of the animal. Therefore, the insect is driven towards the location with the most similitude to its memory. Local homing adds itself to the already long list of behaviours requiring distance information performed daily by insects, such as catching prey, landing, and flying.

Information on visual surroundings and especially depth information is probably learned when the bumblebee leaves its nest for the first time by flying in loops around it. Its movements in space may give it, through the

experienced optic-flow, an indication of the geometric arrangement of the environment. However, this information, depending on the details of how the animal moves may lead to distance information in different frames of reference, i.e. either it would express the distance between environmental objects relative to the bee (egocentric information) or distance between environmental objects and a location in space (geocentric information). From my observations in chapter 4, it seems that bumblebees do not try to accommodate their movements in an attempt to follow one strategy in preference to the other. Bumblebees must be flexible enough to be able to use and memorize this distance information despite the significant difference in its meaning. This conclusion suggests that there are still open questions about how the insect's visual system obtains distance from such a complex source. In fact, small but also large rotations, where distance information cannot be obtained, permanently occur during the execution of learning flight manoeuvres around the nest. Moreover, the reference-frame of distance assessment (ego or geocentric) may at first glance seem critical to allow successful navigation, but, according to the guidance strategy described in chapter 2, this aspect is not a problem to enable local-homing. As a matter of fact, the reference frame of the holistic views stored in memory during learning is not relevant in this context. Indeed, their orientation toward the nest is one of the only prerequisites to allow the bumblebee to successfully return home.

The model proposed in this work is rather simple and could be one of many answers to what bumblebees might use to return to their nest site. Indeed, most modelling analyses do not cover the full range of behaviours employed by navigating insects. Often, several aspects might be overlooked by the researcher to simply allow the design of such a model.

The behaviour displayed by bumblebees when learning the surroundings of its nest and then returning back to it is quite far from the per-

formance of most existing navigation models. Contrary to these models, bumblebees may seem quite chaotic to some of us, as they fly frantically in what may seem to be a "wrong" direction, or they decide to land at "biologically irrelevant" places. Only two aspects of this complex behaviour have been reported in this thesis, namely, changes in altitude and the evolution of search behaviour overtime when the bee does not immediately find its nest hole as a consequence of environmental manipulations. In any case, if only these two aspects were taken into account, enormous possible implications on the local homing process could already be imagined. For example, altitude changes could help the bumblebee to follow the indication given by a visually-guided homing strategy and time could influence its decision on where to search for the nest-hole.

Nevertheless, these can only remain at the level of the hypothesis and would require the development and use of specific techniques. For example, in the case of the analysis of the temporal dimension the Hidden Markov Chain model, or in the case of the relevance of altitude changes, some experiments specifically designed for this purpose could respond if these altitude changes are indeed necessary during navigation.

5.2 Afterthought

In this thesis, I gave suggestions and answers to the above questions: what is learned for local-homing and how. However, this work is constrained by the limitation of observing the bumblebees' behaviour in an indoor setting not even remotely similar to what bumblebees encounter

daily in the wild. Of course, there are several advantages to study navigation in this way; the experimenter can control what should be excluded or included in the experimental design allowing to pinpoint specific questions. However, it is audacious to say that the conclusion made in an indoor setting would be efficient to explain the behaviour seen outdoors. Therefore, the different conclusions made in this present work should be extended to what bumblebees can do in the outdoor and how these answers are incorporating themselves in the bumblebee's journey performed in nature.

Overall, the acquisition and the use of distance information could be shown to be critical in the context of local homing. Also, the implication of the active behaviour of bumblebees to follow and acquire this indication might be central in this context. Therefore, this work could contribute to the inspiration of the design of new research questions and development of new homing models, including a broader range of the flying insects behavioural repertoire.

References

1. Akaike, H. *Information theory and the maximum likelihood principle* in *2nd International Symposium on Information Theory* (1973).
2. Akram, M. & Michel, V. Regularisation of the Helmholtz decomposition and its application to geomagnetic field modelling. *GEM - International Journal on Geomathematics.* ISSN: 18692672 (2010).
3. Ardin, P., Mangan, M., Wystrach, A. & Webb, B. How variation in head pitch could affect image matching algorithms for ant navigation. *Journal of Comparative Physiology A: Neuroethology, Sensory, Neural, and Behavioral Physiology.* ISSN: 14321351 (2015).
4. Ardin, P., Peng, F., Mangan, M., Lagogiannis, K. & Webb, B. Using an Insect Mushroom Body Circuit to Encode Route Memory in Complex Natural Environments. *PLoS Computational Biology.* ISSN: 15537358 (2016).
5. Bar-On, Y. M., Phillips, R. & Milo, R. The biomass distribution on Earth. *Proceedings of the National Academy of Sciences of the United States of America.* ISSN: 10916490 (2018).
6. Becker, L. Untersuchungen über das Heimfindevermögen der Bienen. *Zeitschrift für Vergleichende Physiologie.* ISSN: 03407594 (1958).
7. Benhamou, S., Sauvé, J. P. & Bovet, P. Spatial memory in large scale movements: Efficiency and limitation of the egocentric coding process. *Journal of Theoretical Biology.* ISSN: 10958541 (1990).
8. Bertrand, O. J., Doussot, C., Siesenop, T., Ravi, S. & Egelhaaf, M. Visual and movement memories steer bumblebees along habitual routes (In prep.).

9. Bertrand, O. J., Lindemann, J. P. & Egelhaaf, M. A Bio-inspired Collision Avoidance Model Based on Spatial Information Derived from Motion Detectors Leads to Common Routes. *PLoS Computational Biology.* ISSN: 15537358 (2015).

10. Beugnon, G. & Campan, R. Homing in the field cricket, Gryllus campestris. *Journal of Insect Behavior.* ISSN: 08927553 (1989).

11. Bhatia, H., Norgard, G., Pascucci, V. & Bremer, P. T. The Helmholtz-Hodge decomposition - A survey. *IEEE Transactions on Visualization and Computer Graphics.* ISSN: 10772626 (2013).

12. Boeddeker, N., Lindemann, J. P., Egelhaaf, M. & Zeil, J. Responses of blowfly motion-sensitive neurons to reconstructed optic flow along outdoor flight paths. *Journal of comparative physiology. A, Neuroethology, sensory, neural, and behavioral physiology.* ISSN: 03407594 (2005).

13. Boeddeker, N., Dittmar, L., Stürzl, W. & Egelhaaf, M. *The fine structure of honeybee head and body yaw movements in a homing task* in *Proceedings of the Royal Society B: Biological Sciences* (2010). ISBN: 0962-8452.

14. Boeddeker, N. & Hemmi, J. M. Visual gaze control during peering flight manoeuvres in honeybees. *Proceedings of the Royal Society B: Biological Sciences.* ISSN: 14712970 (2010).

15. Boeddeker, N., Mertes, M., Dittmar, L. & Egelhaaf, M. Bumblebee homing: The fine structure of head turning movements. *PLoS ONE* **10.** ISSN: 19326203 (2015).

16. Boles, L. C. & Lohmann, K. J. True navigation and magnetic maps in spiny lobsters. *Nature.* ISSN: 00280836 (2003).

17. Bradburn, M. J., Clark, T. G., Love, S. B. & Altman, D. G. *Survival Analysis Part II: Multivariate data analysis- An introduction to concepts and methods* 2003.

18. Bregy, P., Sommer, S. & Wehner, R. Nest-mark orientation versus vector navigation in desert ants. *Journal of Experimental Biology.* ISSN: 00220949 (2008).

19. Brower, L. P. Studies on the Migration of the Monarch Butterfly I. Breeding Populations of Danaus Plexippus and D. Gilippus Berenice in South Central Florida. *Ecology.* ISSN: 0012-9658 (1961).

20. Brower, L. P., Calvert, W. H., Hedrick, L. E. & Christian, J. Biological observations on an overwintering colony of monarch butterflies (Danaus plexippus, Danaidae) in Mexico. *Journal of the Lepidopterists' Society* (1977).

21. Buehlmann, C., Hansson, B. S. & Knaden, M. Desert ants learn vibration and magnetic landmarks. *PLoS ONE.* ISSN: 19326203 (2012).

22. Buehlmann, C., Hansson, B. S. & Knaden, M. Path integration controls nest-plume following in desert ants. *Current Biology.* ISSN: 09609822 (2012).

23. Cammaerts, M. C., Attygalle, A. B., Evershed, R. P. & Morgan, E. D. The pheromonal activity of chiral 3 octanol for Myrmica ants. *Physiological Entomology.* ISSN: 13653032 (1985).

24. Capaldi, E. & Dyer, F. The role of orientation flights on homing performance in honeybees. *The Journal of Experimental Biology* **202,** 1655–1666. ISSN: 0022-0949 (1999).

25. Capaldi, E. A. *et al.* Ontogeny of orientation flight in the honeybee revealed by harmonic radar. *Nature.* ISSN: 00280836 (2000).

26. Cartwright, B. A. & Collett, T. S. How honey bees use landmarks to guide their return to a food source. *Nature.* ISSN: 00280836 (1982).

27. Cartwright, B. A. & Collett, T. S. Landmark learning in bees - Experiments and models. *Journal of Comparative Physiology A.* ISSN: 03407594 (1983).

28. Chapman, A. D. Numbers of Living Species in Australia and the World. *Heritage* (2009).

29. Cheeseman, J. F. *et al.* Reply to Cheung et al.: The cognitive map hypothesis remains the best interpretation of the data in honeybee navigation. *Proceedings of the National Academy of Sciences* **111,** E4398–E4398. ISSN: 0027-8424 (2014).

30. Chelazzi, G. Eco-ethological aspects of homing behaviour in molluscs. *Ethology Ecology and Evolution.* ISSN: 18287131 (1990).

31. Cheng, K, Collett, T. S., Pickhard, A & Wehner, R. The use of visual landmarks by honeybees: Bees weight landmarks according to their distance from the goal. *Journal of Comparative Physiology A.* ISSN: 03407594 (1987).

32. Cheung, A. Animal path integration: A model of positional uncertainty along tortuous paths. *Journal of Theoretical Biology.* ISSN: 00225193 (2014).

33. Cheung, A. & Vickerstaff, R. Finding the way with a noisy brain. *PLoS Computational Biology.* ISSN: 1553734X (2010).

34. Chittka, L., Williams, N. M., Rasmussen, H. & Thomson, J. D. Navigation without vision: Bumblebee orientation in complete darkness. *Proceedings of the Royal Society B: Biological Sciences.* ISSN: 14712970 (1999).

35. Clark, T. G., Bradburn, M. J., Love, S. B. & Altman, D. G. Survival Analysis Part I: Basic concepts and first analyses. ISSN: 00070920 (2003).

36. Collett, M., Collett, T. S., Bisch, S. & Wehner, R. Local and global vectors in desert ant navigation. *Nature.* ISSN: 00280836 (1998).

37. Collett, M. How navigational guidance systems are combined in a desert ant. *Current Biology* **22,** 927–932. ISSN: 09609822 (2012).

38. Collett, M., Chittka, L. & Collett, T. S. Spatial memory in insect navigation. *Current Biology* **23,** R789–R800. ISSN: 09609822. `http://dx.doi.org/10.1016/j.cub.2013.07.020` (2013).

39. Collett, M. & Collett, T. S. *Path Integration: Combining Optic Flow with Compass Orientation* 2017.

40. Collett, T. S., de Ibarra, N. H., Riabinina, O. & Philippides, A. Coordinating compass-based and nest-based flight directions during bumblebee learning and return flights. *Journal of Experimental Biology* **216,** 1105–1113. ISSN: 0022-0949 (2013).

41. Collett, T. S., Dillmann, E., Giger, A. & Wehner, R. Visual landmarks and route following in desert ants. *Journal of Comparative Physiology A.* ISSN: 03407594 (1992).

42. Collett, T. S. & Lehrer, M. Looking and learning: A spatial pattern in the orientation flight of the wasp Vespula vulgaris. *Proceedings of the Royal Society B: Biological Sciences.* ISSN: 14712970 (1993).

43. Collett, T. S. & Collett, M. Path integration in insects. ISSN: 09594388 (2000).

44. Collett, T. S. & Graham, P. Insect navigation: Do honeybees learn to follow highways? *Current Biology.* ISSN: 09609822 (2015).

45. Collett, T. S. & Zeil, J. Flights of learning. *Current Directions in Psychological Science.* ISSN: 09637214 (1996).

46. Collett, T. S. & Zeil, J. Insect learning flights and walks. *Current Biology.* ISSN: 09609822 (2018).

47. Crall, J. D., Chang, J. J., Oppenheimer, R. L. & Combes, S. A. Foraging in an unsteady world: Bumblebee flight performance in fieldrealistic turbulence. *Interface Focus.* ISSN: 20428901 (2017).

48. Cruse, H. & Wehner, R. No need for a cognitive map: Decentralized memory for insect navigation. *PLoS Computational Biology.* ISSN: 1553734X (2011).

49. Czaczkes, T. J., Grüter, C., Ellis, L., Wood, E. & Ratnieks, F. L. Ant foraging on complex trails: Route learning and the role of trail pheromones in Lasius niger. *Journal of Experimental Biology.* ISSN: 00220949 (2013).

50. Dacke, M. & Srinivasan, M. V. Honeybee navigation: Distance estimation in the third dimension. *Journal of Experimental Biology.* ISSN: 00220949 (2007).

51. Dacke, M., Baird, E., Byrne, M., Scholtz, C. H. & Warrant, E. J. Dung beetles use the milky way for orientation. *Current Biology.* ISSN: 09609822 (2013).

52. Darwin, C. Origin of certain instincts. *Nature.* ISSN: 00280836 (1873).

53. Degen, J., Hovestadt, T., Storms, M. & Menzel, R. Exploratory behavior of re-orienting foragers differs from other flight patterns of honeybees. *PLOS ONE* **13,** 1–14. `https://doi.org/10.1371/journal.pone.0202171` (Aug. 2018).

54. Derdikman, D. *et al.* Fragmentation of grid cell maps in a multicompartment environment. *Nature Neuroscience.* ISSN: 10976256 (2009).

55. Dewar, A. D., Philippides, A. & Graham, P. What is the relationship between visual environment and the form of ant learning-walks? An in silico investigation of insect navigation. *Adaptive Behavior.* ISSN: 17412633 (2014).

56. Dittmar, L., Sturzl, W., Baird, E., Boeddeker, N. & Egelhaaf, M. Goal seeking in honeybees: matching of optic flow snapshots? *Journal of Experimental Biology.* ISSN: 0022-0949 (2010).

57. Dittmar, L., Egelhaaf, M., Stürzl, W. & Boeddeker, N. The Behavioral Relevance of Landmark Texture for Honeybee Homing. *Frontiers in Behavioral Neuroscience* **5** (2011).

58. Dyer, F. C. & Gould, J. L. Honey Bee Orientation: A Backup System for Cloudy Days. *Science* **214,** 1041–1042. ISSN: 0036-8075 (2006).

59. Eckmeier, D. *et al.* Gaze strategy in the free flying zebra finch (Taeniopygia guttata). *PLoS ONE.* ISSN: 19326203 (2008).

60. Egelhaaf, M., Boeddeker, N., Kern, R., Kurtz, R. & Lindemann, J. P. Spatial vision in insects is facilitated by shaping the dynamics of visual input through behavioral action. *Frontiers in neural circuits* **6,** 108. `http://www.pubmedcentral.nih.gov/articlerender.fcgi?artid=3526811{\&}tool=pmfcentrez{\&}rendertype=abstract` (2012).

61. Egelhaaf, M., Kern, R. & Lindemann, J. P. Motion as a source of environmental information: A fresh view on biological motion computation by insect brains. *Frontiers in Neural Circuits.* ISSN: 16625110 (2014).

62. Emilio Baldaccini, N., Schiff, N. & Fiaschi, V. Homing behaviour of pigeons confined to a new loft distant from their home. *Monitore Zoologico Italiano - Italian Journal of Zoology.* ISSN: 00269786 (1976).

63. Esch, H. E. & Burns, J. E. Distance estimation by foraging honeybees. *Journal of Experimental Biology.* ISSN: 00220949 (1996).

64. Etienne, A. S. & Jeffery, K. J. *Path integration in mammals* 2004.

65. Evans, L. J. & Raine, N. E. Changes in learning and foraging behaviour within developing bumble bee (Bombus terrestris) colonies. *PLoS ONE.* ISSN: 19326203 (2014).

66. Fleischmann, P. *Starting foraging life: Early calibration and daily use of the navigational system in Cataglyphis ants* PhD thesis (Jan. 2019).

67. Fleischmann, P. N., Christian, M., Müller, V. L., Rössler, W. & Wehner, R. Ontogeny of learning walks and the acquisition of landmark information in desert ants, Cataglyphis fortis. *Journal of Experimental Biology.* ISSN: 00220949 (2016).

68. Fleischmann, P. N., Grob, R., Wehner, R. & Rössler, W. Species-specific differences in the fine structure of learning walk elements in Cataglyphis ants. *Journal of Experimental Biology.* ISSN: 00220949 (2017).

69. Fleischmann, P. N., Grob, R., Müller, V. L., Wehner, R. & Rössler, W. The Geomagnetic Field Is a Compass Cue in Cataglyphis Ant Navigation. *Current Biology.* ISSN: 09609822 (2018).

70. Franz, M. O. & Mallot, H. A. Biomimetic robot navigation. *Robotics and Autonomous Systems.* ISSN: 09218890 (2000).

71. Gonsek, A. & Bertrand, O. J. Following similar routes: a method for path classification in cluttered environment. *Modern Methods in Neuroethology, Frontiers in Behavioral Neuroscience* (in prep.).

72. Goulson, J. L. *Bumblebees: Behaviour, Ecology, and Conservation.Second Edition* (Oxford University Press, New York, Hardback, 2010).

73. Gourichon, S., Meyer, J. A. & Pirim, P. Using coloured snapshots for short-range guidance in mobile robots. *International Journal of Robotics Research.* ISSN: 02783649 (1998).

74. Graham, P. & Mangan, M. Insect navigation: do ants live in the now? *Journal of Experimental Biology* **218,** 819–823. ISSN: 0022-0949 (2015).

75. Graham, P., Philippides, A. & Baddeley, B. Animal cognition: Multi-modal interactions in ant learning. *Current Biology.* ISSN: 09609822 (2010).

76. Hardcastle, B. J. & Krapp, H. G. Evolution of Biological Image Stabilization. *Current Biology.* ISSN: 09609822 (2016).

77. Hengstenberg, R. *Multisensory control in insect oculomotor systems.* 1993.

78. Hennig, P. & Egelhaaf, M. Neuronal encoding of object and distance information: A model simulation study on naturalistic optic flow processing: Functional analysis on optic flow processing. *Frontiers in Neural Circuits.* ISSN: 16625110 (2012).

79. Hoffmann, G. The search behavior of the desert isopod Hemilepistus reaumuri as compared with a systematic search. *Behavioral Ecology and Sociobiology.* ISSN: 14320762 (1983).

80. Hoinville, T. & Wehner, R. Optimal multiguidance integration in insect navigation. *Proceedings of the National Academy of Sciences.* ISSN: 0027-8424 (2018).

81. Holm, S. A simple sequentially rejective multiple test procedure. *Scandinavian journal of statistics* (1979).

82. Horn, B. K. P. *Robot Vision* ISBN: 0262081598 (MIT Press, Cambridge, MA, USA, 1986).

83. Hugues, I. & Hase, T. *Measurements and their Uncertainties: A Practical Guide to Modern Error Analysis* (Oxford University Press Inc., UK, 2010).

84. Humphries, N. E. *et al.* Environmental context explains Lévy and Brownian movement patterns of marine predators. *Nature.* ISSN: 00280836 (2010).

85. Huth, J. E. *Before the Bubble* 1–10. ISBN: 9780674072824. `http://www.jstor.org/stable/j.ctt3fgtxg.3` (Harvard University Press, 2013).

86. John, C. R. *et al.* M3C: Monte Carlo reference-based consensus clustering. *Scientific Reports.* ISSN: 20452322 (2020).

87. Judd, S. P. D. & Collett, T. S. Multiple stored views an landmark guidance in ants. *Nature.* ISSN: 00280836 (1998).

88. Kaplan, M. Bumblebees sense electric fields in flowers. *Nature.* ISSN: 0028-0836 (2013).

89. Kaufman, L. & Rousseeuw., P. *Clustering by means of Medoids* in *Statistical Data Analysis Based on the L1 Norm and Related Methods* (1987).

90. Kern, R., van Hateren, J. H. & Egelhaaf, M. Representation of behaviourally relevant information by blowfly motion-sensitive visual interneurons requires precise compensatory head movements. *Journal of Experimental Biology* **209,** 1251–1260. ISSN: 0022-0949. eprint: `https://jeb.biologists.org/content/209/7/1251.full.pdf`. `https://jeb.biologists.org/content/209/7/1251` (2006).

91. Kern, R., Van Hateren, J. H., Michaelis, C., Lindemann, J. P. & Egelhaaf, M. Function of a fly motion-sensitive neuron matches eye movements during free flight. *PLoS Biology.* ISSN: 15457885 (2005).

92. Koenderink, J. J. & van Doorn, A. J. Facts on optic flow. *Biological Cybernetics.* ISSN: 0340-1200 (1987).

93. Kraft, P., Evangelista, C., Dacke, M., Labhart, T. & Srinivasan, M. V. Honeybee navigation: Following routes using polarized-light cues. *Philosophical Transactions of the Royal Society B: Biological Sciences.* ISSN: 14712970 (2011).

94. Krakauer, D. C. Simple connectionist models of spatial memory in bees. *Journal of Theoretical Biology.* ISSN: 00225193 (1995).

95. Lambrinos, D., Möller, R., Labhart, T., Pfeifer, R. & Wehner, R. Mobile robot employing insect strategies for navigation. *Robotics and Autonomous Systems.* ISSN: 09218890 (2000).

96. Lawson, D. A., Chittka, L., Whitney, H. M. & Rands, S. A. Bumblebees distinguish floral scent patterns, and can transfer these to corresponding visual patterns. *Proceedings of the Royal Society B: Biological Sciences.* ISSN: 14712954 (2018).

97. Lebhardt, F. & Ronacher, B. Transfer of directional information between the polarization compass and the sun compass in desert ants. *Journal of Comparative Physiology A: Neuroethology, Sensory, Neural, and Behavioral Physiology.* ISSN: 14321351 (2015).

98. Lehrer, M. Why do bees turn back and look? *Journal of Comparative Physiology A.* ISSN: 03407594 (1993).

99. Lehrer, M. & Collett, T. S. Approaching and departing bees learn different cues to the distance of a landmark. *Journal of Comparative Physiology A.* ISSN: 03407594 (1994).

100. Lehrer, M. & Srinivasan, M. V. Object detection by honeybees: Why do they land on edges? *Journal of Comparative Physiology A.* ISSN: 03407594 (1993).

101. Lent, D. D., Graham, P. & Collett, T. S. Visual scene perception in navigating wood ants. *Current Biology.* ISSN: 09609822 (2013).

102. Li, J., Lindemann, J. & Egelhaaf, M. Local motion adaptation enhances the representation of spatial structure at EMD arrays. *PLoS Computational Biology.* ISSN: 15537358 (2017).

103. Lichtenstein, L., Sommerlandt, F. M. & Spaethe, J. Dumb and lazy? A comparison of color learning and memory retrieval in drones and workers of the buff-tailed bumblebee, bombus terrestris, by means of per conditioning. *PLoS ONE.* ISSN: 19326203 (2015).

104. Lihoreau, M., Chittka, L. & Raine, N. E. Travel optimization by foraging bumblebees through readjustments of traplines after discovery of new feeding locations. *American Naturalist.* ISSN: 00030147 (2010).

105. Lipp, H.-P. *et al.* Pigeon Homing along Highways and Exits. *Current biology : CB* **14,** 1239–49 (Aug. 2004).

106. Lobecke, A. *Local homing of the bumblebee, Bombus terrestris.* PhD thesis (Jan. 2018).

107. Lobecke, A., Kern, R. & Egelhaaf, M. Taking a goal-centred dynamic snapshot as a possibility for local homing in initially naïve bumblebees. *Journal of Experimental Biology* **221** (2018).

108. Mandal, S. *How do animals find their way back home? A brief overview of homing behavior with special reference to social Hymenoptera* 2018.

109. Mangan, M. & Webb, B. Modelling place memory in crickets. *Biological Cybernetics.* ISSN: 03401200 (2009).

110. Mangan, M. & Webb, B. Spontaneous formation of multiple routes in individual desert ants (Cataglyphis velox). *Behavioral Ecology.* ISSN: 10452249 (2012).

111. Marchant, J. Did Vikings navigate by polarized light? *Nature.* ISSN: 0028-0836 (2011).

112. Maschwitz, U. & Mühlenberg, M. Zur jagdstrategie einiger orientalicher Leptogenys-arten (Formicidae: Ponerinae). *Oecologia.* ISSN: 00298549 (1975).

113. Menzel, R. *et al.* Honey bees navigate according to a map-like spatial memory. *Proceedings of the National Academy of Sciences.* ISSN: 0027-8424 (2005).

114. Mertes, M., Dittmar, L., Egelhaaf, M. & Boeddeker, N. Visual motion-sensitive neurons in the bumblebee brain convey information about landmarks during a navigational task. *Frontiers in Behavioral Neuroscience* **8** (2014).

115. Milford, M. *Vision-based place recognition: How low can you go?* in *International Journal of Robotics Research* (2013).

116. Müller, M. & Wehner, R. The hidden spiral: systematic search and path integration in desert ants, Cataglyphis fortis. *Journal of Comparative Physiology A.* ISSN: 03407594 (1994).

117. Möller, R. Do insects use templates or parameters for landmark navigation? *Journal of Theoretical Biology.* ISSN: 00225193 (2001).

118. Möller, R. & Vardy, A. Local visual homing by matched-filter descent in image distances. *Biological Cybernetics.* ISSN: 03401200 (2006).

119. Montello, D. R. Landmarks are Exaggerated. *KI - Künstliche Intelligenz.* ISSN: 0933-1875 (2017).

120. Morris, R. G. Spatial localization does not require the presence of local cues. *Learning and Motivation.* ISSN: 00239690 (1981).

121. Moser, E. I., Kropff, E. & Moser, M.-B. Place Cells, Grid Cells, and the Brain's Spatial Representation System. *Annual Review of Neuroscience.* ISSN: 0147-006X (2008).

122. Mronz, M. & Lehmann, F.-O. The free-flight response of Drosophila to motion of the visual environment. *Journal of Experimental Biology.* ISSN: 0022-0949 (2008).

123. Muller, M. & Wehner, R. Path integration in desert ants, Cataglyphis fortis. *Proceedings of the National Academy of Sciences.* ISSN: 0027-8424 (1988).

124. Müller, M. & Wehner, R. Path integration provides a scaffold for landmark learning in desert ants. *Current Biology.* ISSN: 09609822 (2010).

125. Müller, M. M., Bertrand, O. J., Differt, D. & Egelhaaf, M. The problem of home choice in skyline-based homing. *PLoS ONE.* ISSN: 19326203 (2018).

126. Murray, T. & Zeil, J. Quantifying navigational information: The catchment volumes of panoramic snapshots in outdoor scenes. *PLoS ONE.* ISSN: 19326203 (2017).

127. Nason, G. & Scott, D. W. Multivariate Density Estimation: Theory, Practice, and Visualization. *Journal of the Royal Statistical Society. Series A (Statistics in Society).* ISSN: 09641998 (1993).

128. Nicholson, D. J., Judd, S. P., Cartwright, B. A. & Collett, T. S. Learning walks and landmark guidance in wood ants (Formica rufa). *Journal of Experimental Biology.* ISSN: 00220949 (1999).

129. Orians GH, P. N. *On the theory of central place foraging* 155–177 (1979).

130. Osborne, J. L. *et al.* A landscape-scale study of bumble bee foraging range and constancy, using harmonic radar. *Journal of Applied Ecology.* ISSN: 00218901 (1999).

131. Papi, F. *Animal Homing edited by F. Papi.* ISBN: 94-011-1588-5 (1992).

132. Pete, A. E., Kress, D., Dimitrov, M. A. & Lentink, D. The role of passive avian head stabilization in flapping flight. *Journal of the Royal Society Interface.* ISSN: 17425662 (2015).

133. Peto, R. *et al.* Design and analysis of randomized clinical trials requiring prolonged observation of each patient. II. Analysis and examples. *British Journal of Cancer.* ISSN: 15321827 (1977).

134. Philippides, A., de Ibarra, N. H., Riabinina, O. & Collett, T. S. Bumblebee calligraphy: the design and control of flight motifs in the learning and return flights of Bombus terrestris. *Journal of Experimental Biology.* ISSN: 0022-0949 (2013).

135. Portelli, G., Ruffier, F. & Franceschini, N. Honeybees change their height to restore their optic flow. *Journal of Comparative Physiology A: Neuroethology, Sensory, Neural, and Behavioral Physiology.* ISSN: 03407594 (2010).

136. Raderschall, C. A., Narendra, A. & Zeil, J. Head roll stabilisation in the nocturnal bull ant *Myrmecia pyriformis* : implications for visual navigation. *The Journal of Experimental Biology.* ISSN: 0022-0949 (2016).

137. Ravi, S. *et al.* Hummingbird flight stability and control in freestream turbulent winds. *Journal of Experimental Biology.* ISSN: 0022-0949 (2015).

138. Ravi, S., Crall, J. D., Fisher, A. & Combes, S. A. Rolling with the flow: Bumblebees flying in unsteady wakes. *Journal of Experimental Biology.* ISSN: 00220949 (2013).

139. Ravi, S. *et al.* Gap perception in bumblebees. *Journal of Experimental Biology* **222.** ISSN: 0022-0949 (2019).

140. Reynolds, A. M. *et al.* Displaced honey bees perform optimal scale-free search flights. *Ecology* **88,** 1955–1961. ISSN: 00129658 (2007).

141. Riabinina, O., de Ibarra, N. H., Philippides, A. & Collett, T. S. Head movements and the optic flow generated during the learning flights of bumblebees. *Journal of Experimental Biology.* ISSN: 0022-0949 (2014).

142. Robert, T., Frasnelli, E., de Ibarra, N. H. & Collett, T. S. Variations on a theme: bumblebee learning flights from the nest and from flowers. *The Journal of Experimental Biology.* ISSN: 0022-0949 (2018).

143. Ros, I. G. & Biewener, A. A. Pigeons (C. livia) follow their head during turning flight: Head stabilization underlies the visual control of flight. *Frontiers in Neuroscience.* ISSN: 1662453X (2017).

144. Samet, N., Zeil, J., Mair, E., Boeddeker, N. & Stürzl, W. Ground-nesting insects could use visual tracking for monitoring nest position during learning flights. ISSN: 16113349 (2014).

145. Schone, H. & Strausfeld, C. *Spatial Orientation* ISBN: 978-1-4008-5684-8. `https://www.degruyter.com/view/title/508823` (Princeton University Press, Princeton, 2014).

146. Schulte, P., Zeil, J. & Stürzl, W. An insect-inspired model for acquiring views for homing. *Biological Cybernetics.* ISSN: 14320770 (2019).

147. Schultheiss, P., Cheng, K. & Reynolds, A. M. Searching behavior in social Hymenoptera. *Learning and Motivation* **50,** 59–67. ISSN: 00239690 (2015).

148. Schultheiss, P. *et al.* Similarities and differences in path integration and search in two species of desert ants inhabiting a visually rich and a visually barren habitat. *Behavioral Ecology and Sociobiology.* ISSN: 03405443 (2016).

149. Schwegmann, A., Lindemann, J. P. & Egelhaaf, M. Depth information in natural environments derived from optic flow by insect motion detection system: a model analysis. *Frontiers in Computational Neuroscience* **8** (2014).

150. *scikit-learn 0.22.1* 2007-2019.

151. Secundus, P. t. E. G. P. & Secundus], P. t. E. G. P. in *Clarendon Ancient History Series: The Elder Pliny on the Human Animal: Natural History Book 7* (2016).

152. Seidl, T. & Wehner, R. Visual and tactile learning of ground structures in desert ants. *Journal of Experimental Biology.* ISSN: 00220949 (2006).

153. Si, A., Srinivasan, M. V. & Zhang, S. Honeybee navigation: Properties of the visually driven 'odometer'. *Journal of Experimental Biology.* ISSN: 00220949 (2003).

154. Sims, D. W. *et al.* Scaling laws of marine predator search behaviour. *Nature.* ISSN: 14764687 (2008).

155. Skorupski, P. & Chittka, L. Photoreceptor spectral sensitivity in the bumblebee, Bombus impatiens (Hymenoptera: Apidae). *PLoS ONE.* ISSN: 19326203 (2010).

156. Solvi, C., Al-Khudhairy, S. G. & Chittka, L. Bumble bees display cross-modal object recognition between visual and tactile senses. *Science.* ISSN: 10959203 (2020).

157. Sovrano, V. A., Rigosi, E. & Vallortigara, G. Spatial reorientation by geometry in bumblebees. *PLoS ONE.* ISSN: 19326203 (2012).

158. Srinivasan, M. V. Pattern recognition in the honeybee: Recent progress. *Journal of Insect Physiology* **40,** 183–194. ISSN: 00221910 (1994).

159. Srinivasan, M. V., Zhang, S., Altwein, M. & Tautz, J. Honeybee navigation: Nature and calibration of the 'odometer'. *Science.* ISSN: 00368075 (2000).

160. Steck, K. *Just follow your nose: Homing by olfactory cues in ants* 2012.

161. Stoica, P. & Moses, R. *Spectral Analysis of Signals* (Upper Saddle River:Prentice-Hall, NJ, 2005).

162. Stone, T., Differt, D., Milford, M. & Webb, B. *Skyline-based localisation for aggressively manoeuvring robots using UV sensors and spherical harmonics* in (2016). ISBN: 9781467380263.

163. Stone, T., Mangan, M., Ardin, P. & Webb, B. *Sky segmentation with ultraviolet images can be used for navigation* in (2015).

164. Stone, T., Mangan, M., Wystrach, A. & Webb, B. Rotation invariant visual processing for spatial memory in insects. *Interface Focus.* ISSN: 20428901 (2018).

165. Stürzl, W., Zeil, J., Boeddeker, N. & Hemmi, J. M. How wasps acquire and use views for homing. *Current Biology.* ISSN: 09609822 (2016).

166. Sun, X., Yue, S. & Mangan, M. Modelling the Insect Navigation Toolkit: How the Mushroom Bodies and Central Complex Coordinate Guidance Strategies. *bioRxiv* (2019).

167. Tautz, J. *et al.* Honeybee odometry: Performance in varying natural terrain. *PLoS Biology.* ISSN: 15449173 (2004).

168. Taylor, G. J. *et al.* Bumblebee visual allometry results in locally improved resolution and globally improved sensitivity. *eLife.* ISSN: 2050084X (2019).

169. Timbergen, N. Über die Orienterung des Bienenwolfes (Philanthus triangulum Fabr.). *Zeitschrift für Vergleichende Physiologie* (1932).

170. Tinbergen, N. Über die Orientierung des Bienenwolfes (Philanthus triangulum Fabr.) - II. Die Bienenjagd. *Zeitschrift für Vergleichende Physiologie.* ISSN: 03407594 (1935).

171. Todd, J. G., Kain, J. S. & De Bivort, B. L. Systematic exploration of unsupervised methods for mapping behavior. *Physical Biology.* ISSN: 14783975 (2017).

172. Trullier, O., Wiener, S. I., Berthoz, A. & Meyer, J. A. Biologically based artificial navigation systems: Review and prospects. *Progress in Neurobiology.* ISSN: 03010082 (1997).

173. Tsoar, A. *et al.* Large-scale navigational map in a mammal. *Proceedings of the National Academy of Sciences of the United States of America.* ISSN: 00278424 (2011).

174. Ullrich, T. W., Kern, R. & Egelhaaf, M. Influence of environmental information in natural scenes and the effects of motion adaptation on a fly motion-sensitive neuron during simulated flight. *Biology Open.* ISSN: 20466390 (2015).

175. Van Der Maaten, L. & Hinton, G. Visualizing data using t-SNE. *Journal of Machine Learning Research.* ISSN: 15324435 (2008).

176. Van Hateren, J. H. & Schilstra, C. Blowfly flight and optic flow. II. Head movements during flight. *Journal of Experimental Biology.* ISSN: 00220949 (1999).

177. Vardy, A. *Biologically Plausible Methods for Robot Visual Homing, School of Computer Science* PhD thesis (Carleton University, 2005).

178. Vardy, A. & Möller, R. Biologically plausible visual homing methods based on optical flow techniques. *Connection Science.* ISSN: 09540091 (2005).

179. Vardy, A. & Oppacher, F. *Low-level visual homing* in *Lecture Notes in Artificial Intelligence (Subseries of Lecture Notes in Computer Science)* (2003). ISBN: 3540200576.

180. Viollet, S. & Zeil, J. Feed-forward and visual feedback control of head roll orientation in wasps (polistes humilis, vespidae, hymenoptera). *Journal of Experimental Biology.* ISSN: 00220949 (2013).

181. Von Frisch, K. *The dance language and orientation of bees* Belknap/Ha (Cambridge, 1967).

182. Warrant, E. & Dacke, M. Vision and Visual Navigation in Nocturnal Insects. *Annual Review of Entomology.* ISSN: 0066-4170 (2011).

183. Warrant, E. J. Seeing in the dark: vision and visual behaviour in nocturnal bees and wasps. *Journal of Experimental Biology* **211,** 1737–1746. ISSN: 0022-0949 (2008).

184. Webb, B. The internal maps of insects. *Journal of Experimental Biology.* ISSN: 00220949 (2019).

185. Wehner, R., Meier, C. & Zollikofer, C. The ontogeny of foraging behaviour in desert ants, Cataglyphis bicolor. *Ecological Entomology.* ISSN: 03076946 (2004).

186. Wehner, R., Michel, B. & Antonsen, P. Visual navigation in insects: Coupling of egocentric and geocentric information. *Journal of Experimental Biology.* ISSN: 00220949 (1996).

187. Wehner, R. & Srinivasan, M. V. Searching behaviour of desert ants, genus Cataglyphis (Formicidae, Hymenoptera). *Journal of Comparative Physiology A.* ISSN: 03407594 (1981).

188. Wehner, R. The architecture of the desert ant's navigational toolkit (Hymenoptera: Formicidae). *Myrmecological News.* ISSN: 19944136 (2009).

189. Wilson, E. O. & Hölldobler, B. *Eusociality: Origin and consequences* 2005.

190. Wolf, S. & Chittka, L. Male bumblebees, Bombus terrestris, perform equally well as workers in a serial colour-learning task. *Animal Behaviour.* ISSN: 00033472 (2016).

191. Woltring, H. J. On optimal smoothing and derivative estimation from noisy displacement data in biomechanics. *Human Movement Science.* ISSN: 01679457. arXiv: 23 (1985).

192. Woodgate, J. L., Makinson, J. C., Lim, K. S., Reynolds, A. M. & Chittka, L. Life-long radar tracking of bumblebees. *PLoS ONE.* ISSN: 19326203 (2016).

193. Wystrach, A., Beugnon, G. & Cheng, K. Ants might use different view-matching strategies on and off the route. *Journal of Experimental Biology* **215,** 44–55. ISSN: 0022-0949 (2012).

194. Wystrach, A., Dewar, A., Philippides, A. & Graham, P. How do field of view and resolution affect the information content of panoramic scenes for visual navigation? A computational investigation. *Journal of Comparative Physiology A: Neuroethology, Sensory, Neural, and Behavioral Physiology.* ISSN: 14321351 (2016).

195. Wystrach, A. & Graham, P. What can we learn from studies of insect navigation? *Animal Behaviour* **84,** 13–20. ISSN: 00033472. http://dx.doi.org/10.1016/j.anbehav.2012.04.017 (2012).

196. Wystrach, A., Mangan, M. & Webb, B. Optimal cue integration in ants. *Proceedings of the Royal Society B: Biological Sciences.* ISSN: 14712954 (2015).

197. Wystrach, A., Philippides, A., Aurejac, A., Cheng, K. & Graham, P. Visual scanning behaviours and their role in the navigation of the Australian desert ant Melophorus bagoti. *Journal of Compara-*

tive Physiology A: Neuroethology, Sensory, Neural, and Behavioral Physiology. ISSN: 14321351 (2014).

198. Wystrach, A., Schwarz, S., Baniel, A. & Cheng, K. Backtracking behaviour in lost ants: An additional strategy in their navigational toolkit. *Proceedings of the Royal Society B: Biological Sciences.* ISSN: 14712954 (2013).

199. Wystrach, A., Schwarz, S., Graham, P. & Cheng, K. Running paths to nowhere: repetition of routes shows how navigating ants modulate online the weights accorded to cues. *Animal Cognition.* ISSN: 14359448 (2019).

200. Wystrach, A., Schwarz, S., Schultheiss, P., Baniel, A. & Cheng, K. Multiple sources of celestial compass information in the Central Australian desert ant Melophorus bagoti. *Journal of Comparative Physiology A: Neuroethology, Sensory, Neural, and Behavioral Physiology.* ISSN: 14321351 (2014).

201. Zeil, J. Orientation flights of solitary wasps (Cerceris; Sphecidae; Hymenoptera): I. Description of flight. *Journal of Comparative Physiology A: Sensory, Neural and Behavioral Physiology.* ISSN: 14321351 (1993).

202. Zeil, J. Orientation flights of solitary wasps (Cerceris; Sphecidae; Hymenoptera): II. Similarities between orientation and return flights and the use of motion parallax. *Journal of Comparative Physiology A: Sensory, Neural and Behavioral Physiology.* ISSN: 14321351 (1993).

203. Zeil, J., Hofmann, M. I. & Chahl, J. S. Catchment areas of panoramic snapshots in outdoor scenes. *Journal of the Optical Society of America A.* ISSN: 1084-7529 (2003).